UNIVERSITÀ DEGLI STUDI DELL'INSUBRIA

DOTTORATO DI RICERCA IN SCIENZE DELLA VITA E BIOTECNOLOGIE

XXXIII CICLO

Multi-step biocatalytic depolymerization of lignin

Depolimerizzazione della lignina mediante biocatalisi multi-step

Docente guida: Prof. **LOREDANO POLLEGIONI**
Tutor: Dott.ssa **ELENA ROSINI**

Tesi di dottorato di:
ELISA VIGNALI
Matr. 717812

Dip. Biotecnologie e Scienze della Vita - Università degli Studi dell'Insubria

Anno accademico 2019-2020

Abstract

Lignin is, beside cellulose and hemicellulose, one of the three components of the lignocellulosic biomass. Since the peculiar phenyl-propanoic structure, lignin represents the first renewable source of aromatics on Earth: the valorisation of this biopolymer represents a primary target of the bioeconomy and circular economy. The present Ph.D. thesis highlights different biochemical strategies for lignin valorisation, focusing on the use of different enzymes as high-selective and efficient biocatalysts.

Firstly, the N246A variant of the dye-decolorizing peroxidase DypB from *Rhodococcus jostii* RHA1 (Rh_DypB) and the superoxide dismutase MnSOD-1 from *Sphingobium* sp. T2 (i.e. two bacterial lignin-degrading enzymes) were overexpressed in a recombinant form in the BL21(DE3) strain of *Escherichia coli* and biochemical characterized. In particular, for the first time, Rh_DypB was fully obtained as folded holoenzyme (>100 mg/L, >90% purity) thus avoiding the need for a further time-consuming and expensive reconstitution step of the apoprotein. Rh_DypB is a versatile biocatalyst with an improved manganese peroxidase activity, showing suitable biochemical properties for biotechnological purposes, such as a good thermostability (a melting temperature value of 63-65 °C) and tolerance to compounds used in industrial solubilisation processes (i.e. Rh_DypB is active in the presence of 1 M NaCl, 10% DMSO, and 5% Tween-80). It allowed the oxidation of a large number of lignin model compounds, the cleavage of the β-O-4 linkage in a lignin model dimer (12.5 μmol/min mg enzyme), the decolorization of different dyes (i.e. Remazol Brilliant Blue R, Azure B, Reactive Black 5) and the degradation of Aflatoxin B_1 into the less toxic metabolite Aflatoxin Q_1 (96% yield, 96 h).

Interestingly, MnSOD-1 was obtained in a recombinant form with a 5-fold increase in volumetric yield in comparison to reported studies (i.e. ≈100 mg/L vs. 19.5 mg/L), high activity (518 ± 5.3 U/mg) and a great stability after 24 h of incubation at different pH values (from 3.0 to 9.0, residual activity >90%). MnSOD-1 was used, beside different bacterial commercial and recombinant laccases, in an extensive

quantitative study on the depolymerization yields of technical lignins through a bio-catalytic approach. The use of a miniaturized colorimetric screening method for the identification of oxidation/degradation products from lignin allowed the set up of the optimal incubation conditions through the rapid collection and comparison of more than 240 results (i.e. >48 different lignin/enzyme combinations). Moreover, the acetone-fractionation of the technical lignins was used as mild process to increase the homogeneity (i.e. reduction of polidispersity) of the starting material: in this way an improvement in the enzymatic degradation yield in comparison with the corresponding unfractionated samples was observed. Remarkably, ferulic acid (0.86 mg/g lignin) was obtained following the incubation of MnSOD-1 with the acetone soluble fraction of Wheat Straw Lignin (1 h, pH 8.2) and vanillin (0.35 mg/g lignin) was obtained from the incubation of the recombinant laccase BALL from *Bacillus licheniformis* with the acetone soluble fraction of Kraft lignin (2 h, pH 5.0).

Secondly, the first synthetic multi-enzymatic pathway for the bioconversion of vanillin (the only globally commercialised aromatic compound obtained from lignin degradation) into the value-added product *cis,cis*-muconic acid (a precursor of a large number of plastic materials) was set up. Each of the four reaction steps was optimized and the economic aspects underlying the set up of the bioconversion were evaluated (e.g., the use of a bi-enzymatic system for the THF cofactor regeneration and the use of lyophilised cells expressing the AroY decarboxylase in order to avoid the expensive reconstitution of the apoenzyme with its FMN cofactor). Finally, the one pot reaction was assayed in the presence of 3 mM vanillin: 1 g of *cis,cis*-muconic acid was produced at the 70% of the commercial cost (>95% yield, ≈ 15 h). This efficient and inexpensive approach represents an improvement in comparison with the reported enzymatic conversion of vanillin into *cis,cis*-muconic acid through a whole-cell system (69% yield, 48 h).

Contents

1. Introduction

1.1. Lignin

Lignin, from the Latin word *lignunm* which means wood, is a major component of cell walls in several plants and in some algae[1]. In the cell walls, lignin forms cross-links with the carbohydrates cellulose and hemicellulose, resulting in a complex lignocellulosic matrix (Figure 1)[2,3].

Lignin consists in an aromatic amorphous hetero-polymer with different physiological functions: it confers rigidity and strength to the stem and the bole of the higher plants, it facilitates the transport of water and nutrients among plant tissues and it provides a barrier against insects and microbial attack[4]. It is, after cellulose, the second most abundant substance on Earth and, since its peculiar chemical structure composed of phenylpropane units, it represents the first renewable source of aromatics[2,5].

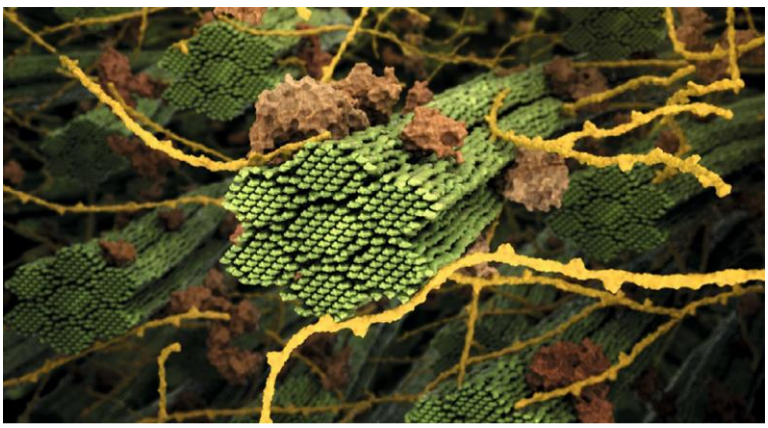

Figure 1. Simulated structure of the lignocellulosic matrix. Cellulose (β-1,4-glucan) consists of unbranched polysaccharide chains, with β-(1→4) linkages between D-glucose units. Seven microfibrills arrange to form a fiber (green). Hemicellulose (yellow) includes different type of heteropolymers which can contain glucose, xylose, arabinose, mannose, galactose and deoxy rhamnose units. Lignin (brown) is a branched amorphous polymer. Adapted by permission from Springer, Nature Reviews Chemistry, reference[3], copyright 2018.

1.2. Chemical structure and biosynthesis

Lignin is a three-dimensional amorphous polymer consisting of substituted phenylpropane units[2]. It is a physically and chemically heterogeneous material,

which complex structure varies between species, within species and according to environmental factors during biosynthesis[6,7]. Lignin is optically inactive and it is formed by repeated monomeric phenylpropane units of the *para*-hydroxyphenyl (H), guaiacyl (G) and syringyl (S) types (Figure 2A)[6,8,9]. Hardwood lignins mainly contain guaiacyl and syringyl units, meanwhile *p*-hydroxyphenyl units are predominant in lignins from nonwoody annual fibers[8]. The lignin polymer is the result of C-O-C and C-C linkages between the monomeric units. The most representative type of linkage is the β-O-4, which is about the 50% of the total lignin interunit linkage (ca. 45% in softwoods and up to 60-65% in hardwoods)[8,10,11]. Other common lignin interunit linkages are the resinol (β-β), phenylcoumaran (β-5), 5-5', α-O-4 and 4-O-5 moieties (Figure 2B)[2,6,8].

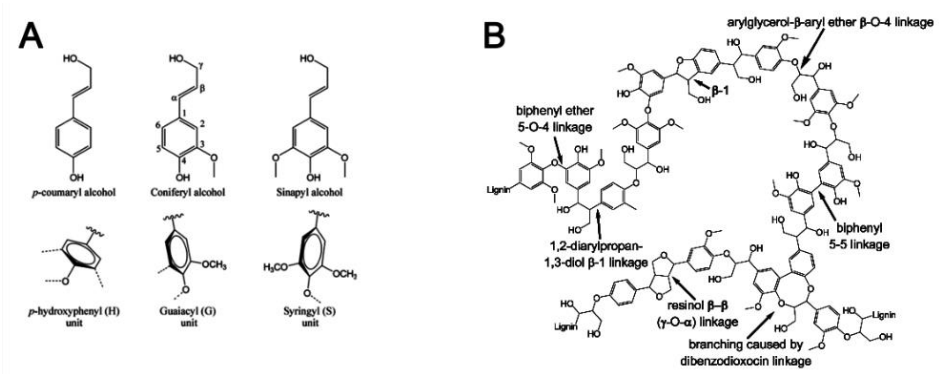

Figure 2. Insights into lignin structure and composition. A) Monolignols and *p*-hydroxyphenyl (H), guaiacyl (G) and syringyl (S) units. B) Schematic representation of lignin structure. The more representative linkages are indicated by arrows. Adapted with permission from reference[6] . Copyright 2015 FEBS Journal.

In nature, lignin is the result of three biosynthetic steps: i) synthesis of its constituents (monolignols); ii) transfer into the cell wall; iii) final radical polymerization[6].

The monolignols (coniferyl, sinapyl and *p*-coumaryl alcohols) are synthetized from L-phenylalanine and, in the case of grasses, also from L-tyrosine[9,12,13]. These two amino acids, produced in the plastid through the shikimate pathway, are channelled into the phenylpropanoid pathway, yielding different hydroxy carboxylic acids and

their activated coenzyme A (CoA) esters. In particular, the enzyme phenylalanine ammonium-lyase (PAL) catalyses the non-oxidative deamination of L-phenylalanine into cinnamic acid, which is the precursor in the production of synapic, caffeic, ferulic, 5-hydroxyferulic and *p*-coumarylic acids[13]. This latter compound can also be yielded through L-tyrosine deamination, which is catalysed by tyrosine ammonium-lyase (TAL)[13]. Then, the 4-cumarate:CoA ligase (4CL) catalyses the activation of *p*-coumaryl, ferulic and sinapic acids into CoA-thioesters, which are subsequently reduced by the cinnamoyl-CoA reductase (CCR) and the cinnamyl alcohol dehydrogenase (CAD) into respective alcohol monolignols[13].

Monolignols are relative toxic and unstable compounds, therefore the glycosylation of their phenolic hydroxyl group, performed by different glucosyl-transferases, is essential to allow the glucoside-monolignols to be both stored in the vacuole and transferred into the cell wall[9,12].

In the cell wall, monolignols are de-glycosylated and subsequently oxidized (i.e. dehydrogenated) by laccases and peroxidases to form phenolic radicals. Hence, the radical-radical coupling between reactive monomers can occur and covalent carbon–carbon or carbon–oxygen (ether) bonds are formed[6,9]. Since monolignol radicals mainly couple at their β positions, the β-β, β-O-4, and β-5 dimers are the only obtained[9,14]. Lignin polymer grows one unit at a time, by adding monomers (radicals) to the existing chain according to an endwise coupling[9,14]. Branching reactions, instead, can occur when two sequential reactions are possible at the growing end, i.e. the phenolic end, of the polymer[14]. Even though the exact mechanism underlying polymerization and controlling the relative abundance of phenylpropane units is still questioning, reported evidences support that the radical polymerization can not be an uncontrolled process and that the availability of monolignol radicals is determinant in the resulting lignin structure[9,14].

Lignin structure is intensively investigated with different analytic techniques, including degradative techniques (pyrolysis-gas-chromatograpy-mass spectrometry, thioacidolysis and derivatization followed by reductive cleavage, nitrobenzene oxidation) and spectroscopic ones (NMR, IR, UV and Raman

spectroscopy)[9,15,16]. Even though the firsts can be very precise in recognition of specific functional groups and structural moieties, being indirect methods they suffer of bias in deduction of the overall structure[15,16]. On the contrary, spectroscopic methods can directly elucidate lignin moieties, in a quantitative and high-resolving way[15]. In particular, the bidimensional [^{1}H;^{13}C] Heteronuclear Single Quantum Coherence NMR spectroscopy (2D-HSQC NMR) has appeared to be not only a relatively rapid and sensitive technique (31.6-fold more sensitive than ^{13}C-NMR), but also to be suitable for *in situ* application (avoiding lignin separation processes)[16]. Therefore, it results the most promising for the investigation of the actual structural features of native lignin.

1.3. Lignin biodegradation

In land ecosystems, the degradation of lignocellulose is mandatory for carbon recycling[6,17]. Even though the recalcitrant structure of lignin hinders its degradation, several types of microorganisms (mainly fungal and bacterial species) perform lignin depolymerisation through a multi-enzymatic process (Figure 3)[6,17–19].

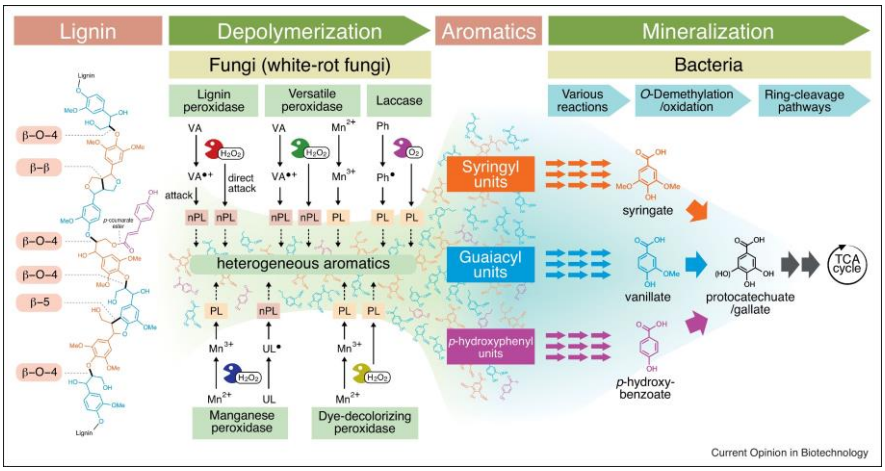

Figure 3. Lignin biodegradation. The process involves first extracellular oxidative reactions (depolymerization) for the formation of low-molecular weight aromatics followed by intracellular metabolic bioconversion of aromatics into carbon and energy sources (mineralisation). Reprinted from reference[19]. Copyright 2019 with permission from Elsevier.

The main enzymes involved in lignin depolymerisation are lignin peroxidases (LiPs), manganese peroxidase (MnPs), versatile peroxidase (VPs), dye-decolorizing peroxidases (DyPs) and laccases, but several accessory enzymes (i.e. aryl-alcohol oxidase, glyoxal oxidase, aryl-alcohol dehydrogenases and quinone reductases), have been reported to enhance delignification[6,19,20]. Notably, the molecular mass of lignocellulolytic extracellular enzymes not allow them to penetrate the intact wood cell wall. Therefore, the initial steps in delignification are probably triggered by small chemical oxidizers such as enzyme mediators and reactive oxygen species[6,17]. Particularly, mediators are low molecular mass compounds which, once oxidised, generate stable radicals acting as electron shuttles[6]. Among mediators, both natural (e.g., 4-hydroxybenzoic acid and 3-hydroxyanthranilate) and synthetic (e.g., 2,2'-azinobis 3-ethylbenzthiazoline-6-sulfonic acid (ABTS), 1-hydroxybenzotriazole (HBT) and acid violuric acid) are known[6].

The main wood decomposing fungi are basidiomycetes, which are distinguished into white-rot and brown-rot organisms according to their different ability of degrade lignin[17]. White-rot basidiomycetes (e.g., *Phanerochaete chrysosporium*, *Trametes versicolor* and *Ceriporiopsis subvermispora*) are the most frequent wood-rotting organisms and they can both degrade lignin selectively or simultaneously with the degradation of hemicellulose and cellulose[17]. Brown-rot fungi, instead, represent only the 7% of wood-rotting basidiomycetes; they typically grow on softwoods and they can degrade cellulose and hemicellulose only after a partial lignin modification[17]. Although only white-rot and brown-rot basidiomycetes can degrade wood extensively, some fungi belonging to the phylum of Ascomycota and a number of bacterial strains within the class of Actinomycetes (e.g., *Streptomyces sp.*, *Rhodococcus sp.*) and Proteobacteria (e.g., *Pseudomonas sp.*, *Bacillus sp.*) are known[6,21]. Even though fungal degradation systems have been more extensively studied comparing with bacterial metabolism, recent studies highlighted the role of bacteria not only in the extracellular lignin depolymerization phase but especially in its catabolism (lignin mineralization)[4,19,21,22].

The possibility to employ bacterial 'biological funneling' to convert a heterogeneous mix of aromatic molecules to a single product and the ease of bacteria engineering increased their attractiveness for biotechnological applications[4,23,24]. In addition, the deepening in the ligninolytic pathways of different soil bacteria allowed to discover beside oxidative enzymes, promising non-radical ligninolytic ones, such as the five-enzymatic system called Lig system from the α-proteobacterium *Sphingobium* sp. SYK-6 which are involved in the selective cleavage of the β-aryl ether bonds[6,25,26].

1.4. Lignin degrading enzymes and their biotechnological relevance

On the basis of their reaction mechanism, ligninolytic enzymes are classified in radical-dependent and non-radical enzymes[26]. The firsts, mainly comprising peroxidases and polyphenol oxidases (laccases), have been extensively studied over the past few decades and they have been already used in several industrial applications[6,26,27].

1.4.1. Peroxidases

Peroxidases are enzymes belonging to the oxidoreductases subclass which can use peroxides as electron acceptors. Peroxidases from ligninolytic microorganisms are successfully used for biopulping and biobleaching in the paper industry[27,28]. In fact, the enzymatic delignification of wood pulp results more effective and lignin-specific than the direct use of microorganisms which, instead, causes the degradation of cellulose fibers and it requires several days of incubation[27]. Furthermore, peroxidases are involved in bio-remediation processes such as soil and water detoxification of phenol, cresol, chlorinated phenolic compounds and recalcitrant xenobiotics (e.g., the herbicide atrazine)[27,28]. Peroxidase activity allows also the degradation of synthetic azo- and anthraquinone dyes, a characteristic appreciated in the textile industry and leather treatments[27,28].

1.4.1.1. Lignin peroxidase (LiP)

Lignin peroxidase, LiP, (EC 1.11.1.14), firstly identified in the 1980s in the white-rot fungus *P. chrysosporium* is a glycoprotein of 38-46 kDa containing 1 mol of iron protoporphyrin IX per 1 mol of protein[6,29]. It catalyses the H_2O_2-dependent oxidative depolymerization of lignin according to the general reaction:

$$\text{1,2 - bis(3,4-dimethoxyphenyl)propane - 1,3 - diol} + H_2O_2 \leftrightarrow$$
$$\leftrightarrow \text{3,4-dimethoxybenzaldehyde} + \text{1-(3,4-dimetoxyphenyl)etan-1,2-diol} + H_2O$$

The first catalytic step is performed in the presence of a molecule of hydrogen peroxide and it consists in a two-electron oxidation of ferric [Fe(III)] LiP to [Fe(IV)=O^+], which is a oxoferryl iron porphyrin radical cation referred as compound I. Subsequently, a substrate (such as veratryl alcohol) acting as electron donor, is oxidised to the radical cation form. This allows first the formation of compound II [Fe(IV)=O] and then the restoring of the initial [Fe(III)] state through two consecutive one-electron reduction steps[6]. Notably, in the presence of an excess of hydrogen peroxide the compound II forms an inactive oxidation state (compound III), which can return to the resting state both spontaneously or by reacting with a veratryl alcohol radical cation[6].

The LiP's redox potential (E_0') of about 1.2 V versus a standard hydrogen electrode, at pH 3.0, enables the enzyme to oxidise both phenolic and nonphenolic compounds, even in the absence of a mediator[6]. Nonetheless, LiPs show an higher activity on monomers and phenol lignin model compounds than on oligomers and nonphenolic substrates[6,30].

1.4.1.2. Manganese peroxidase (MnP)

Manganese peroxidase, MnP, (EC 1.11.1.13), a glycoprotein of 40-50 kDa, is the only heme-peroxidase which can use a single electron for the H_2O_2-dependent oxidation of Mn^{2+} to Mn^{3+}, according to a mechanism for which the ferric resting state [Fe(III)]

is first oxidised into a radical iron cation (compound I) and then into an iron cation (compound II). The stoichiometry of the reaction is as follows:

$$2\ Mn(II) + 2H^{+} + H_2O_2 \leftrightarrow 2\ Mn(III) + 2\ H_2O$$

The Mn^{3+} dissociates from the enzyme and is chelated by carboxylic acids (e.g., oxalate, malate) forming diffusible Mn^{3+}-complexes which act as oxidants of phenolic compounds[6,30]. Contrary to LiP, MnP can not oxidise veratryl alcohol nor nonphenolic substrates[6,30].

1.4.1.3. Versatile peroxidase (VP)

Versatile peroxidase, VP, (EC 1.11.1.16) is a heme-peroxidase of 35-45 kDa firstly discovered in fungi belonging to the *Pleurotus* and *Bjerkandera* genera[31]. Its catalytic cycle is similar to that reported for LiP in which the substrate is oxidised to give compound I and II intermediates[6]. Its high redox potential ($E_0' > + 1.4$ V versus SHE) and its several catalytic sites in the proximity of the heme poket, allow a wide substrate specificity. Accordingly, VP shares with MnP the ability to oxidise Mn^{2+} and with LiP the ability to oxidise veratryl alcohol, but in both the cases with a lower affinity and efficiency[6]. Nonetheless, contrary to LiP and MnP, only VP oxidises hydroquinones and both low- and high-redox-potential dyes[6,31].

1.4.1.4. Dye-decolorizing peroxidase (DyP)

Dye-decolorizing peroxidase, DyP, (EC 1.11.1.19) is a heme-protein belonging to the peroxidase-chlorite dismutase superfamily which has protomer weight of 40-60 kDa and different oligomeric states[32]. DyP was first identified in 1999 in the fungus *Bjerkandera adusta* and characterised for its activity on azo-dyes[21,32]. Nevertheless, to date DyP-type peroxidases have been found to be more commonly expressed in bacteria than fungi or other eukaryotes and they received increased attention due to their involment in lignin degradation[21,32]. Based on primary sequence, DyPs are classified in four classes: A-C (mainly found in bacteria) and D (extracellular fungal

representatives)[6,21,22,32]. Even though in the different types of DyPs at most 15% of primary sequence identity was apparent, structural features (i.e. β-barrel folds and α-helical structural regions) and the binding pocket for hydrogen peroxide are conserved among subclasses[33]. Interestingly, a conserved aspartate was found to be the catalytic residue in the DyP-type peroxidases[33]. This is a DyP-peculiarity compared to the general heme peroxidase mechanism in which a distal histidine is an essential acid-base catalyst[33]. However the details of the structure-function relatioships has to be further investigated in order to better explain the catalytic mechanism[33]. DyP's physiological substrate has not been defined yet, but these enzymes show activity on a broad range of compounds, such as synthetic dyes, monophenolic compounds, veratryl alcohol, carotenoids and lignin model compounds[6,32].

1.4.2. Laccases

Laccase (EC 1.10.3.2, benzenediol:oxygen oxidoreductase) is a polyphenol oxidase of about 60 kDa, belonging to the copper oxidase family[6,30]. The enzyme catalyses in the presence of oxygen the reaction:

$$4 \text{ benzenediol} + O_2 \leftrightarrow 4 \text{ benzosemiquinone} + 2\ H_2O$$

The catalytic site of laccase contains four copper ions (Cu^{2+}) of three different types: a type 1 copper in the T1 site (which having an absorption maximum at the wavelength of 610 nm, confers to laccase the characteristic blue colour), two type 2 coppers in the T2 site and a type 3 copper in the T3 site[6,30]. The latter form a T2/T3 trinuclear cluster. The type 1 copper at the T1 site represents the primary one-electron acceptor in the oxidation of the substrates[6]. In the first step of the catalytic cycle, four electrons from different substrate molecules are one by one transferred from T1 site to the T2/T3 trinuclear cluster through a conserved His-Cys-His motif (the rate-limiting step in catalysis)[6]. Subsequently, the type 2 and 3 coppers are involved in the storage of electrons from the reducing substrates, the binding of

molecular oxygen and its four-electron reduction into a water molecule[6,18,30]. Because of a moderately low redox potentials of about 0.42 - 0.79 V, the enzyme can direct oxidise only phenolic compounds[6]. The presence of suitable mediators (e.g., ABTS, 1-hydrobenzotriazole (1-HBT), violuric acid) expands its substrate spectrum to nonphenolics[6,30].

Like peroxidases, also laccase-mediated systems (LMS) are largely used in the pulp and textile industries during pulp delignification or dye-decolorizing processes[34]. In addition, laccases are applied to eliminate undesirable phenols and to modify the colour of food or beverage in the food industry[34]. Other industrial fields of application of laccases concern the development of nano-biosensors, new enzyme-containing cosmetic formulations and bio-catalysts for the synthetic chemistry[34].

1.5. Valorisation of lignin from the lignocellulosic biomass

Lignocellulosic biomass refers to plant biomass which is composed of cellulose (30-50%), hemicellulose (15-35%), lignin (10-20%) and minor amounts of fibrils and pectin (< 0.1%)[35,36]. On the basis of lignocellulose origin, it can be distinguished in woody feedstock's, agricultural residues, industrial wastes and municipal solid wastes[35,37]. To date, because of its low cost and worldwide availability, lignocellulosic biomass is considered an important renewable feedstock for the production of chemicals, materials and energy[37,38]. Initially, biorefineries focused on the development of the so called sugar-based platforms, valorising the cellulosic and hemicellulosic components for the production of bio-fuels and considering lignin as a raw material to be combusted[35,36,39]. In fact, its calorific power of 26-28 MJ/ton dry lignin is comparable to that of some fossil coals[8,18]. Nevertheless, energy production is, among the several possible applications of lignin, the one with the lowest market value (10 US$ cents/kg)[8].

In order to insert lignin into value-added markets, its peculiar chemical structure has to be considered. In fact, it represents the first renewable source of aromatics and, after cellulose, it is the second most abundant natural polymer on Earth[2,5]. The main

bottleneck consists in the substantial structural differences reported between native proto-lignin samples and technical lignins recovered after lignocellulose pretreatment[7,40]. This is a crucial point for biorefineries extensively discussed in the paragraph 1.5.2. Subsequently, lignin obtained from the biomass pretreatment has to be depolymerised into lower-molecular-weight compounds through thermochemical or biological processes (Figure 4)[41].

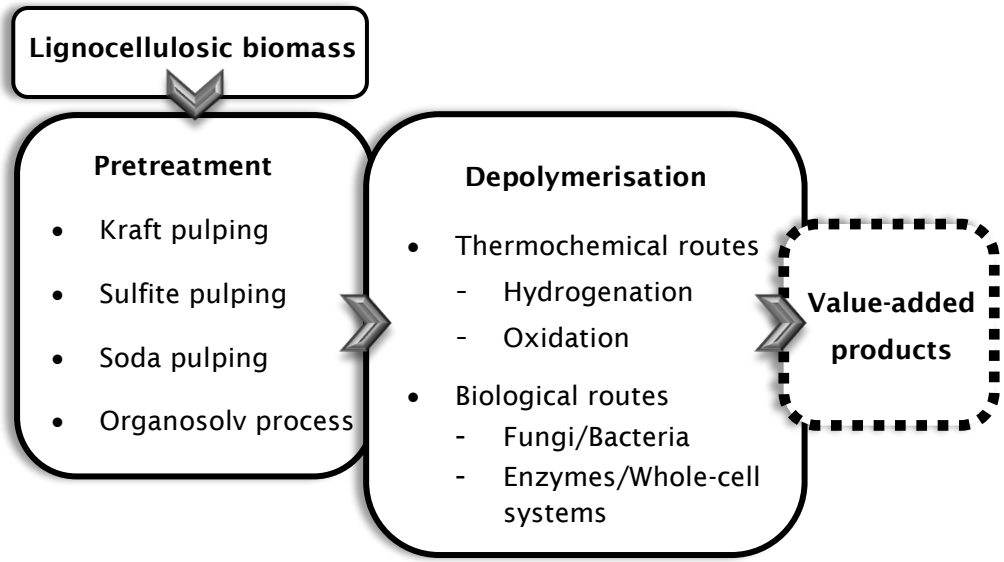

Figure 4. Scheme of the process for lignin valorisation.

Thermochemical approaches (pyrolysis, gasification and reductive, oxidative or acid-base catalytic depolymerisation) are performed under extreme conditions of temperature, pressure and pH values, eventually in the presence of metal catalysts (e.g., Pd, Pt, Ru, Ni, Cu)[41–43]. Instead, the biological approaches involve enzymes or microorganisms and can be performed under mild reaction conditions (see paragraph 1.5.3). Even though the firsts guarantee higher depolymerisation yields than biological treatments, the mixture of monomeric and oligomeric components obtained is generally heterogeneous and it may affect the further valorisation steps[44]: the choice of the optimal depolymerisation option is thus closely related to the target end products[38,42,45].

To date, the possible lignin application has been investigated not only for the production of biofuels (e.g., pyrolytic gas and synthesis gas or "syngas" from the pyrolysis and gasification process, respectively) but also for the production of innovative carbon-based materials and aromatic chemicals (Table 1)[18,38,42].

Table 1. List of the products which can be obtained from lignin.

Process	*Product*	
Lignin combustion	**Process heat, steam**	→ Renewable energy
Gasification	**Synthesis gas (syngas)**	→ Methanol, dimethylether → Diesel
Pyrolysis	**Pyrolytic gas, bio-oil**	→ Green fuels
Hydroliquefication	**Naphthenic and aromatic hydrocarbons**	→ Reformulated gasoline
Technical lignin/ Functionalised lignin	**Macromolecules** • Carbon fibers • Polymer fillers • Thermoset resins • Formaldehyde-free resins • Adhesives and binders	→ Synthetic polymers, materials
Depolymerisation	**Aromatic chemicals** • BTXs (Benzene, Toluene, Xylene) • Lignin monomer molecules - Syringols - Propylphenol - Eugenol - Vanillin and derivatives	→ Synthetic chemistry (polymers, flavors, fragrances)

For instance, lignin can replace synthetic polymers (e.g., polyacrylonitrile) in the synthesis of low-cost carbon fibers[38,44,45]. This represents a promising high-volume lignin application since, annually, the low-cost manufacturing of carbon fibers is about 300 x 10^3 tons[45]. Recently, the automotive industry has shown interest on this topic: energy-efficient light-weight vehicles can be developed by replacing mostly of their steel parts (40-50% of the structural steel mass) with carbon fiber composite

materials[38,45]. Currently, the mechanical properties of the lignin-based carbon fibers are slightly less performing than the petroleum-based counterpart[38]. For this purpose, pure grade lignin and the optimisation of its thermal and melting point properties are required[44].

Lignin is used also, as it or after chemical functionalisation, in the synthesis of other macromolecules, such as polymer modifiers (fillers, additives), resins, adhesives and binders[18,43–45]. In these applications, the addition of lignin during the polymer formulation offers the possibility to modify peculiar properties for existing materials, by employing some intrinsic characteristics of lignin (i.e. presence of reactive groups)[8,42], although both the molecular mass heterogeneity of lignin and the difficulties in controlling its viscosity represent in some cases a technical challenge[43,44]. The development of diisocyanate adhesives in which replacing methylene diphenyl diisocyanate (MDI) with lignin derivatives increased their elasticity modulus and the production of lignin containing resins with an increased in the normalized bond strength are some noteworthy examples reported in literature[8].

In addition, a large number of aromatic chemicals can be obtained from lignin depolymerisation, which are for examples the triad benzene, toluene and xylene (BTX), phenol, substituted coniferols, oxidized lignin monomers (syringaldehyde, vanillin, vanillic acid) and aromatic polyols. Notably, BTXs represent essential building blocks for the synthetic chemistry, with an annually global production volume from petroleum of 36, 10 and 35 x 10^6 tons, respectively[43]. The BTXs, beside to phenol and small amounts of C1 to C3 aliphatic and C6-C7 cycloaliphatic compounds, can be produced from lignin after its non-selective cleavage of C-C and C-O bonds[42–44]. Although technologies for producing BTXs from lignin depolymerisation are already available, in a commercial-scale prospective further efforts are required to improve the efficiency of the downstream of BTXs (i.e. deoxygenation process)[38,43]. The development of solutions to accelerate the use of BTXs as renewable substituents in the existing synthetic processes can have a massive impact on society. In fact, the US Department of Energy estimated that by

converting into BTX the 20% of the lignin (45 million tons) originated from the 1.3 billion tons of biomass available in the United States, the 10% of the these petrochemicals could be replaced[8,42,44].

Among the aromatics obtainable from lignin depolymerisation, guaiacol, syringol, catechol, and especially vanillin and their derivatives, have attracted particular relevance for their potential as building blocks in the synthesis of flavors, fragrances and polymers[22,43,44]. In particular, the globally vanillin market consists in about 20% of lignin-deriving vanillin and the resting 80% of oil-deriving vanillin (less than 1% is extracted from natural sources)[38]. Vanillin is one of the three lignin-deriving products currently commercialised (beside dimethyl sulfide and dimethyl sulfoxide)[38,43]. Vanillin is isolated through the oxidation of lignin in alkaline conditions, while dimethyl sulfide is obtained from the reaction of kraft lignin with molten sulfur in basic conditions and moreover dimethyl sulfoxide is the result of dimethyl sulfide oxidation with nitrogen dioxide[43].

Finally, focusing on some properties of lignin such as its biocompatibility, biodegradability, antimicrobial activity and thermo-stability, its potential use for advanced applications in the fields of biomedicine, bioremediation and energy storage have been investigated[38]. In particular, several studies demonstrated the possibility to use lignin for the production of hydrogels, nanotubes, nanowires and batteries, even though still at a laboratory-scale[38].

Overall, lignin valorisation is globally perceived as an urgent topic: in the last years the trend in publications grew exponentially (from 7 papers in 2008 to 108 papers in 2016)[42] and considering the patents filed in the last ten years in the World Intellectual Property Organization (WIPO) containing the word “lignin” on the front page, ca. 60% were registered in the period 2016-2020 (7,864 documents out of 13,054 documents, data updated to March 2020). In the 2015 the global production of lignin was approximately 100 x 10^6 tons/year, valued at US$ 732.7 million but it is expected to reach $913.1 million by 2025 with a compound annual growth rate (CAGR, i.e. the rate of return index) of 2.2%[38]. The main challenges in lignin valorisation regard both the set-up of optimal conditions for the pretreatment of

the biomass and the development of effective lignin depolymerising strategies[8,39]. In this scenario, biotechnologies play a key role in the design of bio-catalysed solutions involving enzymes and microorganisms (paragraph 1.5.3)[19,37,46].

1.5.1. Circular economy

Starting in the late 1970s, people began to perceive the necessity of a more sustainable economic model, to face some of the emerging social and environmental problems. The constant and rapid growth of the world population, the effects of climate changes, the indiscriminate exploitation of soil and ecosystems and the strict dependence on fossil non-renewable resources led to the introduction of the concept of "Bioeconomy", which combines profit and strategic development with the respect for society and natural resources (Figure 5)[47].

In particular, the branch of the circular economy proposes an alternative to the traditional linear productive approach by discouraging the use of virgin fossil sources (petroleum, coal and natural gas) and promoting a close-loop system able to maximise the recovery of raw materials derived from wastes[37,39,48]. Although a single definition is not available, this approach is well resumed by four key words (the "4Rs") identified by the European Union, which are reuse, reduce, recycle and recover of waste[48]. A proposed definition of "waste" is "any organic material apart from the primary ones" and, in this perspective, nearly all wastes currently have some value (e.g., lignin is used as fuel to power paper mills)[39]. Nevertheless, the aim of the circular economic system is to obtain higher value from waste by realising integrated facilities (biorefineries) which are competitive with the fossil-based ones[37,39,47]. The potential of the waste as resource is enormous, since it annually represents hundreds of megatonnes (i.e., $>10^8$ t) across the world[39]. In particular, the lignocellulosic biomass (which production is estimated to exceed 2×10^{11} t/year worldwide[22,39]) is considered the most suitable renewable feedstock to replace chemicals and fuels from fossil sources[37]. For instance, in order to manage the growing concern over the global effect of greenhouse gas emission, the United

States funded several programs for the increasing in biomass percentage as commodities from 5% in 2005 to 18% in 2020, and 25% by 2030[38]. Moreover, the use of biomass as renewable source has not only important environmental effects but can also assure to each country independence from fossil reserves which, since they are mainly located in confined areas on Earth, they have sometimes been subjected to speculation and they have been causes of international conflicts[38].

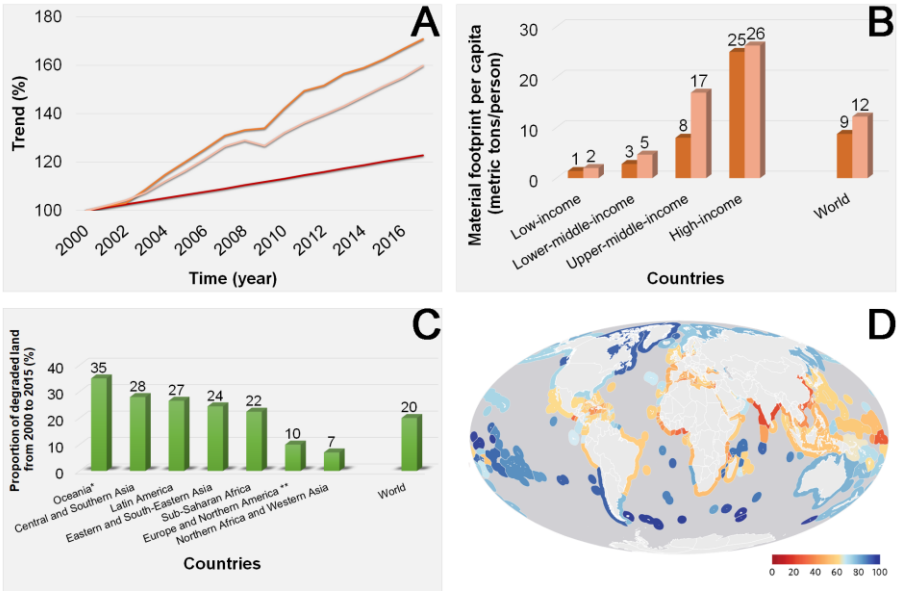

Figure 5. Overview of the global socio-economic and environmental trends. Data from the "Global Sustainable Development Report 2019"[49] of the United Nations . A) Population (red line), material footprint (orange line) and GDP growth index (pink line), 2000–2017 (baseline 2000=100). B) Material footprint per capita, 2000 (orange) and 2017 (light orange) (metric tons per person). In 2017 the material footprint per capita of high-income countries was about the 60 per cent higher than the upper-middle-income countries and more than 13 times the level of low-income countries. C) Proportion of degraded land from 2000 to 2015 (percentage); *Including Australia, New Zealand and Papua New Guinea but excluding the islands of Oceania. **Excluding Switzerland and the United States. D) Clean water scores for 220 coastal regions, assessed on a scale of 0 (very polluted, in red) to 100 (clean, in blue).

The circular economy model can have a positive impact both for developing countries (especially by addressing the waste management crisis) and the developed ones[50]. Advantages include cost saving, job creation and innovation[50]. According to an evaluation realised by the Ellen MacArthur Foundation, in the European Union up to 600 €billion can annually be saved by shifting toward a

circular economic model thanks to the associated reduction in the net resources spending[50]. In addition, it claims that the shift can improve resource productivity by up to 3% annually, and generate an annual net benefit of 1.8 €trillion[50]. Nonetheless, one of the major barriers for the transformation of the linear economic system into the circular one, consists in the skills gap in the workforce[49,50]. Investment in innovation, facilities and education is both important to promote the circular economic model and to increase in the employment in the short term. As for job opportunities, the renewable energy is considered worldwide a driving sector. In 2030 a slight decline in fossil fuel employment is expected to be compensated by a 28% increase in renewable energy jobs[51]. In this scenario, employment remains concentrated in the technologies used today, which are bioenergy, solar, hydropower and wind, with 9.1, 8.5, 3.8 and 2.2 million jobs respectively[51].

A concise insight on the impact of the circular economic model in Europe is proposed in Figure 6.

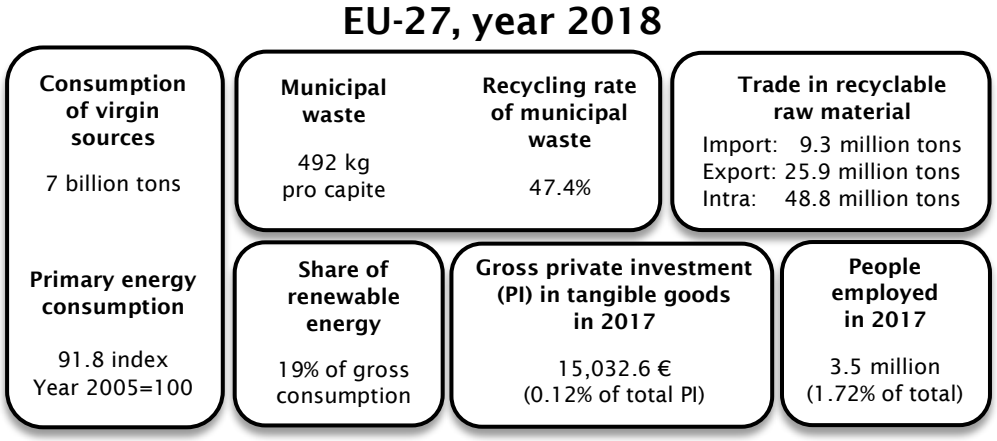

Figure 6. Overview of the impact of the Circular Economy (CE) in Europe (27 countries, without United Kingdom) in 2017-2018. Data from Eurostat 2020 (https://ec.europa.eu/eurostat/web/main/home). In 2018, 7 billion tons of virgin sources were consumed in Europe (3.4% compared to 2007). Total energy consumption decreased in 4% compared to 2007 (1,120 tons of oil equivalent, TOE, excluding supply to the processing sector of energy and to the energy industries themselves) and 19% of gross energy consumption was supplied by renewables. In 2017, 0.12% of total private investment in tangible goods was addressed to CE and 1.72% of the total European workers was employed in the CE sector. In the same year, the 11.2% of input material for domestic use was re-used (circularity rate index) and the greenhouse gas emission index was 81 (year 1990=100).

For all benefits reported (Table 2), circular economy has been demonstrated to effectively promote the reaching of several of the Sustainable Development Goals (SDG) set out in the document "Transforming our World: The 2030 Agenda for Sustainable Development" released in the 2015 by the United Nations[50].

Table 2. Circular economy: environmental, economic and social achievements.

Input	→ CIRCULAR ECONOMY →	Output
	Environmental sector	
- Reduction in virgin material and energy input - Virgin input are predominantly/to the extent possible renewable from productive ecosystems		- Reduction in waste and emissions - Reuse of resources in production-consumption systems - Renewables are CO_2 neutral fuels
	Economic sector	
- Reduced raw material and energy costs - The value in resources is used many times, not only once - Responsible and green market potential		- Value leaks are reduced - Reduced waste management costs - New markets are found for the value in resources
	Social sector	
- Investment in innovation and facilities		- New employment opportunities - Increased independence from fossil sources (located in confined areas)

Obviously, the feasibility of the circular economic system has to consider the diverse characteristics of each country (i.e. type of waste produced, facilities available) and both the Life Cycle Assessment (LCA) and the Life Cycle Costing Analysis (LCCA) are essential tools applied for comprehensive environmental and economic evaluations[38,47,48]. There will be no single bioeconomy, but rather as many bioeconomies as there are ecosystems and socioeconomic models[47]. Furthermore,

a deep understanding of the underlying science and engineering is required for a profitable transition into a circular economic system[47].

1.5.2. Pretreatments of the lignocellulosic biomass for lignin isolation

The first step in the biomass valorisation is its fractionation into lignin, cellulose and hemicellulose[2,8,52]. The Klason method, the Björkman' and the Brauns' processes, based on the acidic/enzymatic hydrolysis or the solvent-mediated precipitation of carbohydrates, are the main routes for the isolation of native lignin to be used for quantitative and structural studies[42]. On the other hand, the traditional routes for the pretreatment of the lignocellulosic biomass aim the complete delignification of the lignocellulose, focusing on the total recovery of cellulose to be used in the paper industry (pulping techniques) or the recovery of the fermentable polysaccharides for the production of biofuels[52]. The so called "technical lignins" obtained from these processes are by-products largely available on the market, mainly commercialized by MeadWestvaco Cooperation and Borregaard Industries[20,38]. The re-utilisation and valorisation of technical lignins represent an opportunity for modern biorefineries[7,52]. Nevertheless, they differ dramatically from the corresponding native lignin since, during the processing, multiple reactions such as lignin depolymerisation, condensation of lignin fragments and formation of new functional groups occur[2,7,20,46]. Thus, their non-uniform structure and the presence of several organic and inorganic impurities have limited their use in high-value-added applications[53]. The features of the main technical lignins are listed below and resumed in Table 3.

1.5.2.1. Kraft lignin

The kraft pulping is the prevalent chemical processing in the world, producing the 85% of the total lignin[53]. The deriving kraft lignin is mostly commercialised by MeadWestvaco and Metso Corporation (developer of the LignoBoost technology for lignin recovery)[2,52]. The process is based on the reaction of the wood chips with the

so called white liquor, an aqueous solution of sodium hydroxide and sodium sulphide, under high-temperatures conditions (155-175 °C)[46,52]. The strongly alkaline environment of the cooking process causes the breaking of the aromatic ether bonds in the lignin and the formation of soluble thio-lignin fragments (black liquor) which can be precipitated in a condensed form upon acidification[8,41]. The molecular weight of the recovered lignin is in the range of 1,500 and 5,000 grams per mole[53], showing a low amount in β-O-4 ether linkages and a sulphur content of 0.5-3.0 wt%[20]. In addition, a residual ash content of 1 to 5 wt% remains after the cooking and washing with diluted sulphuric acid steps[53]. Annually, only 100,000 tons out of 63×10^4 tons of kraft lignin produced are valorised to obtain carbon fibers, binders, ion-exchange resins, carriers for fertilizers and pesticides and low molecular weight aromatics[53].

1.5.2.2. Lignosulphonates

The lignosulphonate process occurs in the presence of sulphite (HSO_3^- and SO_3^{2-} ions) and usually either calcium or magnesium as counterions, in the pH range of 2 to 12[2,53]. Lignosulphonates are obtained after sulphonation, degradation and solubilisation steps of native lignin. They result as water-soluble anionic polyelectrolytes, which sulphonation degree is estimated in 0.4-0.5 per phenylpropanoid unit[20,53]. Lignosulphonates contain a large number of charged groups (phenolic hydroxyl, carboxylic and sulphur containing groups), which confer them unique colloidal properties[46]. They are thus suitable as stabilizers in colloidal suspensions, dispersing agents, detergents, glues, surfactants, adhesives and cement additives[53]. Annually, around 1 million tons of lignosulphonates are produced as dry solids and commercialised, especially by Borregaard LignoTech (about 500,000 metric tons per year)[53].

1.5.2.3. Soda lignin

Soda pulping consists in a sulphur-free process mainly used for the processing of annual crops (flax, straws, bagasse) and some hardwoods[53]. The cooking is carried out at 160-170 °C, in the presence of sodium hydroxide and, optionally, anthraquinone, which acts as enhancer of the reductive cleavage of ether bonds[20,53]. Soda lignin is highly condensed, shows a low β-O-4 ether bonds content and, in comparison to kraft lignin and lignosulphonates, its chemical composition is more similar to that of native lignin[8,40,53]. Since the high purity and biocompatibility of soda lignin, it is used in the synthesis of polymers and to produce phenolic resins and dispersants[53].

1.5.2.4. Organosolv lignin

In the organosolv process lignin is separated from polysaccharides via its solubilisation, using a cooking mixture of water and organic solvents, such as acetic acid, formic acid, ethanol and peroxiorganic acids[2,41,53]. Some of the organosolv processes have been commercially registered (FormicoFib, Alcell, Acetosolv, Organocell and ASAM) and scaled at the industrial level[2,53]. The process, usually used to dissolve biomass from corn, wheat, bamboo and pine wood[41], allows the recovery of high-pure sulphur-free lignin[2,40,53]. Unlike alkaline lignins and lignosulphonates, organosolv lignin has a low molecular weight (500-5,000 grams per mole) and, being hydrophobic, it is poorly water-soluble[40]. In addition to the applications found for alkaline lignin, organosolv lignin is very attractive as filler in the formulation of inks, varnishes and paints[53]. The main disadvantage of this process is the high cost of solvent recovery[2].

1.5.2.5. Ionic liquid lignin

The use of ionic liquids for the biomass processing is focused on the use of organic salts (e.g., 1-ethyl-3-methylimidazolium acetate, 1-butyl-3-methylimidazolium chloride) which remain as liquids at relatively low temperatures (their melting point

has to be lower than 100 °C)[41,53,54]. The process is quite promising but has not yet available on an industrial scale because of the high cost of ionic liquids[41,54]. In addition, the process highlighted different fractionation levels according to the starting material[53,54]. For instance, for bagasse samples in the presence of alkylbenzenesulfonate ionic liquid, the lignin dissolution is up to the 93%, instead for softwood and hardwood lignin, dissolution is only of the 26.1% and 34.9%, respectively[53]. At the end of each process, lignin is recovered by precipitation via addition of an antisolvent (water, acetonitrile, acetone, dichloromethane, or a mixture of these), and the ionic liquid can be recycled[54]. The properties of ionic liquid lignin are comparable to organosolv lignin and its field of application are similar to soda and organosolv lignins[53].

Table 3. Chemical composition of technical lignins. Main data were obtained from[8,53].

Parameter	KL*	LS*	SL*	OL*	ILL*
Scale	Industrial	Industrial	Industrial	Industrial/ Pilot	Demo
Molecular weight, M_w (gram/mol)	1,500-5,000 (up to 25,000)	1,000-50,000 (up to 150,000)	1,000-3,000 (up to 15,000)	500-5,000	≈2,000
Polydispersity	2.5-3.5	4.2-7.0	2.5-3.5	1.5	-
Sulphur content (%)	1.0-3.0	3.5-8.0	0	0	1.5
Carbohydrates (%)	1.0-2.3	-	1.5-3.0	1.0-3.0	0.1
Ash content (%)	0.5-3.0	4.0-8.0	0.7-2.3	1.7	0.6-2.0

* KL = Kraft Lignin, LS = Lignosulfonates, SL = Soda Lignin, OS = Organosolv Lignin, ILL = Ionic Liquid Lignin

1.5.3. Biological approaches for lignin valorisation

The depolymerisation of lignin obtained from lignocellulosic pretreament is a necessary step for its valorisation (Figure 4). Beside thermochemical depolymerising

approaches, the biological ones, involving microorganisms or biocatalysts, have been intensively studied[20,22,26]. In fact, they can overcome the high heterogeneity of lignin better than traditional chemical strategies[4,42]. The main advantage in adopting biological routes consists in the lignin fragmentation through high-selective cleavages under reproducible and mild reaction conditions[18,26]. Therefore, mixtures enriched in the target product are obtained through a controlled, quite inexpensive and safe process (i.e. aqueous reaction medium, moderate temperatures, absence in toxic chemicals, management of not hazardous waste)[26]. On the other hand, thermochemical methods generally show higher depolymerisation yields in shorter times[18,42]. In this view, metabolic engineering, protein engineering and hybrid processes which combine both chemical and biological steps, are valid solutions to increase in the efficiency of biological approaches[20,55].

1.5.3.1. Microorganisms: fungi and bacteria

In nature, lignin biodegradation is a process involving different fungi and bacteria (paragraph 1.3). In particular, fungi belonging to the white-rot basidiomycetes play e key role in lignin depolymerisation while several ligninolytic bacteria have shown to mineralise aromatics from lignin through specific “upper” and “lower” funnelling pathways[4,26].

As for white-rot fungi, difficulties related to their cultivation and the complexity of their biosynthetic pathways have hampered their biotechnological use[20]. Nevertheless, Solid State Fermentation (SSF) processes have been investigated as environmentally and economically friendly alternative to the existing pretreatments of the lignocellulosic biomass[22,37]. This promising approach, usually followed by a bacterial anaerobic digestion step for the production of biogas, is limited by the long incubation time required[22]. For instance, using yard trimmings (which represent a major part in the municipal lignocellulosic waste), a delignification yield of 14.8-20.2% was obtained after 30 days of treatment with *Ceriporiopsis subvermispora*, resulting in the production of 34.9-44.6 L kg^{-1} methane from the combined system[37].

On the other hand, bacteria are involved both in the biotechnological degradation of lignin and in its valorisation. For instance, *Novosphingobium sp.* B-7 was demonstrated to secrete extracellular manganese peroxidases and laccases which enable it to grow using kraft lignin as the sole carbon source[56]. After seven days of incubation, a 34.7% of lignin degradation occurred. The result is comparable to the 37%, 33% and 30% lignin degradation yields reported for the bacteria *Paenibacillus sp.*, *Aneurinibacillus aneurinilyticus* and *Bacillus sp.*, respectively[56]. Several low-molecular aromatic products were identified, including 3,5-dimethylbenzaldehyde, *p*-hydroxybenzoic acid and vanillate[56].

In addition, the investigation of the funnelling pathways in ligninolytic bacteria revealed their potential in the production of several value-added compounds from aromatics deriving from lignin degradation[18,22]. As general mechanism, the "upper pathways" convert aromatics into few central intermediates, which are catechol and protocatechuate for aerobic microorganisms, and resorcinol and phloroglucinol for the anaerobic ones[4,18]. The "lower pathways" catalyse the cleavage of the aromatic ring of the central intermediates in order to provide carbon for the central metabolism process (e.g., citric acid cycle) for cell growth, self-maintenance and eventually bioproducts accumulation (i.e. fatty acids and polyhydroxyalkanoates (PHAs) in oleaginous species)[4,18]. To date, bacteria (e.g., belonging to the *Pseudomonas* and the *Rhodococcus* genera) have been extensively studied both for the accumulation of microbial lipids suitable for biodiesel production and PHAs useful for the synthesis of biodegradable bioplastic, but also for the production of vanillin and dicarboxylic acids (muconate, lactate, pyruvate)[18,20,57].

For instance, *R. opacus* NRRL B-3311 was reported to accumulate 32 mg/L of lipids after 72h of growth on a thermochemically pretreated lignin[22], and 1.83 g/L lipids were reported for *R. opacus* PD630 fed-batch fermented in the presence of chemo-enzymatically pretreated lignin[20].

The PHAs are secondary metabolites produced by specialized microorganism under stress conditions[18]. As in the previous case, the yields of production are quite low: *P. putida* growing on lignin hydrolysate produces 250 mg/L of PHAs[20], while for

Cupriavidus basilensis B-8 growing on kraft lignin the PHAs production is of 128 mg/L under batch condition, with an improvement up to 319.4 mg/L using a fed-batch fermentation[18].

Among the valuable chemicals constituting a platform for synthetic industry, the bioproduction of vanillin and *cis,cis*-muconic acid has been mainly investigated[18,20,57]. Overall, results reported for different microorganisms (i.e. *Bacillus sp.*, *Amycolatopsis sp.*, *Pediococcus sp.*) growing on different lignin feedstock show that vanillin accumulation is lower than 0.8 mg/L, with remarkable exceptions for bacteria growing on lignin model compounds (i.e. *Streptomyces setonii* produces 6.4 g/L of vanillin from ferulate)[18,20,22]. Notably, the deletion of the gene encoding for vanillin dehydrogenase in *R. jostii* RHA1 allowed the accumulation of vanillin up to 96 mg/L in 144 hours, using as substrate a medium containing 2.5% wheat straw lignin and supplemented with 0.5% glucose[18,57]. Nonetheless, these results are far from the reported yields of 11.64-13.39% lignin conversion into vanillin, using chemical depolymerising processes[22].

The production of muconic acid from lignin via chemical routes instead, accounts for the 4% in yield, and thus, contrary to vanillin, it is not a lignin-deriving product commercialised yet[22]. To date, noteworthy results have been obtained using bacteria as producers of the higher-value *cis,cis* isomer of muconate, which is exploited in the synthetic production of nylon and plastic materials. These are the production of 64.2 g/L *cis,cis*-muconate from catechol, 50 g/L from *p*-coumaric acid or even, 13 g/L *cis,cis*-muconate from a lignin hydrolysate by using three different engineered strains of *P. putida*, respectively[20]. The mutant *Amycolatopsis* sp. MA-2 instead, was reported to accumulate 85 g/L *cis,cis*-muconate from catechol and 1.8 g/L *cis,cis*-muconate from a hydrothermally pretreated softwood lignin[22].

Beside the great opportunity in lignin valorisation represented by the exploitation of microbial metabolisms, the main drawbacks consist in the low product titers, the low capability of microorganisms in using water-insoluble fraction of lignin and their low tolerance to inhibitor compounds potentially deriving from lignin pretreatments (Table 4)[4,20,57].

Table 4. Comparison of the different biological approaches for lignin valorisation.

Biological approach	***Advantages***	***Disadvantages***	***Optimisation routes***
Degrading fungi	• Environmentally friendly pretreatment of the lignocellulosic biomass	• Time-consuming • Low efficiency • Complex genome manipulation and growing conditions	• Environmental screening for metabolic diversity • Metabolic engineering
Degrading bacteria	• Selective lignin degradation • Funnelling pathways for lignin valorisation	• Moderate efficiency • Low tolerance to inhibitors	
Enzymatic catalysis	• High-selective lignin degradation • Combination of enzymes from different sources • Enzyme immobilisation	• Cofactor regeneration • Production costs of enzyme	• Chemo-enzymatic treatment • Protein engineering
Whole-cell catalysis	• Cofactors regeneration • No purification of enzymes • Design of multi-enzymatic *de novo* pathways	• Substrate permeation across membrane	• Synthetic biology

In this view, studies on metabolic engineering and screening of the environmentally biological diversity represent an efficient strategy to identify the ideal aromatics tolerant high-accumulating domesticated microorganism to be used in industrial bioreactors[4,22].

1.5.3.2. Biocatalysts: ligninolytic enzymes and whole-cell systems

The valorisation of lignin via ligninolytic enzymes and whole-cell systems (which consist in "microbial factories" specifically designed using the advances in synthetic

biology and metabolic engineering[58]) aims to mimic the synergistic biocatalytic activities observed in nature during lignin biodegradation[46]. In this view, multiple reaction steps are simultaneously performed in one reactor by enzymatic or by engineered whole-cell catalysts[46]. To date, isolated enzymes and whole cells are both effective biocatalytic systems industrially used, even in biorefineries (i.e. Accellerase® DUET and Cellic® CTec2 commercialised by Genencor® and Novozymes, respectively) and paper pulp industry (i.e. Resinase® commercialised by Novo Nordisk) to enhance cellulose and glycerides depolymerisation[59,60].

Overall, the main advantage of the enzymatic catalysis consists in its high regio-, chemo-, diastereo- and enantio-selectivity[26,58–60]. Although pure enzymes can work only under optimal pH and temperature conditions, they can also tolerate co-solvents used to solubilise low-water soluble substrates[6,59]. In addition, they allow the catalysis of specific reactions, using simple equipment and procedures[59,60]. Compared to whole cells, isolated enzymes used in one-pot reactions ensure no side-reactions and an increased in efficiency, since substrates have not to be transported across membranes[58,59]. Nonetheless, whole cell systems are usually preferred either when the isolation and purification of a certain enzyme is expensive or time consuming, and in multi-enzymatic processes (especially if the enzymes involved require co-factors recycling)[58,59]. Furthermore, the intracellular environment can protect low-stable enzymes during catalysis[59].

In order to enhance lignin depolymerisation, several radical- and no radical-dependent enzymes have been biochemically characterised and used alone or in multi-enzymatic reactions. For instance, the extracellular manganese superoxide dismutases MnSOD-1 and MnSOD-2 from *Sphingobacterium sp*. T2 were the only dismutases identified as microbial lignin-oxidizing enzyme[61]. The enzymes were recombinant expressed in *Escherichia coli*, characterised and individually used for the depolymerisation of wheat straw Organosolv and Kraft lignin samples (in the presence of KO_2 as superoxide anion donor) resulting in the production of a number of aromatics (i.e. vanillin, vanillic acid, 4-hydroxybenzoic acid, 2-methoxyhydroquinone, guaiacol)[61]. In this case, genome sequencing and

comparative alignments were fundamental tools for the expansion of the range of bacterial enzymes capable of lignin oxidation.

Structural characterisation and mutagenesis are other important tools to enhance enzymatic activities, as demonstrated for the bacterial dye-decolorizing peroxidase DypB from *R. jostii* RHA1 which catalytic site was successfully engineered (site-directed mutagenesis) in order to improve its activity toward manganese (the apparent k_{cat} and k_{cat}/K_m values of the enzyme for Mn^{2+} increased by 80- and 15-fold, respectively)[62]. The DypB variant N246A was then demonstrated to catalyse in one hour the manganese mediated depolymerisation of hard wood kraft lignin and of its lower molecular weight solvent-extracted fractions[62]. Syringaldehyde and 2,6-dimethoxybenzoquinone were the major degradation products identified, obtained with yield of 18 and 21 μg/mg lignin, respectively[62].

As for the multi-enzymatic approach, five recombinant, no radical-dependent enzymes (Lig system) were demonstrated to catalyse in less than two hours the complete one-pot conversion of the lignin model dimer guaiacylglycerol-β-guaiacyl ether (GGE) into the final products 3-hydroxy-1-(4-hydroxy-3-methoxyphenyl)propan-1-one and guaiacol[25]. Therefore the system, both providing the cleavage of the β-O-4 linkage (which is the most abundant in lignin) and the regeneration of the NAD^+ cofactor, represents a valuable, inexpensive enzymatic cascade for lignin valorisation[25]. In addition, lignin depolymerisation was achieved by a multi-step biocatalytic approach involving a first oxidative step catalysed by a laccase-mediator system followed by the selective cleavage of the β-O-4 linkages catalysed by β-etherases[63]. Also in this case, cofactor regeneration was essential to provide the recycling of glutathione; the overall process yield is of 12.5-16% of OrganoCat lignin depolymerisation and the production of 1% coniferylaldehyde[63].

Among the bio-solutions to improve lignin depolymerisation, chemo-enzymatic treatments combine relative-mild reaction conditions with the efficiency of the chemical approach. For example, up to 45% depolymerisation yields were reported for a combined system consisting in a mediator-laccase oxidative step performed in a buffered solution at pH 5.0, followed by a formic acid-induced lignin

depolymerisation step[64]. The immobilisation of laccase on superparamagnetic nanoparticles allows the easy separation and reuse of the biocatalysts after treatment, while the use of the Response Surface Methodology (RSM) improved the optimisation of the incubation conditions (time of incubation, amount of mediator)[64].

Whole cell approach instead has been mainly used for lignin valorisation. For example, 0.3 g/L vanillin and 0.1 g/L vanillyl alcohol were obtained from eugenol through a two-step process. In the first step, 5 g/L ferulic acid are produced from eugenol by a recombinant XL1-Blue strain of *E. coli* expressing the genes encoding for feruloyl-CoA synthase and enoyl-CoA hydratase/aldolase form *Pseudomonas sp.* strain HR199 while, in the second step, vanillin and vanillyl alcohol are accumulated from ferulate[20]. Furthermore, up to 14.7 g/L ferulic acid were produced from eugenol within 30 h in a 30-liter fermenter (93.3% molar yield) by using a XL1-Blue strain of *E. coli* expressing coniferyl alcohol/aldehyde dehydrogenase from *Pseudomonas sp.* strain HR199 and a vanillyl alcohol oxidase from *Penicillium simplicissimum* CBS 170.90[20].

In addition, the DH1 strain of *E. coli* was successfully engineered with the *cis,cis*-muconate anabolic pathway, by co-transformation and co-expression of genes from different natural producers (e.g., belonging to the genera *Klebsiella, Sphingobium, Pseudomonas*)[65]. The engineered strain produced up to 314 mg/L *cis,cis*-muconate from vanillin (deriving from a thermochemically pretreated Kraft lignin), corresponding to 0.69 $g_{ccMA}/g_{vanillin}$[65].

Enzymes and whole-cell systems are thus promising approaches for the biotechnological valorisation of lignin (Table 4)[20,46]. Catalysts from different sources can be combined to reach synergistic results and, in some cases, in order to reduce costs they can even be immobilised on specific supports and be re-used[20,58,59]. Contrary to the microbial approach (paragraph 1.5.3.1) catalysts show higher delignification rate, a wider tolerance to temperature and pH ranges and they do not consume sugar nor require nutrient supplementation[37,58,59]. Furthermore,

molecular and synthetic biology provide powerful tools (i.e. directed evolution, DNA shuffling, random mutagenesis) for even improve natural enzymatic or metabolic features (i.e. enzymatic thermostability or activity, fatty acid composition of the cellular membrane) to biotechnological purposes[59]. In this view, the deep in the investigation of the microbial metabolic diversity (e.g., extremophiles) is fundamental and it will allow to design specific biocatalysts, such as *de novo* pathways for whole cell systems[58,59].

2. Aim of the work

Lignin is, beside cellulose and hemicellulose, one of the three components of the lignocellulosic biomass. It is, after cellulose, the second most abundant substance on Earth and, since its peculiar chemical composition arising from *para*-hydroxyphenyl, guaiacyl and syringyl units, it represents the first renewable source of aromatics. Nevertheless, the obtainment of value-added aromatic molecules through its degradation is mainly hindered by the high stability and recalcitrance of its structure. Therefore, in the past this biopolymer was underutilised and it was mainly burned for power generation, since its calorific power of 26-28 MJ/ton dry lignin is comparable to that of some fossil coals.

The current and traditional linear material and energy flow model, which is mainly based on the exploitation of virgin sources (such as the fossil ones) according to the principle of "extract, produce, use, dump" is unsustainable and therefore it has to be integrated with the strategic and eco-friendly development model described by the bioeconomy and the circular economy paradigms.

In this scenario, the valorisation of lignin is a main biotechnological challenge which aims to perform its degradation by biological approaches in order to obtain value-added aromatics to be used as building blocks for synthetic pathways.

This Ph.D. project is aimed to explore different biochemical strategies for lignin valorisation, focusing on the use of different enzymes as high-selective and efficient biocatalysts able to perform either single-catalysed reactions or to act synergistically in multi-enzymatic reactions.

The enzymatic tool-box containing 26 ligninolytic and auxiliary-ligninolytic activities, which is available at the host laboratory "The Protein Factory 2.0", will be added of two bacterial enzymes (i.e. the N246A variant of the dye-decolorizing peroxidase DypB from *Rhodococcus jostii* RHA1 and the superoxide dismutase MnSOD-1 from *Sphingobium sp.* T2) recently reported to be involved in lignin degradation. In order to investigate their potential and versatility as biocatalysts, these two enzymes will be expressed in recombinant form, isolated and biochemically characterised.

Moreover, the project is aimed to elucidate the composition of degradation products, both in qualitative and quantitative terms, from different technical lignin samples enzymatically treated. Actually, enzymes can perform selective reactions resulting in the driven production of specific products of interest. Accordingly, a rapid miniaturised screening method for the identification of the optimal lignin/enzyme incubation conditions will be used in the design of the multi-variant experiments. In order to overcome the main bottleneck in the scaled-up application of biocatalysis for lignin degradation, the degradation yields will be investigated through a solvent-based fractionation of the starting material.

Finally, since vanillin is the only globally commercialised aromatic obtained from lignin degradation, a synthetic multi-enzymatic pathway for its valorisation into *cis,cis*-muconic acid, the precursor in the synthesis of nylon and of a large number of plastic materials, will be investigated. The one-pot bioconversion of vanillin will be set-up in the presence of different enzymatic activities working synergistically.

3. Results

Applied Microbiology and Biotechnology
https://doi.org/10.1007/s00253-018-9409-3

BIOTECHNOLOGICALLY RELEVANT ENZYMES AND PROTEINS

Characterization and use of a bacterial lignin peroxidase with an improved manganese-oxidative activity

Elisa Vignali[1] · Fabio Tonin[1,2] · Loredano Pollegioni[1] · Elena Rosini[1]

Received: 24 July 2018 / Revised: 18 September 2018 / Accepted: 19 September 2018

Abstract
Peroxidases are well-known biocatalysts produced by all organisms, especially microorganisms, and used in a number of biotechnological applications. The enzyme DypB from the lignin-degrading bacterium *Rhodococcus jostii* was recently shown to degrade solvent-obtained fractions of a Kraft lignin. In order to promote the practical use, the N246A variant of DypB, named Rh_DypB, was overexpressed in *E. coli* using a designed synthetic gene: by employing optimized conditions, the enzyme was fully produced as folded holoenzyme, thus avoiding the need for a further time-consuming and expensive reconstitution step. By a single chromatographic purification step, > 100 mg enzyme/L fermentation broth with a > 90% purity was produced. Rh_DypB shows a classical peroxidase activity which is significantly increased by adding Mn^{2+} ions: kinetic parameters for H_2O_2, Mn^{2+}, ABTS, and 2,6-DMP were determined. The recombinant enzyme shows a good thermostability (melting temperature of 63–65 °C), is stable at pH 6–7, and maintains a large part of the starting activity following incubation for 24 h at 25–37 °C. Rh_DypB activity is not affected by 1 M NaCl, 10% DMSO, and 5% Tween-80, i.e., compounds used for dye decolorization or lignin-solubilization processes. The enzyme shows broad dye-decolorization activity, especially in the presence of Mn^{2+}, oxidizes various aromatic monomers from lignin, and cleaves the guaiacylglycerol-β-guaiacyl ether (GGE), i.e., the Cα-Cβ bond of the dimeric lignin model molecule of β-O-4 linkages. Under optimized conditions, 2 mM GGE was fully cleaved by recombinant Rh_DypB, generating guaiacol in only 10 min, at a rate of 12.5 μmol/min mg enzyme.

Keywords Lignin peroxidase · Dye-decolorizing peroxidase · Ligninolytic enzymes · Lignin valorization · Heme incorporation

Introduction

Lignin is a main pillar of future biorefining processes since it represents a potentially valuable, renewable source of aromatic chemicals. Lignin is an aromatic polymer showing a structural complexity derived from radical polymerization of three monomers (guaiacyl, syringyl, and p-hydroxyphenyl units) linked by carbon-carbon and carbon-oxygen bonds. The main bottleneck in utilizing lignin is its intrinsic recalcitrance to breakdown (Boerjan et al. 2003).

Despite 30 years of investigating fungal enzymes active on lignin, these studies did not generate a feasible process for lignin degradation (Tien and Kirk 1983; Glenn and Gold 1985; Eggert et al. 1997; Leonowicz et al. 1999; Fernandez-Fueyo et al. 2014). Laccases and peroxidases are the most widely used enzymes. Here, the fungus *Phanerochaete chrysosporium* produces both a heme-dependent manganese peroxidase (MnP) and a heme-containing lignin peroxidase (LiP) (Glenn and Gold 1985; Glenn et al. 1986; Miki et al. 1986). *P. chrysosporium* is of main biotechnological relevance for its ability to cleave lignin model molecules; it is unique in being able to catalyze the oxidation of Mn^{2+} to Mn^{3+}, which can then oxidize a range of compounds comprising lignin model compounds. For recent reviews concerning the enzymatic processes active on the main lignin linkages, see Wong (2009), Pollegioni et al. (2015), Gupta et al. (2016), de Gonzalo et al. (2016), and Longe et al. (2016).

In recent years, bacteria belonging to three classes (actinomycetes, α-proteobacteria, and γ-proteobacteria) have attracted attention owing to their ability to metabolize lignin by employing both general oxidative activities (peroxidases and laccases) and enzymes active on specific bonds (Sánchez

✉ Elena Rosini
elena.rosini@uninsubria.it

[1] Department of Biotechnology and Life Sciences, University of Insubria, via Dunant 3, 21100 Varese, Italy

[2] Present address: Department of Biotechnology, Delft University of Technology, Delft, The Netherlands

Published online: 09 October 2018

2009; Bugg et al. 2011; Bugg and Rahmanpour 2015; Pollegioni et al. 2015).

Concerning lignin-degrading bacteria, the first bacterial lignin peroxidase, i.e., the extracellular DypB, was recently characterized from *Rhodococcus jostii* RHA1 (Ahmad et al. 2011). This peroxidase shows an improved activity in presence of Mn^{2+}, and is able to break down wheat straw lignocellulose and to catalyze the cleavage of the Cα-Cβ bond of β-aryl ether of lignin model molecules. Dyp (dye-decolorizing peroxidase) enzymes belong to the chlorite dismutase superfamily: the C-terminal domain hosts the heme and a histidine residue acts as the fifth ligand to the iron of heme on the proximal side. Two conserved aspartate and arginine residues (namely, D153 and R244, numbering referring to the *R. jostii* RHA1 enzyme) are located in the distal heme environment, and N246 in the distal heme pocket interacts with the distal solvent ligand (Sugano et al. 2007). D153 and N246 seem involved in the modulation of the reactivity of the intermediate compound I during catalysis (Singh et al. 2012). Substitution of N246 with an alanine significantly increased the k_{cat}, the k_{cat}/K_m ratio for Mn^{2+}, and the corresponding K_m value because the first coordination sphere was composed of solvent (Singh et al. 2013). This DypB variant acted on solvent-fractionated fractions of hardwood kraft lignin at different average molecular weights, solubilizing various compounds that were identified by HPLC and GC-MS analyses, among them 2,6-dimethoxybenzoquinone and 4-hydroxy-3,5-dimethylbenzaldehyde (syringaldehyde) (Singh et al. 2013). For a review, see de Gonzalo et al. (2016).

These results highlighted the potential of DypB as biocatalyst. Accordingly, in this work, we focused on the setup of an efficient recombinant production system of N246A DypB (named Rh_DypB) that allowed, for the first time, to express the enzyme in the full holoenzyme, active form. The main folding and chemical-physical properties of the purified recombinant Rh_DypB were investigated, as was the effect on activity and stability of compounds frequently used in lignin depolymerization. In particular, we focused on Rh_DypB kinetic properties on hydrogen peroxide, manganese, and two additional substrates and on the dye-decolorizing activity. Rh_DypB was employed on various monomeric and a dimeric lignin model compounds.

Materials and methods

Materials

2,2-Azino-bis(3-ethylbenzothiazoline-6-sulfonic acid) (ABTS), 2,6-dimethoxybenzyl alcohol (2,6-DMP), phenyl alcohols, remazol brilliant blue R (RBBR), azure B (AB), and reactive black (RB5) were bought from Sigma-Aldrich (Milano, Italy). Guaiacylglycerol-β-guaiacyl ether (GGE) was purchased from Zentek s.r.l. (Milano, Italy).

Design and cloning of cDNA encoding for Rh_DypB enzyme

The synthetic gene encoding the N246A variant of DypB from *R. jostii* RHA1 (Rh_DypB) (Singh et al. 2013) was designed by back translation of the protein sequence deposited in the GeneBank database (GI: 442570838). The gene (accession no. MH292860) was added of sequences corresponding to *NdeI* (CATATG) and *XhoI* (CTCGAG) restriction sites and the codon usage was optimized for expression in *E. coli*. *Rh_DypB* cDNA was inserted in the pET24b(+) vector (Merck Millipore, Vimodrone, Italy) using the *NdeI* and *XhoI* sites, to give a 6.5-kb construct (pET24-Rh_DypB). During the subcloning procedure, six codons (encoding for six histidines) were added to the 3′-end of the *Rh_DypB* gene.

Rh_DypB expression and purification

BL21(DE3) *E. coli* cells (Merck Millipore) transformed with pET24-Rh_DypB expression plasmid were grown under aerobic conditions at 37 °C in Terrific Broth medium (TB, 24 g/L yeast extract, 12 g/L bacto-tryptone, 8 mL/L glycerol, 9.4 g/L K_2HPO_4, 2.2 g/L KH_2PO_4). At an OD_{600nm}~1.0, Rh_DypB expression was induced by adding 0.25 mM isopropyl β-D-1-thiogalactopyranoside (IPTG) and 0.25 g/L hemin chloride (stock solution 12.5 g/L dissolved in 10 mM NaOH). The cells were incubated at 20 °C for 18 h and for another 3 h without shaking (microaerobic cultivation phase) to promote heme incorporation. Cells were lysed by sonication; the crude extract was centrifuged at 39000*g* for 1 h at 4 °C.

The enzyme was purified using a HiTrap chelating affinity column (GE Healthcare, Milano, Italy) previously loaded with 100 mM $NiCl_2$ and equilibrated with 20 mM MOPS buffer, pH 7.5, with addition of 80 mM NaCl and 5% (*v*/*v*) glycerol. Rh_DypB was eluted with the same buffer with addition of 500 mM imidazole; the fractions were equilibrated with 20 mM MOPS buffer (pH 7.5), 80 mM NaCl, and 5% (*v*/*v*) glycerol by a gel-permeation chromatography (PD10 column, GE Healthcare). The amount of Rh_DypB enzyme was determined by using the absorbance intensity at 280 nm and a molar extinction coefficient of 120 mM^{-1} cm^{-1} (Singh et al. 2012).

Activity and kinetic measurements

The reference peroxidase activity assay was performed on 0.1 mM H_2O_2 and 1 mM ABTS, in 50 mM sodium malonate buffer, pH 5.0, to which 2 mM $MnCl_2$ was added. One unit of activity corresponds to the amount of enzyme that consumed 1 μmol substrate in 1 min at 25 °C, pH 5.0. The apparent

kinetic parameters were determined spectrophotometrically at 25 °C on $MnCl_2$ (2–10,000 μM, $\varepsilon_{270nm} = 11{,}590\ M^{-1}\ cm^{-1}$), ABTS (1–60,000 μM, $\varepsilon_{420nm} = 36{,}000\ M^{-1}\ cm^{-1}$) or 2,6-DMP (0.01–30,000 μM, $\varepsilon_{468nm} = 49{,}600\ M^{-1}\ cm^{-1}$), in 50 mM sodium malonate buffer, pH 5.0, to which H_2O_2 (0.3 or 1.5 mM) was added. The apparent kinetic parameters were also evaluated for H_2O_2 in 50 mM sodium malonate buffer, pH 5.0, in presence of 50 mM ABTS. The kinetic results were analyzed using a classical Michaelis-Menten equation or modified to account for a substrate inhibition effect (Cleland 1983; Rosini et al. 2012).

The pH dependence of the peroxidase activity on 5 mM 2,6-DMP was determined using a multicomponent buffer (Harris et al. 2001): 15 mM Tris, 15 mM phosphoric acid, 15 mM sodium carbonate, and 250 mM potassium chloride, pH 3.0–9.0. Furthermore, the pH dependence of the enzymatic activity was determined on the same substrate after adding 0.1 mM H_2O_2 and 2 mM $MnCl_2$ in 50 mM sodium malonate buffer in the pH range 4.0–7.0.

To investigate the enzyme stability, the residual activity was assayed after the enzyme (5 μM) was incubated for 24 h at different pH values in the multicomponent buffer, 25 °C. The dependence on temperature of the peroxidase activity was assessed by measuring ABTS oxidation (with or without 2 mM $MnCl_2$) in the 15–85 °C temperature range. The effect of dimethyl sulfoxide (DMSO), sodium chloride, and Tween-80 concentration on Rh_DypB activity on 1 mM ABTS was determined using the standard peroxidase activity assay.

Spectral measurements

A Jasco FP-750 instrument (Jasco, Cremella, Italy) was used for all fluorescence measurements. Spectra were recorded from 300 to 400 nm using an excitation wavelength of 280 nm and from 580 to 680 nm with excitation at 400 nm for tryptophan and heme fluorescence emission, respectively; bandwidths of 5 and 10 nm were set for excitation and emission, respectively.

Circular dichroism (CD) spectra were recorded on a J-810 Jasco spectropolarimeter (Caldinelli et al. 2005). The secondary structure was estimated by using K2D3 software (Louis-Jeune et al. 2012).

All spectral experiments were performed in 20 mM MOPS, 80 mM NaCl buffer, pH 7.5.

The temperature-induced loss of secondary and tertiary structure was monitored by following the tryptophan fluorescence at 340 nm and the CD signal at 220 nm. Both the fluorimeter and the spectropolarimeter were equipped with a software-driven Peltier-based temperature controller (temperature gradient of 0.5 °C/min) (Caldinelli et al. 2009).

Dye decolorization

The dyes remazol brilliant blue R (RBBR), azure B (AB), and reactive black 5 (RB5) were used to evaluate the decolorization capability of Rh_DypB. The reaction mixture contained 0.1 mM dye and 0.1 mM H_2O_2, to which 2.5 μM Rh_DypB was added (1 mL final volume). Either 50 mM sodium acetate, pH 4.0, or 50 mM sodium malonate, pH 6.0, to which 2 mM $MnCl_2$ was added, was used as buffer. After overnight incubation at 30 °C on a rotary wheel, the absorbance spectra (from 400 to 800 nm) were recorded on a Jasco V-580 spectrophotometer. The control reactions were performed under the same conditions without adding the enzyme.

The dye decolorization was expressed as a percentage, as follows:

$D = [(Abs_{t0} - Abs_{t24})]/Abs_{t0} \times 100$, where D is the decolorization level (%), and Abs_{t0} and Abs_{t24} are the absorbance values before and after treatment, recorded at 595 nm, 648 nm, and 597 nm for RBBR, AB, and RB5 dyes, respectively.

Screening procedure

Different benzyl alcohols were dissolved in 50 mM sodium malonate buffer, pH 6.0, at 2 mM final concentration. Reaction mixtures with addition of 2 mM $MnCl_2$, 0.1 mM H_2O_2, and Rh_DypB (0.25 U, 0.5 μM) were incubated at 25 °C on a rotatory wheel (final volume of 1 mL). For colorimetric screening, 20 μL of sample was withdrawn at different times, with addition of 30 μL 100 mM HCl, and transferred in a 96-well plate (Tonin et al. 2017). Fifty microliters of 1 mM 2,4-dinitrophenylhydrazine (2,4-DNP) dissolved in 100 mM HCl was added in each well. One hundred microliters of 1 N NaOH was added after incubation at 25 °C for 5 min and the absorbance at 450 nm was recorded using a microtiter plate reader (Sunrise, Tecan, Männedorf, Switzerland). The absorbance values determined for control samples (in the absence of substrate or enzyme) were subtracted from all samples. Values are reported as mean ± standard deviation ($n = 3$).

GGE bioconversion

A 10 mM GGE solution was prepared by dissolving 32 mg of substrate in 100 μL DMSO and bringing to volume (10 mL) with water. The assay mixture containing 50 mM sodium malonate buffer, pH 6.0, 2 mM GGE, 2 mM $MnCl_2$, 1 mM H_2O_2, and 0.25 U Rh_DypB (0.5 μM) was incubated on a rotatory wheel at 25 °C (2.5 mL final volume). At fixed times, 200 μL of the reaction mixture was withdrawn, added of 400 μL of a 0.1% (*v*/*v*) TFA aqueous solution, centrifuged for 1 min at 13,000 rpm: 20 μL of the supernatant was analyzed by HPLC analyses using a Luna 5 μm C18(2) column (Phenomenex, 150/4.6 mm), detection set at 310 nm. Elution

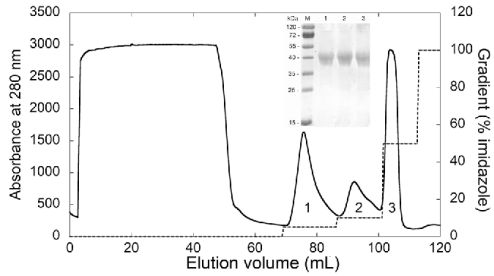

Fig. 1 Step gradient elution profile during the purification of recombinant Rh_DypB on a HiTrap chelating column. Insert: SDS-PAGE analysis of fractions eluted at different imidazole concentration (——): 1, 2, 3 = 25, 50, 250 mM imidazole. Gel was stained with Coomassie blue. (M) Molecular weight marker proteins

gradient: 0–5 min, 20 to 30% MeOH/H_2O; 5–12 min, 30 to 50% MeOH/H_2O; 12–25 min, 50 to 80% MeOH/H_2O. The retention times (t_R) of GGE and guaiacol were 18.8 min and 17.8 min, respectively.

Results

Expression and purification of Rh_DypB

Recombinant N246A DypB (named Rh_DypB) from *R. jostii* was expressed in the host *E. coli* BL21(DE3) strain transformed with the pET24-Rh_DypB plasmid, grown at 37 °C in TB medium, adding IPTG and hemin chloride at an OD_{600nm}~1.0, and collecting cells after further 18 h at 20 °C under shaking (aerobic conditions). An incomplete heme incorporation and a low enzymatic activity were observed under these expression conditions (see below). Metal ion physiology in *E. coli* is dependent on oxygen availability; an increased intracellular concentration and solubility of copper and iron was observed under anaerobic growth conditions (Partridge et al. 2007; Durão et al. 2008; Tonin et al. 2016). Therefore, to promote heme incorporation, *E. coli* cells were grown for another 3 h under static conditions (microaerobic conditions) (Tonin et al. 2016). The recombinant His-tagged Rh_DypB was purified in a single step by HiTrap chelating affinity chromatography. Recombinant Rh_DypB was isolated as a single band at ~ 40 kDa; ~ 100 mg of purified Rh_DypB/L fermentation broth was obtained, with a > 90% purity as judged by SDS-PAGE analysis (Fig. 1). The Rh_DypB fractions eluted from metal-chelating chromatography at 25, 50, and 250 mM imidazole concentration showed a similar degree of purity and different Rz values (Reinheitzahl value, defined by the ratio between the Soret absorbance band and the absorbance at 280 nm, see Fig. 2b), suggesting a different degree of heme incorporation that affects the correct folding of the recombinant Rh_DypB. The higher Rz value was obtained for the recombinant Rh_DypB eluted at 250 mM imidazole (~ 2.4): this fraction was used for subsequent biochemical characterization.

By changing the aeration from shaking (aerobic cultures) to static conditions (microaerobic cultures), an increase in the Rz value was obtained, reaching a figure of 2.4 (see Fig. 2a), in agreement with the value previously reported for this enzymatic variant (Singh et al. 2012). A Soret band at 404 nm was apparent in the absorbance spectrum; the presence of high-spin ferric heme is supported by a charge transfer band at 623 nm (Fig. 2b) (Singh et al. 2012). Worthy of note is that these spectral features are not apparent for the recombinant enzyme produced under aerobic conditions (see Fig. 2a). The switch from aerobic to microaerobic conditions causes changes in gene expression associated with metal ion physiology in only 10 min. In particular, an enhanced abundance of transcripts involved in iron management was apparent

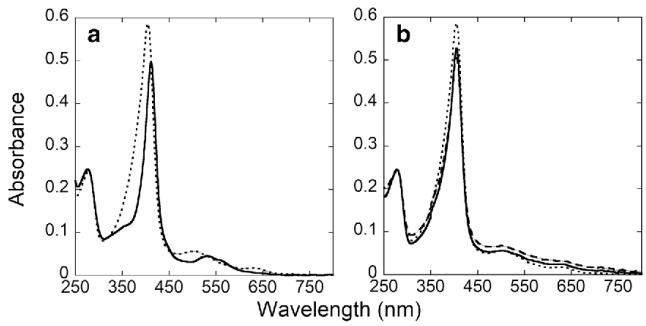

Fig. 2 UV-Vis absorbance spectra of recombinant Rh_DypB (5 μM) in 20 mM MOPS, 80 mM NaCl, 5% glycerol (pH 7.5, 15 °C). **a** Spectral analysis of Rh_DypB obtained under aerobic (continuous line) and microaerobic conditions (dotted line). **b** Spectral analysis of fractions eluted from HiTrap column at different imidazole concentrations (see Fig. 1): 25 mM (continuous line), 50 mM (dashed line), and 250 mM (dotted line) imidazole

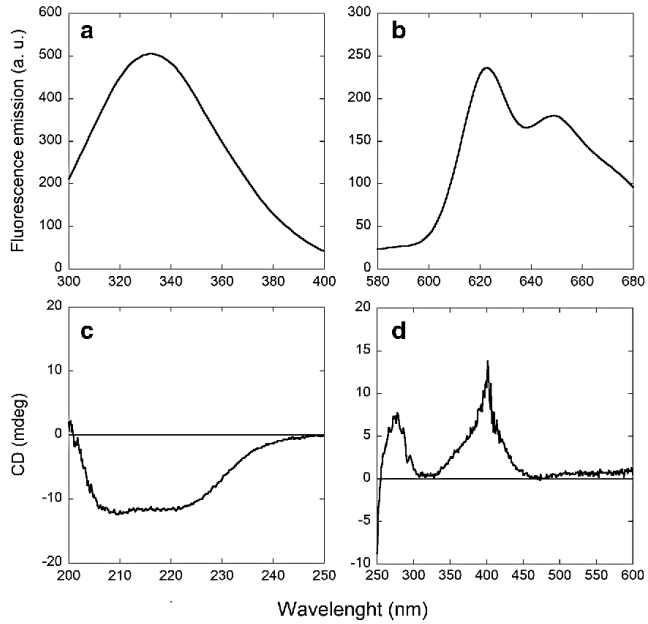

Fig. 3 Spectral analyses of recombinant Rh_DypB. **a** Protein fluorescence spectrum recorded from 300 to 400 nm with excitation at 280 nm (0.1 mg protein/mL). **b** Heme fluorescence spectrum recorded from 580 to 680 nm with excitation at 400 nm (0.1 mg protein/mL). **c** Far-UV CD spectrum (0.1 mg protein/mL). **d** Near-UV CD spectrum (0.8 mg protein/mL). The Rh_DypB enzyme was equilibrated at 15 °C in 20 mM MOPS, pH 7.5, 80 mM NaCl, 5% glycerol

(Partridge et al. 2007). The higher abundance of transcripts encoding the ferrous ion transporter FeoAB and the ferritin-like iron-storage protein allow the increased availability of iron under microaerobic conditions. Notably, the optimization of the codon usage of the synthetic gene and the identification of optimized expression conditions made it possible, for the first time, to incorporate heme and avoid the time-consuming and expensive apoprotein reconstitution step. The recombinant Rh_DypB exhibits peroxidase activity on ABTS; interestingly, by changing from aerobic to microaerobic conditions, a ≈ 10-fold increase in enzymatic activity was apparent (data not shown). Moreover, a further increase up to 5-fold was obtained in the presence of 2 mM $MnCl_2$ (i.e., 6 s^{-1} vs. 1.2 s^{-1} corresponding to 9.5 U/mg vs. 2.0 U/mg protein), as previously reported by Ahmad et al. (2011).

Structural characterization of Rh_DypB

Recombinant Rh_DypB was eluted in size-exclusion chromatography as a single peak corresponding to a ~ 155 kDa, tetrameric form. Spectral analyses of tertiary structure highlighted a high fluorescence intensity, although Rh_DypB only contains two Trp residues (Fig. 3a), and a very low signal in the near-UV CD spectrum (see Fig. 3d). Interestingly, porphyrin fluorescence emission peaks at 620 nm and 650 nm were apparent, with excitation at the Soret wavelength of 400 nm (Fig. 3b).

Concerning the secondary structure, a α-helix and β-strand content of ~ 29% and ~ 19%, respectively, were estimated from the far-UV CD spectrum (by means of K2D3 software, Fig. 3c), in fairly good agreement with the secondary structure

Table 1 Kinetic parameters of recombinant Rh_DypB peroxidase on Mn^{2+}, ABTS, and 2,6-DMP. The activity was assayed in 50 mM sodium malonate pH 5.0, 25 °C

Mn^{2+}			ABTS			2,6-DMP		
(A) In presence of 1.5 mM H_2O_2								
k_{cat} (s^{-1})	K_m (mM)	k_{cat}/K_m	k_{cat} (s^{-1})	K_m (mM)	k_{cat}/K_m	k_{cat} (s^{-1})	K_m (mM)	k_{cat}/K_m
19.0 ± 1.9	11.2 ± 1.1	1.7 ± 0.3	12.6 ± 1.3	14.9 ± 1.5	1.2 ± 0.1	0.45 ± 0.05	29.5 ± 3.0	0.02 ± 0.01
(B) In presence of 0.3 mM H_2O_2								
21.4 ± 0.6	3.1 ± 0.3	6.9 ± 0.7	15.4 ± 0.73	15.6 ± 1.3	0.98 ± 0.1	0.50 ± 0.08	17.5 ± 2.7	0.03 ± 0.01

Table 2 Kinetic parameters of recombinant Rh_DypB peroxidase on H_2O_2. The activity was assayed in 50 mM sodium malonate pH 5.0, 25 °C, in presence of 50 mM ABTS

k_{cat} (s^{-1})	K_m (mM)	k_{cat}/K_m	K_i (mM)
21.3 ± 1.9	0.03 ± 0.01	710 ± 85	2.2 ± 0.2
Addition of 2 mM Mn^{2+}			
34.0 ± 1.2	0.04 ± 0.01	850 ± 91	2.8 ± 0.3

content determined from the crystal structure (PDB code 3VEE, a value of 28% and 21% was apparent, respectively) (Singh et al. 2012).

Studies on the temperature sensitivity of heme fluorescence (a probe of tertiary structure modifications) and of far-UV signal (taken as reporter of secondary structure modification) gave similar T_m values (i.e., 63.3 ± 0.6 °C and 64.3 ± 0.3 °C, respectively).

Kinetic properties

At first, the apparent kinetic parameters of recombinant Rh_DypB peroxidase were determined at 25 °C in 50 mM sodium malonate buffer, pH 5.0, in the presence of different concentrations of Mn^{2+}, the nonphenolic ABTS and the phenolic 2,6-DMP substrates using a 1.5 mM H_2O_2 final concentration (see Materials and Methods section) (Table 1). Based on the apparent K_m value for ABTS, kinetic parameters were determined for H_2O_2 in presence of 50 mM ABTS (Table 2). In all cases, the reaction rates were fitted to a classical Michaelis-Menten equation, modified to account for a substrate inhibition effect with H_2O_2 (K_i~2.2 mM, Table 2). The highest substrate affinity (K_m of 0.03 mM) and enzymatic activity (≈ 20 s^{-1}, Table 2) were observed for H_2O_2 as substrate; interestingly, the enzymatic activity increased 1.6-fold in presence of Mn^{2+} (see Table 2). At this point, taking into account the H_2O_2 substrate inhibition effect, the kinetic parameters on Mn^{2+}, ABTS, and 2,6-DMP were newly determined using a saturating H_2O_2 concentration that did not result in an inhibition effect, i.e., 0.3 mM (Table 1); a higher substrate affinity and kinetic efficiency (up to 3.6-fold) were observed for Mn^{2+} as substrate, in comparison to the values determined at higher H_2O_2 concentration.

Effect of pH and temperature

The peroxidase activity of Rh_DypB was assessed in the temperature range 15–85 °C and in the pH range 3–9. As shown in Fig. 4a, maximal peroxidase activity occurred in the 45–75 °C temperature range; the enzyme is quite thermophilic, showing an optimum at ≈ 65 °C, in agreement with the high T_m values determined following the change in secondary and tertiary structure (see above). Rh_DypB is also quite stable: > 90% of its initial activity was maintained after 24-h incubation at 25 or 37 °C (pH 5.0).

An important issue for the use of ligninolytic enzymes is the pH-dependence of the catalytic activity (Pollegioni et al. 2015). The optimum of the bell-shaped curve was at acidic pH values, showing the highest activity at pH 4.0 (0.1 s^{-1}, Fig. 4b), as for known laccases (Xu 1999; Machczynski et al. 2004; Tonin et al. 2016). Interestingly, in the presence of manganese (i.e., in 50 mM sodium malonate buffer to which 2 mM $MnCl_2$ was added), the peroxidase activity of Rh_DypB showed a maximum at pH 6.0 (corresponding to a figure of 2.4 s^{-1}, see inset Fig. 4b). Concerning the stability, Rh_DypB maintained ≈ 50% of its initial activity in the 3–9 pH range after incubation for 24 h at 25 °C, remarkably showing ≥ 80% of its initial activity at pH 6–7 (data not shown).

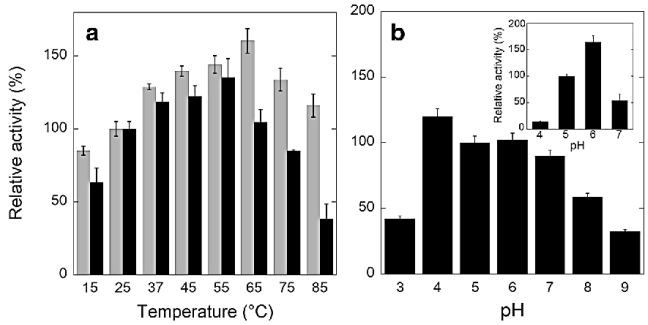

Fig. 4 **a** Effect of temperature on peroxidase activity of Rh_DypB in absence (black) and in presence of manganese (gray) (i.e., in 50 mM sodium malonate buffer with addition of 2 mM $MnCl_2$). **b** Effect of pH on the peroxidase activity of Rh_DypB. Inset: pH-dependence of the peroxidase activity in presence of manganese. Values represent the means of three independent experiments (mean ± standard error). The activity values at 25 °C and pH 5.0 were taken as 100%

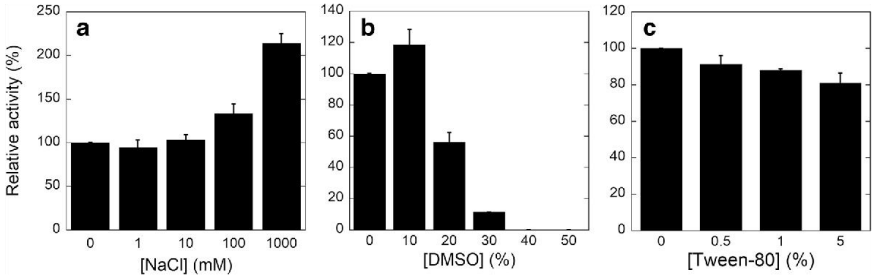

Fig. 5 Effect of NaCl (**a**), DMSO (**b**) and Tween-80 (**c**) concentration on the peroxidase activity of Rh_DypB, determined by measuring ABTS oxidation, at pH 5.0, 25 °C. The value in absence of the different compounds was taken as 100%. Values represent the means of three independent experiments (mean ± standard error)

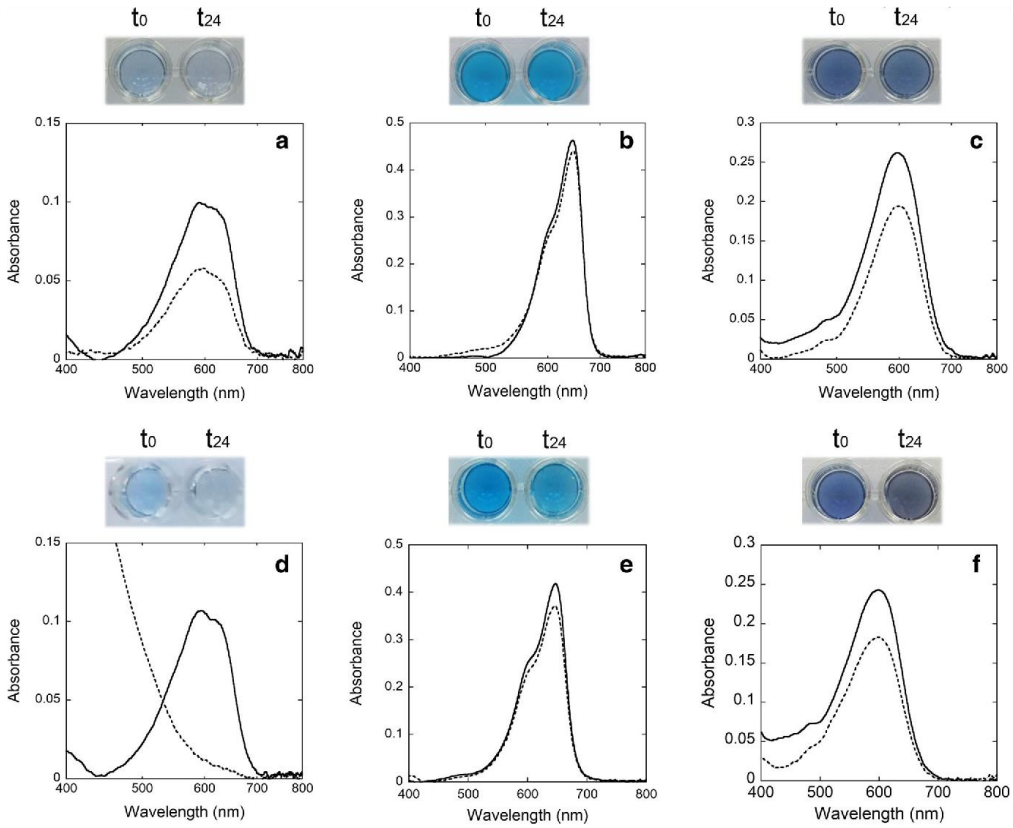

Fig. 6 Screening for dye-decolorizing peroxidase activity of Rh_DypB on RBBR (**a**, **d**), Azure B (**b**, **e**), and RB5 (**c**, **f**) performed on a 96-well microtiter plate, in 50 mM sodium acetate buffer, pH 4.0, 0.1 mM H_2O_2 (panels **a**, **b**, **c**) or 50 mM sodium malonate buffer, pH 6.0, 0.1 mM H_2O_2, 2 mM $MnCl_2$ (panels **d**, **e**, **f**). The dyes (0.1 mM) were treated with 0.5 U Rh_DypB (2.5 μM), resulting in a change in absorbance at 595, 648, and 597 nm, respectively. For each dye, the absorbance spectra before (continuous line) and after 24 h enzyme treatment (dashed line) are shown

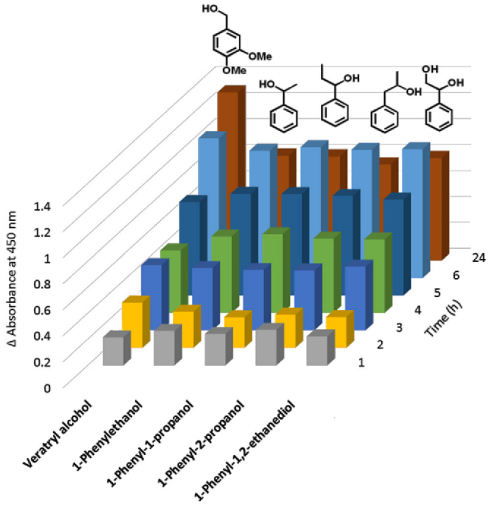

Fig. 7 Screening for phenyl alcohol oxidation performed on a 96-well microtiter plate. Different aromatic compounds were treated with Rh_DypB, resulting in a time-dependent increase in absorbance at 450 nm following reaction with 2,4-DNP at basic pH. No absorbance change with time was apparent in the control wells with no enzyme or substrate added

Effect of sodium chloride, Tween-80, and DMSO concentrations

A further factor affecting peroxidase application in dye decolorizing is the presence of halide ions. Accordingly, the dependence of the peroxidase activity of Rh_DypB from the sodium chloride concentration was investigated: a 2-fold higher enzymatic activity in the presence of 1 M NaCl was apparent (Fig. 5a).

In order to verify the possible application of Rh_DypB in processes requiring solvents, the dependence of enzymatic activity from DMSO (i.e., the most effective organic compound used to solubilize lignin) (Zakzeski et al. 2012; Cheng et al. 2013) was investigated. In the presence of 20% (*v*/*v*) DMSO, Rh_DypB showed ≈ 60% of the activity value assayed in plain buffer (Fig. 5b).

In the field of enzymatic hydrolysis of lignocellulosic biomass, Tween-80 was also demonstrated to increase the hydrolysis yield (Qing et al. 2010). As shown in Fig. 5c, the activity of Rh_DypB was not affected by the surfactant in the reaction medium up to 5% (*v*/*v*) of Tween-80.

Dye-decolorizing activity

The peroxidase activity of Rh_DypB on different dyes (RBBR, Azure B, and RB5) was tested on 96-well microtiter plates under optimal operational conditions (i.e., 50 mM sodium malonate buffer, pH 6.0, to which 0.1 mM H_2O_2 and 2 mM $MnCl_2$ were added) and spectral changes were monitored after 24 h of incubation. As reported in Fig. 6, the enzyme is able to decolorize all tested dyes; notably, a remarkable dye-decolorizing effect was apparent on RBBR (see Fig. 6d). In particular, a decolorization level of ≥ 95%, ≈ 11%, and ≈ 22% was apparent on RBBR, Azure B, and RB5, respectively. On the other hand, a figure of ≈ 50% and ≈ 5% on RBBR and RB5, respectively, was apparent when the peroxidase activity was evaluated in the absence of $MnCl_2$ (i.e., in 50 mM sodium acetate buffer, pH 4.0, see Fig. 6a, c) but no decolorization was observed for Azure B as dye.

Screening of oxidation activity on monomeric lignin model compounds

The ability to oxidize various monomeric lignin model compounds was followed qualitatively by a simple and rapid colorimetric assay (Fig. 7) (Tonin et al. 2017). An increase in the absorbance value at 450 nm was evident for all the evaluated compounds; the higher response was apparent on the veratryl alcohol, a substituted benzyl alcohol.

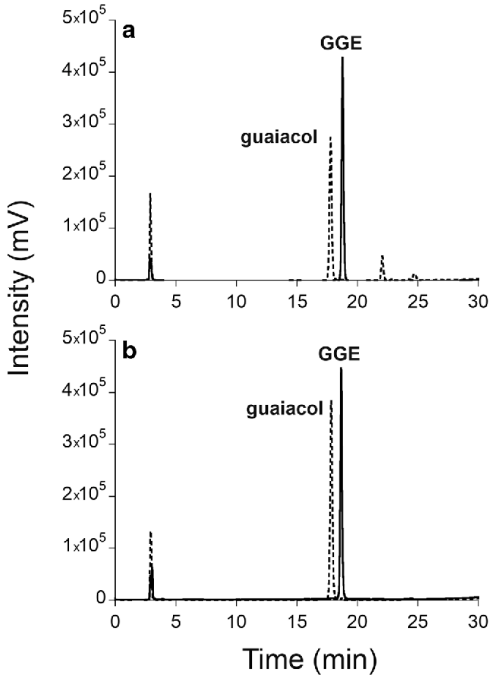

Fig. 8 Bioconversion of GGE by Rh_DypB. HPLC chromatograms of 2 mM GGE conversion before (continuous line) and 10 min after adding Rh_DypB (dashed line), at 25 °C and pH 6.0, in the absence (**a**) and presence (**b**) of 1 mM ascorbic acid

Bioconversion of GGE

The ability of Rh_DypB to act on lignin was investigated on the dimeric lignin model compound guaiacylglycerol-β-guaiacyl ether (GGE), in 50 mM sodium malonate buffer, pH 6.0, to which 2 mM $MnCl_2$ and 1 mM H_2O_2 were added. The substrate was incubated with Rh_DypB and its conversion was assessed by HPLC analysis (Fig. 8). The Cα-Cβ bond cleavage of GGE released guaiacol as product (Ahmad et al. 2011): the complete conversion of 2 mM GGE (R_t = 18.8 min) and a novel peak at a retention time of 17.8 min (guaiacol) were apparent in 10 min (see Fig. 8a). Interestingly, in the presence of 1 mM ascorbic acid (a reducing agent used to avoid guaiacol polymerization) (Hong et al. 2016), an increase in guaiacol production was observed (≈30% higher, see Fig. 8b). The conversion rate corresponded to 12.5 μmol GGE/min mg Rh_DypB. Notably, no bioconversion was observed using commercial manganese peroxidases under the same reaction conditions (such as manganese peroxidase from *Bjerkandera adusta* and *Nematoloma frowardii*) (Tonin et al. 2017).

Discussion

In this work, we report on the successful overexpression of the N246A variant of *R. jostii* RHA1 DypB peroxidase in *E. coli* (Singh et al. 2013). The optimization of the codon usage for *E. coli* expression of the synthetic gene allowed us to produce > 100 mg of recombinant enzyme per liter of fermentation broth in soluble and active form. Owing to a His-tag, the recombinant enzyme could be purified in a single chromatographic step with an overall yield > 90%. Adding hemin chloride at the induction of protein expression and growing for 3 h without shaking before cell collection made it possible, for the first time, to isolate the enzyme as full holoenzyme (as demonstrated by the Rz value), avoiding the use of a reconstitution step. The switch from aerobic to microaerobic growth conditions significantly alters the abundance of transcripts involved in homeostasis of redox-reactive metals (Partridge et al. 2007): an increased abundance of the *feoAB* and *fntB* transcripts encoding the ferrous ion transporter FeoAB and a ferritin-like iron-storage protein was detected that resulted in higher metal solubility (Partridge et al. 2007).

DypB demonstrated peroxidase activity that improves in the presence of Mn^{2+} (Ahmad et al. 2011): recombinant Rh_DypB showed a 5-fold increase in specific activity after adding 2 mM $MnCl_2$. Compared to the previous investigation (Singh et al. 2012), our preparation shows a 6-fold higher maximal activity (34 vs. 5.4 s^{-1}) and a 2.5-fold higher K_m for H_2O_2 (40 vs. 15 μM). This apparent discrepancy largely arises from the different buffer composition (malonate buffer at pH 5.0 with addition of 2 mM Mn^{2+} vs. acetate buffer at pH 5.5) and the ABTS concentration (50 vs. 10 mM).

Recombinant Rh_DypB shows good stability at pH 6–7 and at 25–37 °C (less than 20% of the starting activity is lost following a 24-h incubation), and its activity is not affected by 1 M NaCl, 10% DMSO, or 5% Tween-80. Under optimized conditions (i.e., 50 mM sodium malonate buffer, pH 6.0, 2 mM $MnCl_2$, and 0.1 mM H_2O_2), the enzyme can be used for dye decolorizing in a number of compounds, which is more effective when Mn^{2+} ions are present (Fig. 6). Rh_DypB can also oxidize various monomeric lignin model compounds (Fig. 7) and efficiently cleave the Cα-Cβ bond of GGE, the dimeric lignin model of β-O-4 linkages. The GGE conversion rate was 12.5 μmol/min mg enzyme. Differently from previous studies (Ahmad et al. 2011), a peak corresponding to guaiacol was clearly produced: this is probably due to a faster conversion, which reduces side reactions due to further radical reactions. This conclusion is also supported by the stabilizing effect exerted by ascorbate (Fig. 8b).

Overall, Rh_DypB can be applied in a variety of applications both as a single biocatalyst and as a member of multistep artificial metabolism (Tessaro et al. 2015). Thus, since "future perspectives could include synergy between natural enzymes from different sources (as well as those obtained by protein engineering) and other pretreatment methods that may be required for optimal results in enzyme-based, environmentally friendly, technologies" (Pollegioni et al. 2015), Rh_DypB might represent a novel tool in the strategy for breaking down lignin.

Acknowledgements E.V. is a PhD student of the "Life Sciences and Biotechnology" course at Università degli studi dell'Insubria.

Funding information We thank the financial support from CIB, Consorzio Interuniversitario per le Biotecnologie.

Compliance with ethical standards

Conflict of interest The authors declare that they have no conflict of interest.

Ethical approval This article does not contain any studies with human participants or animals performed by any of the authors.

References

Ahmad M, Roberts JN, Hardiman EM, Singh R, Eltis LD, Bugg TD (2011) Identification of DypB from *Rhodococcus jostii* RHA1 as a lignin peroxidase. Biochemistry 50:5096–5107. https://doi.org/10.1021/bi101892z

Boerjan W, Ralph J, Baucher M (2003) Lignin biosynthesis. Annu Rev Plant Biol 54:519–546. https://doi.org/10.1146/annurev.arplant.54.031902.134938

Bugg TDH, Rahmanpour R (2015) Enzymatic conversion of lignin to renewable chemicals. Curr Opin Chem Biol 29:10–17. https://doi.org/10.1016/j.cbpa.2015.06.009

Bugg TDH, Ahmad M, Hardiman EM, Singh R (2011) The emerging role for bacteria in lignin degradation and bio-product formation. Curr Opin Biotechnol 22:394–400. https://doi.org/10.1016/j.copbio.2010.10.009

Caldinelli L, Iametti S, Barbiroli A, Bonomi F, Fessas D, Molla G, Pilone MS, Pollegioni L (2005) Dissecting the structural determinants of the stability of cholesterol oxidase containing covalently bound flavin. J Biol Chem 280:22572–22581. https://doi.org/10.1074/jbc.M500549200

Caldinelli L, Molla G, Sacchi S, Pilone MS, Pollegioni L (2009) Relevance of weak flavin binding in human D-amino acid oxidase. Protein Sci 18:801–810. https://doi.org/10.1002/pro.86

Cheng K, Sorek H, Zimmermann H, Wemmer DE, Pauly M (2013) Solution-state 2D NMR spectroscopy of plant cell walls enabled by a dimethylsulfoxide-d 6/1-ethyl-3-methylimidazolium acetate solvent. Anal Chem 85:3213–3221. https://doi.org/10.1021/ac303529v

Cleland W (1983) Contemporary enzyme kinetics and mechanism. Academic Press, New York, pp 253–266

de Gonzalo G, Colpa DI, Habib MH, Fraaije MW (2016) Bacterial enzymes involved in lignin degradation. J Biotechnol 236:110–119. https://doi.org/10.1016/j.jbiotec.2016.08.011

Durão P, Chen Z, Fernandes AT, Hildebrandt P, Murgida DH, Todorovic S, Pereira MM, Melo EP, Martins LO (2008) Copper incorporation into recombinant CotA laccase from *Bacillus subtilis*: characterization of fully copper loaded enzymes. J Biol Inorg Chem 13:183–193. https://doi.org/10.1007/s00775-007-0312-0

Eggert C, Temp U, Eriksson KEL (1997) Laccase is essential for lignin degradation by the white-rot fungus *Pycnoporus cinnabarinus*. FEBS Lett 407:89–92

Fernandez-Fueyo E, Castanera R, Ruiz-Dueñas FJ, López-Lucendo MF, Ramírez L, Pisabarro AG, Martínez AT (2014) Ligninolytic peroxidase gene expression by *Pleurotus ostreatus*: differential regulation in lignocellulose medium and effect of temperature and pH. Fungal Genet Biol 72:150–161. https://doi.org/10.1016/j.fgb.2014.02.003

Glenn JK, Gold MH (1985) Purification and characterization of an extracellular Mn(II)-dependent peroxidase from the lignin degrading basidiomycete *Phanerochaete chrysosporium*. Archiv Biochem Biophy 242:329–341

Glenn JK, Akileswaran L, Gold MH (1986) Mn (II) oxidation is the principal function of the extracellular Mn-peroxidase from *Phanerochaete chrysosporium*. Arch Biochem Biophys 251:688–696. https://doi.org/10.1016/0003-9861(86)90378-4

Gupta VK, Kubicek CP, Berrin JG, Wilson DW, Couturier M, Berlin A, Filho EXF, Ezeji T (2016) Fungal enzymes for bio-products from sustainable and waste biomass. Trends Biochem Sci 41:633–645. https://doi.org/10.1016/j.tibs.2016.04.006

Harris CM, Pollegioni L, Ghisla S (2001) pH and kinetic isotope effects in D-amino acid oxidase catalysis. Eur J Biochem 268:5504–5520. https://doi.org/10.1046/j.1432-1033.2001.02462.x

Hong CY, Park SY, Kim SH, Lee SY, Choi WS, Choi IG (2016) Degradation and polymerization of monolignols by *Abortiporus biennis*, and induction of its degradation with a reducing agent. J Microbiol 54:675–685. https://doi.org/10.1007/s12275-016-6158-9

Leonowicz A, Matuszewska A, Luterek J, Ziegenhagen D, Wojtaś-Wasilewska M, Cho NS, Hofrichter M, Rogalski J (1999) Biodegradation of lignin by white rot fungi: review. Fungal Genet Biol 2:175–185. https://doi.org/10.1006/fgbi.1999.1150

Longe L, Garnier G, Saito K (2016) Lignin biodegradation with fungi, bacteria and enzymes for producing chemicals and increasing process efficiency. In: Fang Z, Smith RL (eds) Production of biofuels and chemicals from lignin. Springer, Singapore, pp 147–179

Louis-Jeune C, Andrade-Navarro MA, Perez-Iratxeta C (2012) Prediction of protein secondary structure from circular dichroism using theoretically derived spectra. Proteins 80:374–381. https://doi.org/10.1002/prot.23188

Machczynski MC, Vijgenboom E, Samyn B, Canters GW (2004) Characterization of SLAC: a small laccase from *Streptomyces coelicolor* with unprecedented activity. Protein Sci 13:2388–2397

Miki K, Renganathan V, Gold MH (1986) Mechanism of beta-aryl ether dimeric lignin model compound oxidation by lignin peroxidase by *Phanerochaete chrysosporium*. Biochemistry 25:4790–4796. https://doi.org/10.1021/bi00365a011

Partridge JD, Sanguinetti G, Dibden DP, Roberts RE, Poole RK, Green J (2007) Transition of *Escherichia coli* from aerobic to micro-aerobic conditions involves fast and slow reacting regulatory components. J Biol Chem 282:11230–11237. https://doi.org/10.1074/jbc.M700728200

Pollegioni L, Tonin F, Rosini E (2015) Lignin-degrading enzymes. FEBS J 282:1190–1213. https://doi.org/10.1111/febs.13224

Qing Q, Yang B, Wyman CE (2010) Impact of surfactants on pretreatment of corn stover. Bioresour Technol 101:5941–5951. https://doi.org/10.1016/j.biortech.2010.03.003

Rosini E, Monelli CS, Pollegioni L, Riva S, Monti D (2012) On the substrate preference of glutaryl acylases. J Mol Catal B Enzym 76:52–58. https://doi.org/10.1016/j.molcatb.2011.12.001

Sánchez C (2009) Lignocellulosic residues: biodegradation and bioconversion by fungi. Biotechnol Adv 27:185–194. https://doi.org/10.1016/j.biotechadv.2008.11.001

Singh R, Grigg JC, Armstrong Z, Murphy ME, Eltis LD (2012) Distal heme pocket residues of B-type dye-decolorizing peroxidase arginine but not aspartate is essential for peroxidase activity. J Biol Chem 287:10623–10630. https://doi.org/10.1074/jbc.M111.332171

Singh R, Grigg JC, Qin W, Kadla JF, Murphy ME, Eltis LD (2013) Improved manganese-oxidizing activity of DypB, a peroxidase from a lignolytic bacterium. ACS Chem Biol 8:700–706. https://doi.org/10.1021/cb300608x

Sugano Y, Muramatsu R, Ichiyanagi A, Sato T, Shoda M (2007) DyP, a unique dye-decolorizing peroxidase, represents a novel heme peroxidase family ASP171 replaces the distal histidine of classical peroxidases. J Biol Chem 282:36652–36658. https://doi.org/10.1074/jbc.M706996200

Tessaro D, Pollegioni L, Piubelli L, D'Arrigo P, Servi S (2015) Systems biocatalysis: an artificial metabolism for interconversion of functional groups. ACS Catal 5:1604–1608. https://doi.org/10.1021/cs502064s

Tien M, Kirk T (1983) Lignin-degrading enzyme from the hymenomycete *Phanerochaete chrysosporium*. Science 221:661–663. https://doi.org/10.1126/science.221.4611.661

Tonin F, Melis R, Cordes A, Sanchez-Amat A, Pollegioni L, Rosini E (2016) Comparison of different microbial laccases as tools for industrial uses. New Biotechnol 33:387–398. https://doi.org/10.1016/j.nbt.2016.01.007

Tonin F, Vignali E, Pollegioni L, D'Arrigo P, Rosini E (2017) A novel, simple screening method for investigating the properties of lignin oxidative activity. Enzym Microb Technol 96:143–150. https://doi.org/10.1016/j.enzmictec.2016.10.013

Wong DWS (2009) Structure and action mechanism of ligninolytic enzymes. Appl Biochem Biotechnol 157:174–209. https://doi.org/10.1007/s12010-008-8279-z

Xu F (1999) Recent progress in laccase study: properties, enzymology, production, and applications. In: Flickinger MC, Grew SW (eds) Encyclopedia of bioprocess technology: fermentation, biocatalysis, and bioseparation. John Wiley & Sons, New York, pp 1545–1554

Zakzeski J, Jongerius AL, Bruijnincx PC, Weckhuysen BM (2012) Catalytic lignin valorization process for the production of aromatic chemicals and hydrogen. ChemSusChem 5:1602–1609. https://doi.org/10.1002/cssc.201100699

Chemosphere 250 (2020) 126296

Contents lists available at ScienceDirect

Chemosphere

journal homepage: www.elsevier.com/locate/chemosphere

Enzymatic transformation of aflatoxin B_1 by Rh_DypB peroxidase and characterization of the reaction products

Martina Loi [a], Justin B. Renaud [b], Elena Rosini [c], Loredano Pollegioni [c], Elisa Vignali [c], Miriam Haidukowski [a], Mark W. Sumarah [b], Antonio F. Logrieco [a], Giuseppina Mulè [a, *]

[a] Institute of Sciences of Food Production, National Research Council of Italy (ISPA-CNR), Via G. Amendola 122/O, 70126 Bari, Italy
[b] London Research and Development Centre, Agriculture and Agri-Food Canada, 1391 Sandford Street London, Ontario, Canada, N5V4T3
[c] Department of Biotechnology and Life Sciences, University of Insubria, via Dunant 3, 21100 Varese, Italy

HIGHLIGHTS

- Rh_DypB application could be of great interest for the treatment of contaminated feed.
- Rh_Dyp B peroxidase was applied for aflatoxin B_1 biotransformation.
- Low enzyme and H_2O_2 concentrations were effective to reduce Aflatoxin B_1.
- Aflatoxin B_1 was quantitatively converted to Aflatoxin Q_1.
- AFQ_1 has a lower acute toxicity and mutagenicity than AFB_1.

GRAPHICAL ABSTRACT

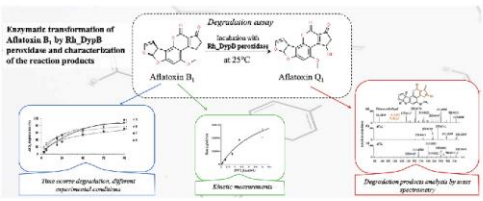

ARTICLE INFO

Article history:
Received 28 October 2019
Received in revised form
17 February 2020
Accepted 20 February 2020
Available online 25 February 2020

Handling Editor:

Keywords:
Aflatoxin B_1
Aflatoxin Q_1
Bioremediation
Dye-decolorizing peroxidase
Reaction products

ABSTRACT

In some environments, a number of crops, notably maize and nuts can be contaminated by aflatoxin B_1 and related compounds resulting from the growth of aflatoxin-producing *Aspergilli*. Fungal peroxidases have been shown to degrade a number of mycotoxins, including aflatoxin B_1 (AFB_1). Therefore, the purpose of this study was to investigate the *in vitro* enzymatic degradation AFB_1 by a recombinant type B dye decolorizing peroxidase (Rh_DypB). Analysis of the reaction products by HPLC-MS analysis showed that under optimized conditions AFB_1 was efficiently transformed by Rh_DypB, reaching a maximum of 96% conversion after 4 days of reaction at 25 °C. Based on high resolution mass spectrometry analysis, AFB_1 was demonstrated to be quantitatively converted to AFQ_1, a compound with a significantly lower toxicity. A number of low molecular mass compounds were also present in the final reaction mixture in small quantities. The results presented in this study are promising for a possible application of the enzyme Rh_DypB for aflatoxin reduction in feed.

1. Introduction

Aflatoxins (AFs) are toxic metabolites produced by *Aspergillus flavus* and *A. parasiticus* along with 11 other uncommon species of *Aspergillus*. Aflatoxin B_1 (AFB_1) is highly toxic to domestic animals and is a potent human carcinogen (World Health Organization, 2019).

* Corresponding author.
E-mail addresses: martina.loi@ispa.cnr.it (M. Loi), justin.renaud@agr.gc.ca (J.B. Renaud), elena.rosini@uninsubria.it (E. Rosini), loredano.pollegioni@uninsubria.it (L. Pollegioni), e.vignali@uninsubria.it (E. Vignali), miriam.haidukowski@ispa.cnr.it (M. Haidukowski), mark.sumarah@agr.gc.ca (M.W. Sumarah), antonio.logrieco@ispa.cnr.it (A.F. Logrieco), giuseppina.mule@ispa.cnr.it (G. Mulè).

https://doi.org/10.1016/j.chemosphere.2020.126296
0045-6535/

Abbreviations

AFs	Aflatoxins
AFB_1	Aflatoxin B_1
AFM_1	Aflatoxin M_1
Rh_DypB	Dye-decolorizing peroxidase type B
ABTS	2,2-azino-bis-[3-ethylbenzothiazoline-6-sulfonic acid]

In food-insecure countries with subtropical climates or that are subject to drought conditions, crops like maize and groundnuts are prone to aflatoxin contamination. Managing this risk requires an integrated approach that spans the management of fungal contamination in the field, in storage and, where possible, practical post-harvest reduction strategies (Leslie and Logrieco, 2014). More than 500 million people, mainly in Africa, are chronically exposed to aflatoxin. This contributes to child stunting, increases the rate of liver cancer and can result in child mortality (Doerge et al., 2018; McMillan et al., 2018; Wild et al., 2015).

There is, however, an important additional negative impact of aflatoxin on human health, namely the decrease in the amount of animal proteins available for food. In many developing countries where aflatoxin is a chronic problem, the poorest quality grain (where it can be spared) is used for animal feed. Poultry species suffer from reductions in growth rate, increased susceptibility to disease, and decreased egg production. In cattle, aflatoxin causes liver and kidney damage, and reduces milk production (Eaton et al., 2010; Pitt et al. 2012). Thus, the use of aflatoxin-contaminated feed contributes to another serious problem in sub-Saharan Africa, i.e. Protein Energy Malnutrition (Bhutta et al., 2017). A practical technique to reduce aflatoxin in highly contaminated maize for feed would make an important contribution to public health in Africa.

Biological methods, such as enzymatic biotransformation, can reduce AFs concentrations in food commodities through a mild and environmental friendly approach. Many enzymes have been recognized as being capable of degrading mycotoxins, such as peroxidases and laccases, recently reviewed (Loi et al., 2017). Laccases have medium to low redox potential ($\leq$ 0.8 V) and may need redox mediators to efficiently degrade mycotoxins (Loi et al., 2018), while peroxidases have higher redox potential ($\geq$ 1.0 V), and are efficient oxidants by themselves. These enzymes are heme containing peroxidases requiring H_2O_2 to oxidize methoxylated aromatics, antraquinones, phenolics and non-phenolics lignin model compounds (Pollegioni et al., 2015).

Peroxidases are known to act on mycotoxins (including AFB_1) (Marimón Sibaja et al., 2019; Yehia, 2014; Tripathi and Mishra, 2011; Chitrangada and Mishra, 2000), although the transformation products and their associated toxicities have been poorly investigated. Oxidation of AFB_1 may result in a more toxic (carcinogenic, according to IARC) metabolite, i.e. 8,9-epoxy-AFB_1. which is the *in vivo* product of cytochrome P450 isozymes (CYP3A4 and CYP1A2) (Rushing and Selim, 2019) as well as other peroxidases (Wang et al., 2019; Wang et al., 2011). The identification of the degradation product is, therefore, a crucial issue.

In preliminary experiments we evaluated the ability of two laccases from *Bacillus licheniformis* and *Trametes versicolor*, two manganese peroxidases from *Bjerkandera adusta* and *Phlebia* sp. Nfb19 (Tonin et al., 2017), and the recombinant N246A variant of dye-decolorizing DypB (Rh_DypB) from *Rhodococcus jostii* (Vignali et al., 2018) to degrade AFB_1. Transformation of the mycotoxin was monitored qualitatively by a simple and rapid colorimetric assay (Tonin et al., 2017). Noteworthy, Rh_DypB showed the highest mycotoxin degradation activity and demonstrated to combine different dye-decolorizing and oxidative activities in a single enzyme, and to have a high yield of recombinant production (up to 100 mg enzyme/L fermentation broth) (Vignali et al., 2018).

The purpose of this study was to investigate the *in vitro* biotransformation of AFB_1 by a recombinant Rh_DypB; the enzymatic reaction was studied using various experimental conditions and the kinetic parameters were assessed. Finally, the reaction products were characterized by mass spectrometry analysis.

2. Materials and methods

2.1. Chemicals and AFB_1 standard preparation

2,2-Azino-bis-[3-ethylbenzothiazoline-6-sulfonic acid] (ABTS) (catalogue number A11557), H_2O_2 (catalogue number H1009), AFB_1 standard (catalogue number 32754, purity > 99%) were purchased from Sigma Aldrich Milan, Italy. Regenerated cellulose (RC) membranes 0.2 mm filters (catalogue number 656102) were obtained from Alltech Italia-Grace Division (Milano, Italy). All solvents (HPLC grade) were purchased from J. T. Baker Inc. (Deventer, The Netherlands). Ultrapure water was produced by a Milli-Q system (Millipore, Bedford, MA, USA).

AFB_1 (Sigma Aldrich, Milan, Italy) was dissolved in toluene:acetonitrile (ACN) (9:1, v/v) to prepare a AFB_1 stock solution (100 μg/mL). The exact concentration of AFB_1 was determined according to Association of Official Analytical Chemists (2000).

2.2. Rh_DypB production and purification

Rh_DypB was produced from BL21 (DE3) *Escherichia coli* cells (catalogue number 69450, Merck Millipore) transformed with pET24-Rh_DypB expression plasmid (Vignali et al., 2018). Recombinant cells were grown under aerobic conditions at 37 °C in Terrific Broth medium (24 g/L yeast extract, 12 g/L bacto-tryptone, 8 mL/L glycerol, 9.4 g/L, K_2HPO_4, 2.2 g/L KH_2PO_4) and induced adding 0.25 mM IPTG and 0.25 g/L hemin chloride at an $OD_{600nm} \approx 1.0$; the highest Rh_DypB expression was achieved under microaerobic conditions. Purification was performed using an HiTrap chelating affinity column (catalogue number 17040901, GE Healthcare, Milano, Italy), previously loaded with 100 mM $NiCl_2$. Column equilibration was performed with 20 mM MOPS buffer, pH 7.5 added with 80 mM NaCl and 5% (v/v) glycerol. Rh_DypB was eluted with the same buffer with addition of 500 mM imidazole, which was then removed by a gel-permeation chromatography (PD10 column, GE Healthcare). The obtained Rh_DypB stock solution (5 U/mg in 50 mM sodium malonate, pH 6.0, 2 mM $MnCl_2$, 0.1 mM H_2O_2, 25 °C) was stored at −20 °C until use.

2.3. Activity measurements

Enzyme activity was measured spectrophotometrically, as reported by Vignali et al. (2018). Briefly, enzyme activity was assayed in 50 mM sodium malonate buffer, pH 6.0 added with 2 mM $MnCl_2$, 0.1 mM H_2O_2 and 1 mM ABTS from the absorbance change at 420 nm recorded in the first minute of measurement ($\epsilon_{420nm} = 36{,}000\ M^{-1}cm^{-1}$). One unit of activity was defined as the amount of enzyme which consumed 1 μmol of substrate in 1 min at 25 °C.

2.4. Aflatoxin B_1 degradation assays with Rh_DypB and kinetic measurements

In order to study and optimize AFB_1 degradation upon enzymatic treatment four different experiments (Table 1, A-D) were

performed. Starting from the already optimized condition (A, Table 1) for Rh_DypB (Vignali et al., 2018), H_2O_2 and enzyme adjustments were made to counteract H_2O_2 consumption, spontaneous decomposition or enzyme denaturation during the assay. AFB_1 degradation assays were carried out in 50 mM sodium malonate buffer, pH 6.0 containing 2 mM $MnCl_2$ and AFB_1 (1 μg/mL). The reaction mixture contained different H_2O_2 and enzyme concentrations, as reported in Table 1.

In control samples, the enzyme solution was replaced by an equal amount of buffer. After gentle mixing, samples were incubated at 25 °C under shaking (150 rpm) and analyzed after 3, 6, 18, 24, 48, 72 and 96 h of reaction. Residual AFB_1 was quantified by HPLC as reported by Loi et al. (2016), and analyzed by high-resolution LC-MS/MS to identify AFB_1 degradation products as described in section 2.5.

Kinetic parameters, K_m and V_{max}, were determined using 0.1 U/mL of Rh_DypB, and increasing AFB_1 concentrations (0.1, 0.33, 0.8, 1.33 and 3 μg/mL) using the amount of substrate converted after 24 h.

2.5. High resolution LC-MS analyses of AFB_1 degradation and characterization of transformation products

The enzymatic reactions with AFB_1 (Table 1) were quenched by adding 200 μL of cold methanol (to denature Rh_DypB) to 100 μL of reaction mixture and incubated in ice for 10 min. Samples were then centrifuged at 9000 g for 5 min at 4 °C to remove precipitated protein and the supernatant was transferred to a HPLC vial.

All samples were analyzed using a Q-Exactive™ Quadrupole Orbitrap mass spectrometer (Thermo Scientific™) coupled to an Agilent 1290 high-performance liquid chromatography (HPLC) system. AFB_1 and transformation products were resolved on a Zorbax Eclipse Plus RRHD C18 column (2.1 × 50 mm, 1.8 μm; catalogue number 959757-902, Agilent) maintained at 35 °C. The mobile phase was water with 0.1% formic acid (A), and acetonitrile with 0.1% formic acid (B) (Optima grade, Fisher Scientific™, Lawn, NJ, USA). Mobile phase B was held at 0% for 30 s, before increasing to 100% over 3 min. B was then held at 100% for 2.5 min before returning to 0% over 30 s. Injections of 6 μL were used with a flow rate of 0.3 mL/min. The following conditions were used for positive HESI: capillary voltage, 3.9 kV; capillary temperature, 400 °C; sheath gas, 17.00 units; auxiliary gas, 8.00 units; probe heater temperature, 450 °C; S-Lens RF level, 45.00. Samples were analyzed using a data-dependent acquisition (DDA) experiment comprised of a full MS scan at 17,500 resolution over a scan range of 70–1000 *m/z*; automatic gain control (AGC) target and maximum injection time (max IT) was 3×10^6 and 64 ms, respectively. The five highest intensity ions from the full scan (excluding isotopes) were sequentially selected using a 1.0 *m/z* isolation window and analyzed at resolution of 17,500; AGC target, 1×10^6; max IT, 64 ms; normalized collision energy (NCE) 50; threshold intensity 1.5×10^5; and dynamic exclusion of 5 s.

2.6. Statistical analyses

Data were expressed as the mean of three replicates ± standard deviation (SD) of at least two independent experiments. Results were analyzed through ANOVA and Student's t-test (paired comparison) performed using STATISTICA software for windows, ver. 7 (Statsoft, Tulsa, Okhla). Differences between samples and relative control were considered significant for a P value < 0.05.

3. Results and discussion

Rh_DypB capability of degrading AFB_1 was tested *in vitro* and optimized using different experimental conditions and kinetic parameters were estimated. Toxin reduction was evaluated by HPLC analyses. To assess whether the enzymatic reaction resulted in the production of less toxic metabolites (i.e. AFB_1 was detoxified), samples were analyzed by mass spectrometry and the reaction products identified.

3.1. Time course degradation of aflatoxin B_1 by Rh_DypB

AFB_1 stability was assessed in 50 mM sodium malonate buffer, pH6 containing 0.1 mM H_2O_2 and 2 mM $MnCl_2$, as well as in samples added with 0.1 mM H_2O_2. AFB_1 was stable in all control samples during the whole extent of the assay (96 h) (recovery 100 ± 0.11%). H_2O_2 treatment has been reported to chemically modify AFB_1, but at higher concentrations than the one used in this study (0.06–2 M vs 0.1 mM) (Karlovsky et al., 2016).

The time course of AFB_1 degradation by Rh_DypB is shown in Fig. 1. The efficacy of a standard degradation assay (Table 1, A) was compared using various experimental conditions, which included the addition of aliquots of 0.1 mM H_2O_2 (Table 1, B), aliquots of both 0.1 mM H_2O_2 and 0.1 U/mL of Rh_DypB (Table 1, C) or higher enzyme (0.5 U/mL) and H_2O_2 (0.2 mM) concentrations (Table 1, D).

In all conditions tested, Rh_DypB was effective at modifying AFB_1, following an exponential decay ($R^2 = 0.9918$; 0.9818; 0.9767; 0.9625). The highest rate of conversion occurred in the first 18 h of assay. After 3 and 6 h the modification was higher under the standard conditions ($P < 0.01$). Regardless of H_2O_2 and Rh_DypB addition, the concentration of AFB_1 was halved within 24 h (51–54%), and then slowly, but continuously removed. AFB_1 biotransformation reached 77% in the standard conditions (A) and 89% with the re-addition of H_2O_2 (B), while, an almost complete biotransformation (96%) was reached when both H_2O_2 and Rh_DypB were added to the reaction mix. The use of higher enzyme concentrations and H_2O_2 amounts (D) did not lead to an increased modification at all tested time points; the biotransformation reached only 71% after 96 h.

H_2O_2 addition was not effective in increasing AFB_1 degradation, likely because it was present in large excess at the beginning of the reaction. Likewise, Rh_DypB re-addition did not significantly increase mycotoxin degradation. The only exception is apparent at 96 h, probably due to enzyme inactivation at long reaction times (C, Fig. 1).

It is worth noting that a high aflatoxin B_1 concentration (1 μg/mL) was used for the experimental design. Although aflatoxins concentration in food is usually lower (μg/kg range), the efficiency of the enzymatic degradation may be reduced under real conditions, depending on matrix composition, humidity, enzyme

Table 1
Aflatoxin B_1 degradation assays parameters.

Assay	H_2O_2 (mM)	Rh_DypB (U/mL)
A	0.1	0.1
B	0.1, aliquots added every 2 h, 4 times a day	0.1
C	0.1, aliquots added every 2 h, 4 times a day	0.1 aliquots added every 24 h
D	0.2	0.5

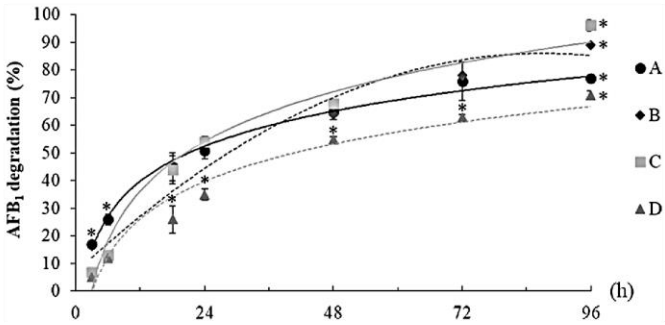

Fig. 1. Time course of biotransformation of AFB_1 by Rh_DypB in sodium malonate buffer 50 mM pH 6, 2 mM $MnCl_2$. A-D. conditions were reported in Table 1. Error bars represent the standard deviation for three independent replicates of two independent experiments. Asterisks (*) indicate a statistically significant difference between samples at the same timepoint ($P < 0.05$).

application etc. In addition, natural contamination may appear as "hot spots"; some parts may appear uncontaminated, while other show extremely high contamination levels. Therefore, although *in vitro*, the results of this study are meaningful and this enzymatic method might be an effective tool to counteract aflatoxins contamination in a real context. In previous studies, a fungal manganese dependent peroxidase from *Pleurotus ostreatus* (Yehia, 2014), a native (Wang et al., 2011) and a commercial (Marimón Sibaja et al., 2019) horse radish peroxidase and a peroxidase extracted from *Alium sativum* (Tripathi and Mishra, 2011) were shown to degrade AFB_1 *in vitro* up to 90%, 57%, 97% and 70%, respectively. Direct comparisons between these studies and our results is not feasible since we used lower concentrations of enzyme and H_2O_2, along with higher amounts of AFB_1. For instance, Marimon-Sibaja and colleagues et al. (2019) used an enzyme/AFB_1 ratio and a H_2O_2 concentration 200 and 20 times higher, respectively, than the one used in this study. A total of 0.4 U/mL were used by Yehia (2014) to obtain a percentage of degradation after 24 h of reaction similar to that reported in our study but only using 0.003 μg/mL of AFB_1 (Yehia, 2014). The findings of our study may have a high impact also for the applicability and sustainability of the enzymatic detoxification process. A first important point is that Rh_DypB is a recombinant enzyme produced in fairly large amounts (100 mg/L). Secondly, the process is effective at low H_2O_2 and enzyme amounts. These points are of main relevance to guarantee the economic sustainability of this biotransformation method. In addition, using mild conditions and low enzyme and H_2O_2 dosages will limit the possible side reactions in a complex material, such as contaminated vegetable commodities.

3.2. Kinetic measurements

The kinetic parameters of Rh_DypB on AFB_1 were determined up to 3.5 μg/mL to ensure a homogeneous mycotoxin concentration in aqueous solution (the maximal mycotoxin concentration used is limited by the poor solubility in aqueous solution, ≤ 10 μg/mL, and the need to avoid interferences from the solvents used for mycotoxin solubilization). The experimental data were fitted using a classical Michaelis-Menten equation as shown in Fig. 2. In the substrate range assayed, the plot is rather linear, indicating that the substrate concentration is far from saturating the enzyme. A maximal rate of ≈0.002 (0.0021 ± 0.0005) μg/mL per min and a K_m of ≈3.2 (3.2 ± 0.6) μg/mL were estimated.

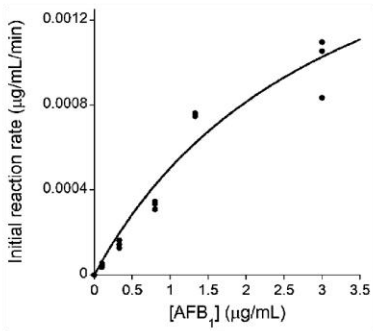

Fig. 2. Michaelis-Menten plot of the rate of conversion after 24 h vs. AFB_1 concentration for 0.1 U/mL Rh_DypB using 0.1 mM H_2O_2 in 50 mM sodium malonate buffer, pH 6.0, at 25 °C.

3.3. High resolution LC-MS/MS analyses of AFB_1 degradation products

AFB_1 showed good ionization efficiency in positive ion mode; the analyte was observed as both the $[M+H]^+$ and $[M+Na]^+$ molecular ion *m/z* 313.0706 and 335.0526.

The ability of Rh_DypB to degrade AFB_1 was also confirmed by high resolution LC-MS analysis (Fig. 3). Following 48 h of reaction at 25 °C of AFB_1 under assay condition A, a marked reduction (61%) of AFB_1 was measured, in accordance with the results obtained by HPLC analyses.

The total ion current chromatograms of the control and Rh_DypB samples were compared for the occurrences of additional peaks that could represent the chemical product of the AFB_1 reaction (Fig. 4). An additional distinct peak (marked with an asterisk in Fig. 4) was observed in the Rh_DypB sample, which was not detected in the control and in reference AFB_1.

Closer inspection of the unknown peak at retention time 2.83 revealed a *m/z* of 351.0475, corresponding to a formula of a sodiated AFB_1 metabolite $[C_{17}H_{12}O_7 + Na]^+$ (−0.01 ppm). This formula represents the addition of a single oxygen to AFB_1 and has the same formula as the known compounds: AFG_1, AFM_1, AFQ_1 and 8,9-AFB_1

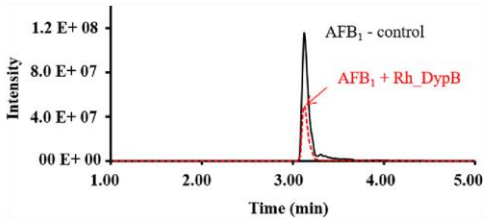

Fig. 3. Extracted ion current chromatograms of aflatoxin B_1 (AFB_1) following 48 h control treatment (black) or Rh_DypB treatment (red). (For interpretation of the references to color in this figure legend, the reader is referred to the Web version of this article.)

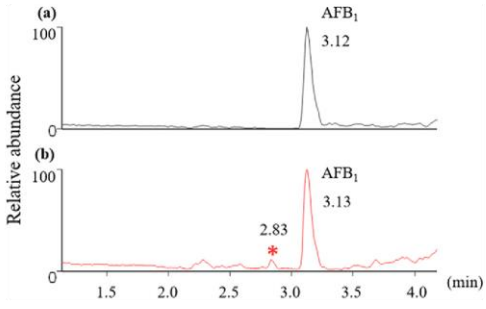

Fig. 4. Total ion chromatograms of (a) AFB_1 control and (b) AFB1+DypB after 48 h of incubation.

epoxide. Comparing the MS/MS spectrum of the unknown AF metabolite to equivalent spectra of AFG_1, AFM_1 (https://massbank.eu/: AC000034, AC000037, AC000046, AC000049), allowed exclusion of AFM_1 and AFG_1 (Fig. 5). Indeed, 8,9-AFB_1 epoxide is known to undergo rapid hydrolysis to AFB_1-dihydrodiol (Johnson et al., 1996), indicating that it is not the observed product.

The unknown Rh_DypB reaction product had a diagnostic product ion at *m/z* 141.0182, corresponding to a formula of $C_6H_5O_4^+$. This product ion suggests that the additional oxygen has been added to the ring A portion of the molecule. The fluorescence of the assay mixture did not decrease over time (data not shown), suggesting that adding oxygen did not disrupt the double bond of ring A, one of the determinant chemical features for AFs fluorescence (Vazquez et al., 2010). AFQ_1 is a known AFB_1 metabolite, which contains a hydroxyl group on the 3α position of ring A. Although this compound is no longer commercially available, the MS/MS spectra was generously provided by Dr. De Boevre (see Supplementary Fig. 1).

Although it was not possible to fully compare the MS/MS spectra obtained in this study (acquired on a Thermo Q-Exactive Orbitrap) with the spectra acquired on a Waters Synapt TOF, there are several diagnostic ions that match between the spectra, notably, *m/z* 283.0599, 206.0574 and 177.0547. Based on these, we concluded that it is highly likely that AFB_1 was hydroxylated by Rh_DypB into AFQ_1.

Any proposed enzymatic treatment of mycotoxins, especially AFB_1, requires careful identification of the reaction products, as they themselves may be equally or even more toxic than the original toxin. For example, the carcinogenicity of AFB_1 is primarily a result of the exo 8,9-epoxyAFB_1, which forms adducts with DNA, reacting with the guanyl N7 (Doerge et al., 2018). Moreover, the identification of the AFB_1 reaction products can be a difficult task since AFB_1 possesses a number of sites where enzymes can act (Bonomo et al., 2017). AFB_1 degradation products by peroxidase were questioned

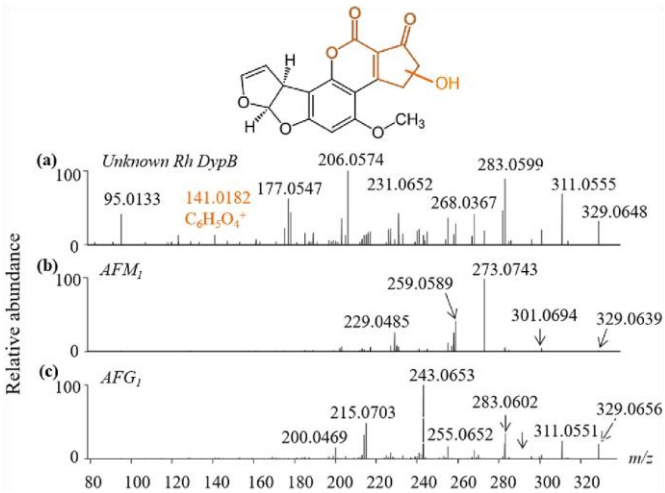

Fig. 5. MS/MS spectra of (a) unknown Rh_DypB product, (b) AFM_1 and (c) AFG_1. Arrows indicate diagnostic product ions.

since the late 70s by Doyle and Marth (1979) and more recently by Wang et al. (2011). In the latter case, oxidation to 8,9-epoxyAFB$_1$ leading to AFB$_1$-8,9-dihydrodiol (the rapid hydrolysis product of 8,9-AFB$_1$ epoxide) was found. In humans, four major metabolic pathways have been described for AFB$_1$: epoxidation to 8,9-epoxyAFB$_1$, ketoreduction to aflatoxicol (AFL), hydroxylation to AFM$_1$, and AFQ$_1$, and demethylation to AFP$_1$ (Deng et al., 2018). This wide variety of possible products is due to the fact that peroxidase can catalyze different reactions, including breaking carbon-carbon bonds, benzylic oxidative cleavage, ortho-demethylation, N-methylation, epoxidation and hydroxylation.

In our study, after Rh_DypB biotransformation, neither 8,9-AFB$_1$ epoxide nor AFB$_1$-8,9-dihydrodiol were detected by LC-MS/MS, suggesting that the C—H hydroxylation pathway is favored compared to the epoxidation of the alkene. Oxidative demethylation was also excluded, as no stable demethylated AFB$_1$ was found. This finding is extremely important because we can exclude the production of 8,9-epoxy-AFB$_1$, the more toxic oxidation product of cytochromes and other peroxidases. AFQ$_1$ was the main product. However, the presence of small quantities of low molecular mass compounds cannot be excluded.

Hsieh et al. (1974) reported that AFQ$_1$ was an order of magnitude less toxic than AFB$_1$ in the chicken embryo test and suggested that it was not mutagenic in an Ames assay. However, a re-analysis of these data indicated a mutagenic activity of AFQ$_1$ (Campbell and Hayes, 1976; Eaton and Gallagher, 1994). Based on available data, AFQ$_1$ has a lower acute toxicity and mutagenicity than AFB$_1$. In rainbow trout, AFQ$_1$ toxicity is ~1% of AFB$_1$, noting that rainbow trout is generally considered the most sensitive species to AFB$_1$ (Eaton and Gallagher, 1994). In mammals, glucuronide and sulphate conjugates are formed prior to the excretion of AFQ$_1$ in urine and feces, thus providing an effective detoxification pathway (Eaton et al., 2010).

4. Conclusions

Rh_DypB peroxidase proved to be an efficient AFB$_1$ biotransformation agent, being effective at low enzyme and H_2O_2 dosages and catalyzing the hydroxylation to AFQ$_1$. Up to 96% of bioconversion was obtained after 96 h of reaction with only 0.1 U/mL of Rh_DypB and 0.1 mM of H_2O_2. Elucidating that Rh_DypB does not catalyze the epoxidation of AFB$_1$, but its hydroxylation to a less toxic metabolite, AFQ$_1$, is a crucial step for the development of a true and safe detoxification process using peroxidases. This application could be of great interest for the treatment of commodities highly contaminated with AFB$_1$ and intended as feed. The main limitation of this study is the lack of evaluation of the enzyme's performance on real matrices and under operational conditions that can significantly affect mycotoxin bioconversion. Therefore, further studies are needed to validate this method in natural contaminated matrixes. Nonetheless, the results presented in this study greatly contribute to expanding the current knowledge on AFB$_1$ biotransformation by Rh_DypB, its reaction products and the range of possible applications of this versatile biocatalyst.

Declaration of competing interest

The authors declare that they have no known competing financial interests or personal relationships that could have appeared to influence the work reported in this paper.

CRediT authorship contribution statement

Martina Loi: Conceptualization, Investigation, Writing - original draft, Writing - review & editing. **Justin B. Renaud:** Methodology, Investigation, Writing - review & editing. **Elena Rosini:** Methodology, Writing - review & editing. **Loredano Pollegioni:** Methodology, Writing - review & editing. **Elisa Vignali:** Investigation. **Miriam Haidukowski:** Investigation, Methodology. **Mark W. Sumarah:** Supervision, Writing - review & editing. **Antonio F. Logrieco:** Supervision, Funding acquisition, Writing - review & editing. **Giuseppina Mulè:** Supervision, Writing - review & editing.

Acknowledgments

We acknowledge Dr. Marthe De Boevre and Prof. Dr. Sarah De Sager for providing the AFQ$_1$ MS/MS spectra. We thank Prof. J. David Miller for helpful comments on the manuscript. The authors acknowledge Dr. Simonetta Martena and Dr Giuseppe Panzarini of the Institute of Sciences of Food Production—CNR for the skilled technical support provided during the realization of this work. This work was financially supported by H2020-E.U.3.2—678781-MycoKey-Integrated and innovative key actions for mycotoxin management in the food and feed chain. EV is a PhD student of the "Life Sciences and Biotechnology" course at Università degli Studi dell'Insubria.

Appendix A. Supplementary data

Supplementary data to this article can be found online at https://doi.org/10.1016/j.chemosphere.2020.126296.

References

Association of Official Analytical Chemists (Aoac), 2000. Official Method 971, 2988.
Bhutta, Z.A., Berkley, J.A., Bandsma, R.H., Kerac, M., Trehan, I., Briend, A., 2017. Severe childhood malnutrition. Nature reviews Disease primers 3, 17067.
Bonomo, S., Jørgensen, F.S., Olsen, L., 2017. Dissecting the cytochrome P450 1A2-and 3A4-mediated metabolism of aflatoxin B1 in ligand and protein contributions. Chemistry—A European Journal 23 (12), 2884—2893.
Campbell, T.C., Hayes, J.R., 1976. The role of aflatoxin metabolism in its toxic lesion. Toxicol. Appl. Pharmacol. 35 (2), 199—222.
Chitrangada, Das, Mishra, H.N., 2000. In vitro degradation of aflatoxin B$_1$ by horse radish peroxidase. Food Chem. 68 (3), 309—313.
Deng, J., Ling, Z., Ni-Ya, Z., Karrow, N.A., Christopher, S.K., De-Sheng, Q., Lv-Hui, S., 2018. Aflatoxin B1 Metabolism: Regulation by Phase I and II Metabolizing Enzymes and Chemoprotective Agents. Mutation Research/reviews in Mutation Research.
Doerge, D.R., Shephard, S.G., Adegoke, G.O., Benford, D., Bhatnagar, D., Bolger, M., Boon, P.E., Cressey, P., Edwards, S., Hambridge, T., Miller, J.D., Mitchell, N.J., Riley, R.T., Wheeler, M.W., 2018. Aflatoxins (Addendum) in Safety Evaluation of Certain Contaminants in Food, WHO FOOD ADDITIVES SERIES: 74 FAO JECFA Monographs 19 Bis, pp. 3—280.
Doyle, M.P., Marth, E.H., 1979. Peroxidase activity in mycelia of *Aspergillus parasiticus* that degrade aflatoxin. Eur. J. Appl. Microbiol. Biotechnol. 7 (2), 211—217.
Eaton, D.L., Gallagher, E.P., 1994. Mechanisms of aflatoxin carcinogenesis. Annu. Rev. Pharmacol. Toxicol. 34 (1), 135—172.
Eaton, D.L., Beima, K.M., Bammler, T.K., Riley, R.T., Voss, K.A., 2010. Hepatotoxic mycotoxins. Comprehensive Toxicology 9, 527—569.
Hsieh, D.P., Salhab, A.S., Wong, J.J., Yang, S.L., 1974. Toxicity of aflatoxin Q1 as evaluated with the chicken embryo and bacterial auxotrophs. Toxicol. Appl. Pharmacol. 30 (2), 237—242.
Johnson, W.W., Harris, T.M., Guengerich, F.P., 1996. Kinetics and mechanism of hydrolysis of aflatoxin B1 exo-8, 9-epoxide and rearrangement of the dihydrodiol. J. Am. Chem. Soc. 118 (35), 8213—8220.
Karlovsky, P., Suman, M., Berthiller, F., De Meester, J., Eisenbrand, G., Perrin, I., et al., 2016. Impact of food processing and detoxification treatments on mycotoxin contamination. Mycotoxin Res. 32 (4), 179—205.
Leslie, J.F., Logrieco, A. (Eds.), 2014. Mycotoxin Reduction in Grain Chains. Wiley Blackwell, Hoboken, NJ.
Loi, M., Fanelli, F., Zucca, P., Liuzzi, V., Quintieri, L., Cimmarusti, M., Monaci, L., Logrieco, A.F., Mulè, G., 2016. Aflatoxin B$_1$ and M$_1$ degradation by Lac 2 from *Pleurotus pulmonarius* and redox mediators. Toxins 8 (9), 245.
Loi, M., Fanelli, F., Liuzzi, V., Logrieco, A., Mulè, G., 2017. Mycotoxin biotransformation by native and commercial enzymes: present and future perspectives. Toxins 9 (4), 111.
Loi, M., Fanelli, F., Cimmarusti, M.T., Mirabelli, V., Haidukowski, M., Logrieco, A.F., Caliandro, R., Mule, G., 2018. *In vitro* single and combined mycotoxins degradation by Ery 4 laccase from *Pleurotus eryngii* and redox mediators. Food Contr. 90, 401—406.
Marimón Sibaja, K.V., de Oliveira Garcia, S., Feltrin, A.C.P., Diaz Remedi, R.,

Cerqueira, M.B.R., Badiale-Furlong, E., Garda-Buffon, J., 2019. Aflatoxin biotransformation by commercial peroxidase and its application in contaminated food. J. Chem. Technol. Biotechnol. 94 (4), 1187–1194.
McMillan, A., Renaud, J.B., Burgess, K.M., Orimadegun, A.E., Akinyinka, O.O., Allen, S.J., Miller, D.J., Reid, G., Sumarah, M.W., 2018. Aflatoxin exposure in Nigerian children with severe acute malnutrition. Food Chem. Toxicol. 111, 356–362.
Pitt, J.I., Wild, C.P., Baan, R.A., Gelderblom, W.C.A., Miller, J.D., Riley, R.T., Wu, F., 2012. Improving Public Health through Mycotoxin Control. International Agency for Research on.
Pollegioni, L., Tonin, F., Rosini, E., 2015. Lignin-degrading enzymes. FEBS J. 282 (7), 1190–1213.
Rushing, B.R., Selim, M.I., 2019. Aflatoxin B_1: a review on metabolism, toxicity, occurrence in food, occupational exposure, and detoxification methods. Food Chem. Toxicol. 124, 81–100.
Tonin, F., Vignali, E., Pollegioni, L., D'Arrigo, P., Rosini, E., 2017. A novel, simple screening method for investigating the properties of lignin oxidative activity. Enzym. Microb. Technol. 96, 143–150.
Tripathi, S., Mishra, H.N., 2011. Modeling and optimization of enzymatic degradation of aflatoxin B 1 (AFB 1) in red chili powder using response surface methodology. Food Bioprocess Technol. 4 (5), 770–780.
Vazquez, I.N., Albores, A.M., Martınez, E.M., Miranda, R., Castro, M., 2010. Role of lactone ring in structural, electronic, and reactivity properties of aflatoxin B1: a theoretical study. Arch. Environ. Contam. Toxicol. 59, 393–406.
Vignali, E., Tonin, F., Pollegioni, L., Rosini, E., 2018. Characterization and use of a bacterial lignin peroxidase with an improved manganese-oxidative activity. Appl. Microbiol. Biotechnol. 102 (24), 10579–10588.
Wang, J., Ogata, M., Hirai, H., Kawagishi, H., 2011. Detoxification of aflatoxin B_1 by manganese peroxidase from the white-rot fungus *Phanerochaete sordida* YK-624. FEMS Microbiol. Lett. 314 (2), 164–169.
Wang, X., Qin, X., Hao, Z., Luo, H., Yao, B., Su, X., 2019. Degradation of four major mycotoxins by eight manganese peroxidases in presence of a dicarboxylic acid. Toxins 11 (10), 566.
Wild, C.P., Miller, J.D., Groopman, J.D. (Eds.), 2015. Mycotoxin Control in Low-And Middle-Income Countries. International Agency for Research on Cancer, Lyon, France.
World Health Organization, 2019. Safety Evaluation of Certain Contaminants in Food: Prepared by the Eighty-Fourth Meeting of the Joint FAO/WHO Expert Committee on Food Additives (JECFA).
Yehia, R.S., 2014. Aflatoxin detoxification by manganese peroxidase purified from *Pleurotus ostreatus*. Braz. J. Microbiol. 45 (1), 127–134.

Enzymatic oxidative valorization of technical lignins and their fractions: a quantitative approach

Introduction

Lignin is an optically inactive three-dimensional aromatic polymer constituted of substituted phenylpropane units (Berlin and Balakshin, 2014; Ponnusamy et al., 2019) and it represents the first renewable source of aromatics on Earth. Therefore, strategies to obtain high value-added aromatic compounds from its degradation are constantly studied and improved (Zakzeski et al., 2010; Schutyser et al. 2018; Banu et al., 2019; Ponnusamy et al., 2019). The thermo-chemical approaches to perform lignin depolymerisation, based on the use of inorganic catalysts (e.g. metals) and extreme incubation conditions in terms of pH and temperatures, allowed the almost complete depolymerisation of various lignin samples, but with the formation of complex and heterogeneous mixtures of degradation products (Beckham et al., 2016; Schutyser et al. 2018). On the other hand, the biological approaches are based on the use of microbial cells and enzymes. Bacterial degradation of kraft lignin generated several aromatic lignin-related compounds, e.g. guaiacol, acetoguaiacone, gallic acid and ferulic acid from treatment with *Aneurinibacillus aneuriniltycus* and 3,4,5-trimethoxybenzaldeyde and ferulic acid from *Bacillus* sp. (Raj et al., 2007), ethanediol, *p*-hydroxybenzoic acid and vanillic acid from *Novosphingobium* sp. B-7 (Chen et al., 2012). As a general rule, the produced amount of aromatics was low, frequently avoiding a quantification. For recent reviews on microbial degradation of lignins see (Asina et al., 2017; Becker and Wittman, 2019). On the other hand, enzymes (e.g., laccases and peroxidases) act under mild reaction conditions and allow highly selective and specific cleavages of the lignin polymer (Lancefield et al., 2016; Pollegioni et al., 2016; Rosini et al., 2016; Chen and Wan, 2017; Picart et al., 2017; Zhu et

al., 2020). The limit in the use of biological approaches mainly concerns the lower depolymerisation yields than the chemical ones, which are comprised between the 65% under specific acidic treatments up to the complete mineralisation in the case of pyrolytic and gasification treatments (Beckham et al., 2016; Agarwal et al., 2018; Schutyser et al., 2018). In this view, the identification of the optimal experimental conditions (i.e. amount of enzyme, incubation time, temperature, pH, …) is fundamental to improve the degradation yields. During the years various works reported the main molecules released from lignin samples following enzymatic treatments (Rashid et al., 2015; Lancefield et al., 2016), but frequently only a qualitative analysis was reported. Quantitative analyses reported a ≈ 12.5% (w/w) oily fraction of low-molecular weight compounds (Wiermans et al., 2013; Picart et al., 2017) or < 0.5 mg/g lignin for selected molecules (Reiter et al., 2013; Singh et al., 2013).

The aim of the present work consists in a quantitative comparison of the degradation products obtained from enzymatic treatments using four oxidative activities on three technical lignins (i.e. softwood lignosulfonate, softwood kraft lignin and wheat straw lignin) following the identification of optimized conditions. Firstly, more than 48 enzyme/lignin combinations were analysed at different times through a rapid, miniaturised colorimetric screening method (Tonin et al., 2017). Then, the optimal identified conditions were assayed in a scaled-up treatment, and the obtained products were extracted with ethyl acetate and quantified by GC-MS analysis. In addition, with the purpose of better identifying the efficacy of the treatment on the various lignin constituents, both kraft and wheat straw organosolv lignin were subjected to an acetone-aided fractionation prior to the depolymerisation step. The high heterogenicity of the lignin structure is well-known, and solvent fractionation represents a simple and quick approach to achieve more homogenous cuts (Gigli and Crestini, 2020). The obtained results provided, for the first time, a

deep investigation not only of the main degradation products from enzymatic treatment of lignins, but especially of their abundance.

Materials and Methods

1. Reagents and enzymes

Softwood Kraft Lignin (SKL), Wheat Straw Lignin (WSL) and Softwood Lignosulfonate (SLS) were kindly provided by Stora Enso (Helsinki, Finland), Compagnie Industrielle de la Matière Végétale (CIMV, Paris, France) and Borregaard (Sarpsborg, Norway), respectively, and used as received. The laccase from *Bacillus licheniformis* (BALL) and the manganese superoxide dismutase from *Sphingobacterium spiritivorum* T2 (MnSOD-1) recombinant enzymes were expressed and purified as reported in (Tonin et al., 2016) and in the Supplementary Materials (see Figures S1-S5 for MnSOD-1 characterization). The laccase from *Funalia trogii* (Lac F) was provided by ASA Spezialenzyme GmbH. The laccase from *Trametes versicolor* (Lac C), 2,2,6,6-tetramethylpiperidine 1-oxyl (TEMPO), 2,2′-azino-bis(3-ethylbenzothiazoline-6-sulfonic acid) diammonium salt (ABTS), 1-hydroxybenzotriazole (HBT), *N*-hydroxyphthalimide (HPI), violuric acid (VA), 2,4-dinitrophenylhydrazine (2,4-DNP), 1,2,3-trihydroxybenzene (pyrogallol), 3,4-dimethoxybenzyl alcohol and ethyl acetate (ACS grade) were purchased from Merck (Merck KGaA, Darmstadt, Germany).

2. Enzymatic assays

Enzymatic activities were assayed at 25 °C with a thermostated Jasco V-580 spectrophotometer (Jasco, Cremella, Italy) as follows. The laccase activity was determined by monitoring the oxidation of 0.5 mM ABTS ($\varepsilon_{420\ nm}$ = 36 mM^{-1} cm^{-1}) at 420 nm in 50 mM sodium acetate, pH 5.0 (Tonin et al., 2016). One enzymatic unit is defined as the amount of enzyme which converts 1 µmol of substrate per min.

The superoxide dismutase activity of MnSOD-1 was determined using the autoxidation pyrogallol assay by monitoring the change of absorbance at 325 nm of the pyrogallol, for 5 min, at 25 °C (He et al., 2007; Li, 2012). The assay was performed in 100 mM Tris-HCl, pH 8.2, 0.1 mM EDTA buffer using 0.25 mM pyrogallol (100 mM stock dissolved in 10 mM HCl). One enzymatic unit is defined as the amount of enzyme that inhibits the autoxidation rate of pyrogallol by 50% (Marklund and Marklund, 1974).

3. Lignin samples: fractionation methods and structural characterization

Acetone soluble (AS) and acetone insoluble (AI) fractions were prepared by suspending SKL and WSL powders (at a concentration of 5 mg/mL) in acetone and letting them dissolve at 23 °C under mild stirring for 12 hours. The AI fraction was collected by filtration and dried under vacuum at 30 °C, while the AS fraction was recovered by solvent removal in a rotavapor at 30 °C. Four samples, acetone soluble kraft lignin (ASKL, 68.7%), acetone insoluble kraft lignin (AIKL 31.3%), acetone soluble wheat straw lignin (ASWL, 75.0%) and acetone insoluble wheat straw lignin (AIWL, 25.0%) were thus obtained with the indicated yields.

Quantitative ^{31}P NMR analysis was performed on lignin samples in accordance with a previously described procedure (Meng et al., 2019). Briefly, a weighed amount of sample (30 mg) was dissolved in a pyridine/CDCl3 1.6:1 mixture phosphitylated by reaction with Cl-TMDP. Cholesterol was used as internal standard. The spectra were recorded by collecting at least 256 scans on a 300 MHz Bruker instrument.

GPC was carried out on a Shimadzu HPLC system equipped with a Plgel MiniMIX-C column. HPLC-grade DMSO containing 0.1% lithium chloride was employed as eluent (0.2 mL/min, 70 °C). Standard calibration was

performed with polystyrene sulfonate standards (Merck, Mw range 4.3–2600 kDa) and lignin low-molecular weight models (170–941 Da).

4. Enzymatic treatment of unfractionated lignins: screening and scale up

The optimal incubation conditions for the oxidation/degradation of technical lignins (SKL, WSL, and SLS) were identified using a rapid, miniaturising colorimetric screening as previously reported by (Tonin et al., 2017). In particular, lignin samples were dissolved at 50 mg/mL in 50 mM sodium acetate, pH 5.0, with the addition of 20% DMSO in the case of WSL samples. In details, 0.5 mg lignin were incubated with Lac C, Lac F or BALL (0.2 U/mg lignin) enzymes in the presence of 2 mM mediator (i.e. ABTS, TEMPO, HBT, HPI or violuric acid) in 50 mM sodium acetate, pH 5.0 (1 mL final volume). The WSL (4.5 mg) was incubated with MnSOD-1 enzyme (1 U/mg lignin) in the presence of 1 mM pyrogallol, in 50 mM Tris-HCl, pH 8.2, 0.1 mM EDTA. In parallel, control reactions in the absence of enzyme were carried out. All samples were incubated at 30 °C on a rotary wheel: 20 µL of sample were withdrawn at different times (15 min, 2, 5, 24, 30, 48 h) and added of 30 µL of 0.1 N HCl to be analysed in a 96-well microtiter plate with the colorimetric screening procedure. In details, after 5 min of incubation at 25 °C with 50 µL of 1 mM 2,4-DNP (dissolved in 0.1 N HCl), the color was generated by adding 0.1 mL of 1 N NaOH: the absorbance value at 450 nm was measured with a microtiter plate reader (Sunrise, Tecan, Italy). The steps for the microplate setting up were performed using the automated system epMotion 5075 (Eppendorf, Italy). Each sample was analysed in duplicate.

On the basis of the screening results, the optimal combinations of lignin and enzyme (i.e. SLS/Lac C/TEMPO, WLS/Lac F/ABTS, SKL/BALL/TEMPO, and WLS/MnSOD-1) were scaled up to be analysed in GC-MS. In details: a) 40 U laccase (0.2 U laccase/mg lignin) and 2 mM mediator in 50 mM sodium

acetate, pH 5.0, were incubated in a 0.3 L baffled flask containing lignin (5 mg/mL final concentration); b) 0.2 g of WSL, and 0.1 g of AIWL or ASWL were incubated in a 0.5 L baffled flask (1 mg/mL final concentration) with 700 U MnSOD-1 (3.5 U enzyme/mg lignin) in 50 mM TrisHCl, pH 8.2, 1 mM EDTA; c) control reactions in the absence of enzyme. Samples were incubated for 24 h (1 h for WLS/MnSOD-1 enzyme/lignin combination) at 30 °C under 100 rpm shaking.

5. Enzymatic treatment of lignin fractions

ASKL, AIKL, ASWL and AIWL lignin fractions were prepared at 40 mg/mL by adding 0.5 mL 1 N NaOH to the dried powder and bringing to volume with the appropriate buffer.

The ASKL and AIKL (0.1 g, 20 mL, 5 mg/mL), and the ASWL and AIWL samples (0.2 g, 40 mL, 5 mg/mL) were incubated for 2 h at 30 °C under shaking (100 rpm) in 0.3 L baffled flasks in the presence of BALL laccase and 2 mM TEMPO mediator, and Lac F laccase and 2 mM ABTS mediator (0.2 U enzyme/mg lignin), respectively, in 50 mM sodium acetate buffer, pH 5.0. To avoid repolymerization, 2-hours reaction time was used. Furthermore, the ASWL and AIWL (0.1 g, 100 mL, 1 mg/mL) were also incubated in 0.5 L baffled flasks in the presence of 1 mM pyrogallol and 414 U MnSOD-1 (4.14 U/mg lignin) in 50 mM Tris-HCl, pH 8.2, 1 mM EDTA. Samples were incubated for 1 h at 30 °C under a 100 rpm shaking. For all the enzymatic treatments of lignin fractions, reaction controls in the absence of the enzyme were carried out.

6. Solvent extraction and GC-MS analyses

At the end of the incubation, the pH was adjusted to 1.0 by adding 1 N HCl. Subsequently, 1 and 10 mg of 3,4-dimethoxybenzyl alcohol as internal standard (IS) were added to the fractionated and unfractionated lignin

samples, respectively. The extraction of the acidified samples was carried out using ethyl acetate as aprotic solvent in a 3:1 (v/v) ratio. The organic phase was collected, dewatered over anhydrous Na_2SO_4, filtered through Whatman filter paper and dried in a rotary evaporator.

Mass spectrometric analyses of the lignin extracts were performed on acetone-dissolved samples (0.1 mg/mL) before and after *in situ* silylation using N,O-bis(trimethylsilyl)trifluoroacetamide in the presence of dry pyridine. Gas chromatographic separation of the samples was accomplished using a Shimadzu GCMS QP2010 Ultra system (gas chromatograph GC2010 Plus, equipped with Shimadzu autosampler AOC20i) at 70 eV ionization energy. A Supelco fused-silica capillary column SLB-5 ms (30 m long, 0.25 mm thick, 0.25 μm diameter) was used as stationary phase, He (UHP grade) as mobile phase. The system was operated in "linear velocity mode" with a starting pressure of 100 kPa, 280 °C injection temperature, and 200 °C interface temperature, running the following temperature program: 50 °C start temperature for 1 min, 10 °C min^{-1} heating rate, 280 °C final temperature for 15 min. System control and analyses were carried out on a Shimadzu analysis software package Labsolutions–GCMSsolution Version 2.61.

The amount of each compound (m_P) extracted in the organic phase has been quantified as follows:

$$m_P = A_P/A_{IS} \times m_{IS} \times rf_{IS} \qquad (1)$$

where m_{IS} is the mass of the internal standard added, A_P and A_{IS} are the peak areas of the product and of the internal standard, respectively, and rf_{IS}, equal to 0.791, is the fraction of the IS retained in the organic phase after the extraction step.

Results and discussion

1. Structural characterisation of lignin samples

The number-average molecular weight (M_n) and the polydispersity index (PDI = M_W/M_n) of the unfractionated and fractionated lignins, determined by GPC, are shown in Table 1. The PDI of the pristine lignins (i.e. SKL, WSL, and SLS) is fairly large, confirming the heterogeneous nature of this material (Table 1). On the other hand, the fractions highlight a lowering of the PDI with respect to the pristine lignins, indicating that more homogeneous cuts were obtained, in agreement with literature reports (Gigli and Crestini, 2020). By comparing the two fractions of kraft lignin, it can be noticed that AIKL and ASKL display quite different characteristics. Specifically, AIKL shows a higher molecular weight and content of aliphatic OH groups and a lower concentration of phenolic OH functionalities with respect to ASKL (Table 1), being constituted of polymeric and less degraded lignin fragments containing aliphatic side chains. On the other hand, ASKL mainly contains highly branched oligomeric structures. (Crestini et al. 2017)

Table 1. Properties (hydroxyl group content and molecular weight) of lignin samples.

Lignin sample	Aliphatic OH	Phenolic OH	Condensed OH	Carboxylic OH	G-type OH	H-type OH	M_n	PDI
	(mmol/g)						(g/mol)	
SKL	1.77	3.69	1.63	0.36	1.88	0.18	1150	4.1
ASKL	1.41	3.93	1.76	0.39	2.04	0.12	700	1.7
AIKL	2.17	2.51	1.3	0.18	1.10	0.10	2900	2.8
WSL	1.13	1.18	0.52	0.37	0.50	0.16	1550	12
ASWL	1.28	1.88	0.86	0.76	0.79	0.23	650	1.5
AIWL	2.35	2.76	1.43	0.22	1.21	0.12	2700	12
SLS	0.69	1.59	0.76	0.27	0.77	0.06	2500	5.8

PDI: polydispersity index; determined by: a) quantitative ^{31}P NMR spectroscopy; b) gel permeation chromatography in DMSO.

A similar trend was observed for WSL and its fractions. Specifically, AIWL shows a higher molecular weight than the unfractionated lignin and a still broad polydispersity, as already described (Lange et al., 2016). Conversely, the M_n of ASWL, which also displays a consistent reduction of the PDI as compared to both WSL and AIWL, is the lowest among the wheat straw-based samples. As observed in the case of kraft lignin, the higher concentration of aliphatic groups has been determined in the AIWL.

Lastly, SLS contains a low amount of OH groups, which is mainly due to the very low concentration of aliphatic hydroxyl groups as compared to the other lignins here characterized. In addition, a total content of sulphur equal to 6.3% was determined by elemental analysis.

2. Enzymatic treatments

2.1. Screening for optimal lignin/enzyme combinations

A rapid colorimetric screening method based on the selective reaction under basic conditions of 2,4-DNP with carbonyl groups was used to analyse the formation of oxidative degradation products after the incubation (30 °C) of technical SLS, WSL and SKL by Lac C, Lac F, BALL, and MnSOD-1 enzymes (Tonin et al., 2017). Samples were analyzed at different times (15 min, 2, 5, 24, 30, 48 h) and the recorded absorbance value at 450 nm was corrected by the absorption value of the respective control (incubation without enzyme). In this way, more than 48 different lignin/enzyme combinations were assayed, with more than 240 data collected. For the lignosulfonate (SLS), the absorbance maximum was observed after 24 h of incubation with Lac C and TEMPO (Figure 1A). The maximum absorbance responses for WSL were observed after 24 h of incubation with Lac C, Lac F and BALL laccases in the presence of ABTS (Figure 1B). Interestingly, the earlier significant increase in the absorbance at 450 nm was observed after 2 h of incubation of SKL with Lac F/TEMPO, but the maximal absorbance was reached with BALL/TEMPO

after 24 h (Figure 1C). Based on previous studies (Rashid et al., 2015; Lancefield et al., 2016), the treatment with MnSOD-1 was focused on wheat straw organosolv only. The best response for WSL was obtained after 1 h of incubation with MnSOD-1 (Figure S6). Since the absorbance at 450 nm is proportional to the carbonyl groups deriving from the oxidative lignin degradation (Tonin et al., 2017), the screening identified SLS/Lac C/TEMPO, WSL/Lac F/ABTS, SKL/BALL/TEMPO, and WLS/MnSOD-1 as the optimal combinations for the enzymatic oxidation/degradation of unfractionated lignins to be scaled up for GC-MS analyses.

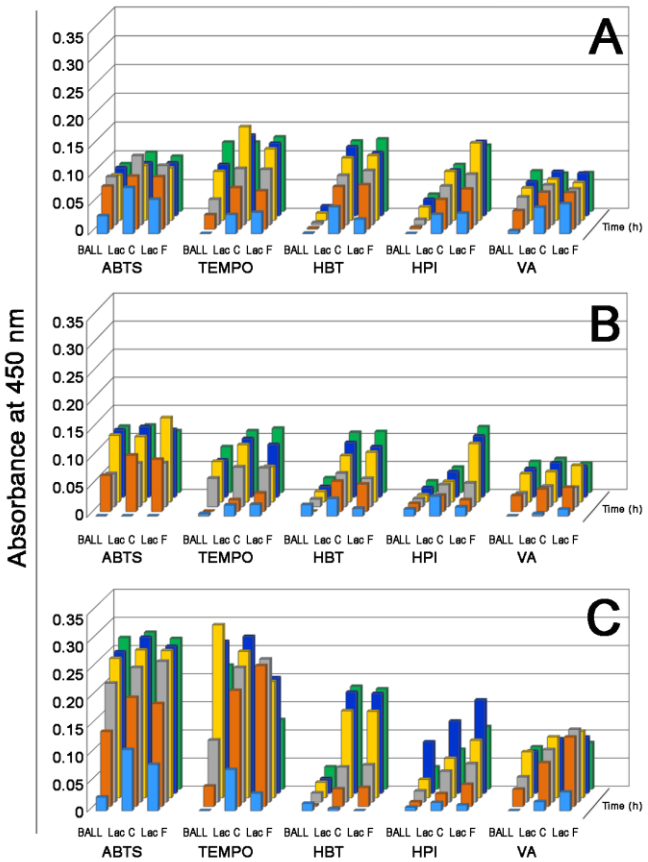

Figure 1. Identification of the optimal lignin/laccase/mediator combination to oxidize/degrade different lignins as detected by the colorimetric screening method. Different colours referred to different times of incubation: light blue: 15 min, orange: 2 h, grey: 5 h, yellow: 24 h, blue: 30 h, green: 48 h. A) Softwood lignosulphonate (SLS); B) wheat straw lignin (WSL); C) softwood kraft lignin (SKL).

2.2. Treatment of WSL and its fractions with Lac F/ABTS or MnSOD-1

WSL was incubated with Lac F and 2 mM ABTS, as well as with the MnSOD-1 enzyme. At the end of the incubation, followed by acidification to pH ≈ 1.0 and extraction with ethyl acetate, the oxidation products were analysed by GC-MS. Table 2 reports the amount (mg) of each product generated per gram of lignin, subtracted of the quantity measured in the control (without the enzyme). The results suggest that both enzymes cleave the lignin interunit bonds and promote the depolymerisation of branched chains, leading to the production of various aromatic compounds and, in a fewer cases, also to short chain aliphatic fragments.

Table 2. Compounds extracted in the organic phase after the treatment of WSL, ASWL and AIWS with Lac F/ABTS and MnSOD-1. The reported values represent the amount of extracted product (mg/g of lignin) in the organic phase as quantified by GC-MS analysis (subtracted of the quantity detected in the reaction control).

	Compound	Lac F/ABTS (mg/g)			MnSOD-1 (mg/g)		
		WSL	ASWL	AIWL	WSL	ASWL	AIWL
Aromatics	4-Methoxy acetophenone					0.448	
	Vanillin			0.023		0.280	0.108
	Veratraldehyde	0.067	0.516	13.02			0.065
	Homoveratric acid			0.280			0.055
	Veratric acid	1.167		1.990		0.131	0.056
	Isovanillic acid					0.208	
	Syringaldehyde			0.139		0.103	0.055
	Acetosyringone					0.148	
	Coniferyl alcohol					0.363	
	p-Coumaric acid						0.114
	Syringic acid				0.419		0.097
	Ferulic acid				0.289	0.858	0.657
	2,6-Dimethoxybenzoquinone	0.621	0.965	2.341			

Substituted biphenyls	4,4'-Dimethoxy-2,2'-dihydroxychalcone			1.324			
	2,2',3,3'-Tetramethoxy-4-methyl-1,1'-biphenyl			0.959			
	2,2',3',3'-Tetramethoxy-1,1'-biphenyl			0.297			
	Diveratryl ether	0.142		2.289			0.118
	2-Hydroxy-2',4,4'-trimethoxy-1,1'-biphenyl			0.179		0.246	
Alkyl chains	Glycerol	0.063					

Lignin fractionation permitted to increase the amount of extracted products with respect to the pristine material (Figure 2).

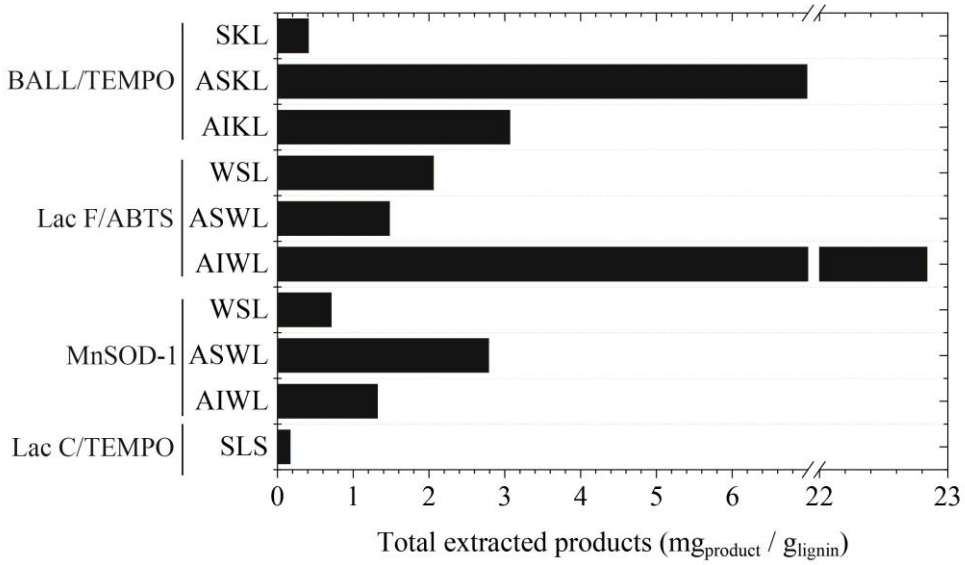

Figure 2. Total extracted products (mg/g of lignin) obtained after the enzymatic treatment. The values, quantified by GC-MS, are reported as net production, i.e. subtracted of the corresponding amounts present in the control without enzyme.

Furthermore, the collected data indicate a higher yield of total monomers produced in the lignin samples treated with LacF/ABTS with respect to those incubated in the presence of the MnSOD-1 enzyme. However, beside AIWL treated with LacF/ABTS, for which a production of almost 23 mg of low

molecular weight compounds per gram of lignin has been measured, all other samples do not significantly differ in terms of total extracted species, being in the range 1-2 mg/g (Figure 2). Conversely, the variety and the structure of the molecules generated by the two enzymes are quite different from sample to sample. A total of 13 different monoaromatics and 5 substituted biphenyls have been identified by quantitative analysis (Table 2). Interestingly, in the WSL treated with LacF/ABTS a very low amount of glycerol (about 0.06 mg/g of lignin) has been also detected. A wider number of compounds was apparent in the AIWL with respect to the WSL, irrespectively of the enzyme used for the oxidation. By calculating the relative content of each molecule extracted in the organic phase (Figure 3), it can be noticed that in the case of the LacF/ABTS system veratraldehyde, veratric acid and 2,6-dimethoxybenzoquinone are present in higher concentration in all samples.

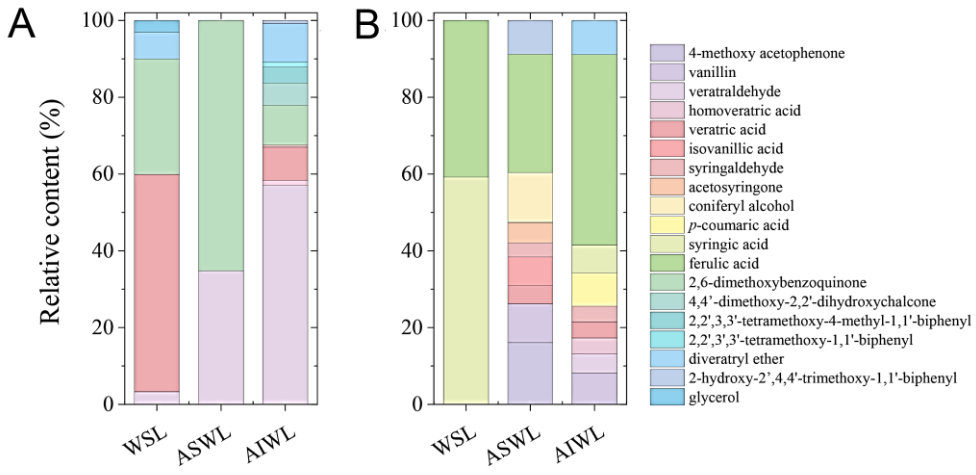

Figure 3. Relative content (%) of each product in the mixture of extracts after the treatment of WSL, ASWL and AIWL with the LacF/ABTS (A) and Mn-SOD-1 (B) enzymatic systems. Yields have been calculated in terms of net production, i.e. subtracted of the corresponding amounts present in the control without enzyme.

On the other hand, ferulic acid, and to a minor extent also coniferyl alcohol and *p*-coumaric acid, are the primary products when the oxidation treatment

is carried out on WSL, ASWL and AIWL in the presence of MnSOD-1. These molecules have not been detected in the lignin extracts treated with the Lac F/ABTS systems. It has been reported that a significant portion of the WSL aliphatic primary alcohols are esterified with coumaric and ferulic acid derivatives (Lange et al., 2016). Therefore, the presence of these molecules in the extracts of WSL, AIWL and ASWL treated with MnSOD-1 system indicates the ability of superoxide dismutase to cleave these end motifs, while laccase does not.

It can thus be concluded that MnSOD-1 mainly causes the formation of phenylpropanoid units (monolignols) with various degrees of oxidation, while by using the Lac F system phenolic moieties arising from Cα-Cβ cleavage (e.g., veratraldehyde and veratric acid) and from aryl-Cα cleavage (2,6-dimethoxybenzoquinone) are mostly extracted. Both enzymes did not lead to a complete oxidation of the depolymerised molecules, as in both cases either alcohols, aldehydes or acids were found. Additionally, it can be pointed out that the substituted biphenyls are mostly constituted of 5-5' motifs or dimeric species deriving from ether-containing moieties, such in the case of 4,4'-dimethoxy-2,2'-dihydroxychalcone and diveratryl ether.

The silylation supported the above discussed data although, as expected, additional compounds have been identified (Table S1). A total of 19 monoaromatic species, five biphenyls and two C3 alkyl chains have been distinguished, all ascribable to depolymerisation of the lignin chains. The trend observed in the quantitative analysis was confirmed, as unfractionated lignin displayed a lower variety of molecules, while a broader number of compounds have been extracted from the fractions (both ASWL and AIWL).

2.3. Treatment of SKL and its fractions with BALL/TEMPO

Based on preliminary results (Section 2.1), SKL and its fractions were incubated with BALL and 2 mM TEMPO at 30 °C for 24 h. The GC-MS

analyses of the extracted samples highlighted the presence of a number of oxidative products as compared with the corresponding controls, confirming the effectiveness of the laccase treatment. Moreover, it demonstrated that the yield of total extracted compounds, in the range 0.4 – 3.5 mg/g of lignin, depends on the starting materials, i.e. SKL, ASKL and AIKL (Figure 2). A total of 9 different compounds, whose structure arises from enzyme-mediated oxidative depolymerization of lignin backbone have been identified (Table 3). Five of them, i.e. apocynin, 4-ethoxy-3-methoxy-benzaldehyde, isoeugenol, vanillin and veratraldehyde are monomeric phenols with various substituents and degree of oxidation, while the other four are substituted biphenyls. Interestingly, no carboxylic acid were quantified in concentration higher than the control, although the presence of 5-methoxy-2-benzoic acid, vanillic acid, and 3-phenyl-2-propenoic acid and of one alkyl species, i.e. 2-propanoic acid, was detected after silylation (Table S2).

Table 3. Compounds extracted in the organic phase after the treatment of SKL, ASKL and AIKL with BALL/TEMPO and of SLS with Lac C/TEMPO. The reported values represent the amount of extracted product (mg/g of lignin) in the organic phase as quantified by GC-MS analysis (subtracted of the quantity detected in the reaction control).

	Compound	BALL/TEMPO (mg/g)			Lac C/ TEMPO (mg/g)
		SKL	ASKL	AIKL	SLS
Aromatics	Apocynin		2.447	0.350	
	4-ethoxy-3-methoxy-benzaldehyde		0.604		
	Diveratryl ether	0.273			
	Isoeugenol		0.565		
	Vanillin			0.350	
	Veratraldehyde	0.047	0.908	2.150	0.174
Substituted biphenyls	2-Hydroxy-2',4,4'-trimethoxy-1,1'-biphenyl	0.087	1.778	0.211	
	bis(4-Hydroxy-3-methoxy)-acetophenone		0.097	0.005	
	Secoisolariciresinol		0.590		

The fractionation not only allowed for the extraction of a wider variety of compounds, but also for an increase in the monomer production with respect to the pristine lignin. As a proof of evidence, the incubation of ASKL and AIKL with BALL/TEMPO respectively produced up to 0.9 mg/g and 2.1 mg/g of veratraldehyde, and 2.4 mg/g and 0.35 mg/g of apocynin, while from the unfractionated lignin much smaller amounts of veratraldehyde (0.05 mg/g) were recovered. The formation of apocynin was not observed. Interestingly, a significant concentration of diveratryl ether, probably deriving from the recombination of two disubstituted benzyl alcohol units, has been found in the extracts of treated SKL lignin (Figure 4). Conversely, this molecule was not identified after the enzymatic oxidative process carried out on the fractions.

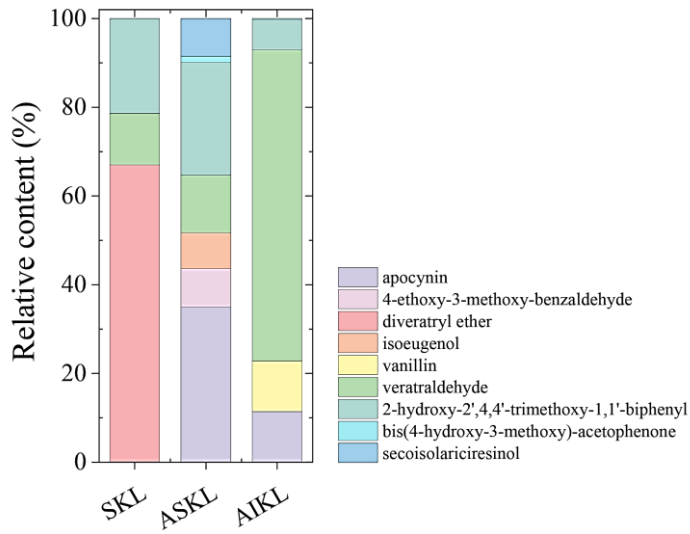

Figure 4. Relative content (%) of each product in the mixture of extracts after the treatment of SKL, ASKL and AIKL with the BALL/TEMPO enzymatic system. Yields have been calculated in terms of net production, i.e. subtracted of the corresponding amounts present in the control without enzyme.

2.4. Treatment of softwood lignosulfonate with Lac C/TEMPO

SLS was incubated with Lac C and 2 mM TEMPO. Afterwards, the treated sample (and the corresponding control in the absence of the enzyme) was acidified to pH ≈ 1.0, extracted with ethyl acetate and analysed by GC-MS.

The results show the production of the solely veratraldehyde, for which 0.174 mg/g were obtained in the organic phase, with a higher concentration than the control (Table 3). After silylation, also the reduced form of this compound, i.e. veratryl alcohol, was detected, a compound present in the control too. Interestingly, no sulphur-containing species have been extracted in the organic phase. This could be either due to the high water solubility of compounds bearing sulfonic acid moieties or to the inability of the laccase system in depolymerizing such motifs.

The total quantity of extracts is significantly lower in comparison to these figures achieved by the oxidative depolymerisation of kraft and organosolv lignins (in agreement with the few available literature about enzymatic treatments of lignosulfonates); on the other hand, a much higher selectivity was achieved as only veratryl alcohol-based species have been recovered from the reaction mixture.

Conclusions

A primary objective of bio-economy is to develop bio-based products, able to compete with their existing petroleum-based counterparts. Lignin depolymerisation, through selective and specific enzymatic treatments, is a key aspect in the biotechnological valorisation of this biopolymer (Pollegioni et al., 2015; Tonin et al., 2016). "You can make anything you want out of lignin" is a frequently heard statement in the scientific community or industry. In the present work, the technical softwood kraft lignin (SKL), wheat straw lignin (WSL) and softwood lignosulfonate (SLS) were incubated with different enzymes and the accumulation of oxidative/degradation products in each sample was monitored through a colorimetric screening (Tonin et al., 2017). By examining more than 240 experimental conditions, those resulting in the maximum intensity of absorbance at 450 nm for the three unfractionated lignin samples were chosen: SLS/Lac C/TEMPO, WSL/Lac F/ABTS,

SKL/BALL/TEMPO laccase/mediator systems (24 h of incubation) and WSL/MnSOD-1 (1 h of incubation). On this basis, the optimal enzyme/lignin combinations were scaled-up. The highest yield in terms of products extracted in the organic phase, calculated by subtracting the amount present in the corresponding untreated control, was obtained for the unfractionated and fractionated wheat straw lignin treated with the Lac F/ABTS laccase/mediator system (22.8 mg total monomers per gram of lignin), with veratraldehyde as the main degradation product (13 mg/g, Table 2). The lowest degree of depolymerisation was obtained in the case of lignosulfonate: only 0.17 mg/g of products were recovered. However, the enzymatic treatment on this sample displayed the highest selectivity among the tested materials, as the only detected product was veratraldehyde.

The amounts of recovered high-added value compounds also favourably compares with data reported in the literature. E.g., the treatment of lignin samples with the LigD/F/G systems yielded the highest productivity for vanillin, reaching a figure < 0.5 mg/g lignin after 50 h (Reiter et al., 2013).

Lastly, it is worth pointing out that the presence of monomers in the raw technical lignins correlates with the severity of pretreatment methods (e.g., kraft, organosolv and sulfonate processes) and it is defined by the broad polydispersity index (Vishtal et al., 2011; Constant et al., 2016). This may negatively affect the degradation yields during an enzymatic oxidative treatment (e.g., for the occurring of re-polymerisation reactions) (Pardo et al., 2018). As shown in Table 1, the unfractionated SKL, WSL and SLS samples are structurally heterogeneous and display wide PDI (i.e. 4.1, 12 and 5.8, respectively). In addition, the pretreatment of the biomass increases in the heterogeneity of technical lignins in terms of molar mass and functional groups distribution, ash and sulphur content, degree of condensation and organic impurities (Lange and Crestini, 2013; Constant et al., 2016). Since the features of the starting lignin play an important role to reach high enzymatic

degradation yields, a simple and green solvent-based fractionation method for the SKL and WSL samples was performed in order to both reduce the monomers content and increase the homogeneity of the lignin samples (Dominguez-Robles et al., 2018). Four lignin fractions (ASKL, AIKL, ASWL and AIWL, Table 1) were thus prepared and used for enzymatic degradation, showing in all the cases an improvement of the total depolymerisation yield in comparison with the unfractionated approach. More in detail, the enzymatic treatment of AI fractions generally resulted in a higher production of extracted monomers in comparison to those obtained from AS fractions.

In conclusion, this study reports a suitable strategy to identify the optimal enzymatic treatment for the degradation of the main technical lignins, i.e. kraft, organosolv and lignosulfonate. The miniaturised screening method (for the identification of the optimal enzyme/lignin incubation conditions) combined with the fractionation of lignin samples (for the obtainment of a more homogeneous starting material) allowed the identification of the most suited experimental setup to achieve improved degradation yields. Moreover, the developed degradation platform highlighted that starting from different raw materials, various added-value end products with different yields could be obtained, therefore representing a successful approach for lignin valorisation.

Keywords: lignocellulosic biomass; lignin depolymerization; ligninolytic enzymes; lignin valorization; quantitative degradation

References

Asina, F. N. U, Brzonova, I., Kozliak, E., Kubátová, A. and Ji, Y. Microbial treatment of industrial lignin: successes, problems and challenges. *Renewable Sustainable Energy Rev.* **77**, 1179-1205 (2017).

Banu, J. R. *et al.* A review on biopolymer production via lignin valorization. *Bioresour. Technol.* **290**, 121790 (2019).

Becker, J. and Wittmann C. A field of dreams: lignin valorization into chemicals, materials, fuels, and health-care products. *Biotechnol. Adv.* **37**, 107360 (2019).

Chen Y., Chai L., Tang C., Yang Z., Zheng Y., Shi Y., Zhang H. Kraft lignin biodegradation by *Novosphingobium* sp. B-7 and analysis of the degradation process. *Bioresour. Technol*. **123**, 682-685 (2012).

Chen, Z., and Wan, C. Biological valorization strategies for converting lignin into fuels and chemicals. *Renewable Sustainable Energy Rev.***73**, 610-621 (2017).

Constant, S. *et al.* New insights into the structure and composition of technical lignins: a comparative characterisation study. *Green Chem.* **18**, 2651–2665 (2016).

Crestini, C., Lange, H., Sette, M. and Argyropoulos, D. S. *Green Chem*., **19**, 4104-4121 (2017)

Domínguez-Robles, J. *et al.* Aqueous acetone fractionation of kraft, organosolv and soda lignins. *Int. J. Bio.l Macromol.* **106**, 979-987 (2018).

Gigli, M. and Crestini, C. Fractionation of industrial lignins: opportunities and challenges. *Green Chem.* **22**, 4722-4746 (2020).

Gornall, A. G., Bardawill, C. J., David, M. M. Determination of serum proteins by means of the biuret reaction. *J Biol Chem*. **177**(2), 751-66 (1949).

He, Y. Z. *et al.* Characterization of a hyperthermostable Fe-superoxide dismutase from hot spring. *Appl. Microbiol. Biotechnol.* **75**, 367–376 (2007).

Lancefield, C. S. *et al.* Investigation of the chemocatalytic and biocatalytic valorization of a range of different lignin preparations: the importance of β-O-4 content. *ACS Sustain. Chem. Eng.* **4**, 6921–6930 (2016).

Lange, H., Schiffels, P., Sette, M., Sevastyanova, O., Crestini, C. Fractional precipitation of wheat straw organosolv lignin: macroscopic properties and structural insights. *ACS Sustain. Chem. Eng.* **4**, 5136−5151 (2016).

Lange, H., *et al.* Oxidative upgrade of lignin – Recent routes reviewed, *Eur. Polym. J.*, **49**, 1151-1173 (2013).

Li, X. Improved pyrogallol autoxidation method: a reliable and cheap superoxide-scavenging assay suitable for all antioxidants. *J. Agric. Food Chem.* **60**, 6418–6424 (2012).

Marklund, S. and Marklund, G. Involvement of the superoxide anion radical in the autoxidation of pyrogallol and a convenient assay for superoxide dismutase. *Eur. J. Biochem.* **47**, 469–474 (1974).

Meng, X. *et al.* Determination of hydroxyl groups in biorefinery resources via quantitative ^{31}P NMR spectroscopy. *Nat. Protoc.* **14**, 2627–2647 (2019).

Pardo, I. *et al.* A highly stable laccase obtained by swapping the second cupredoxin domain. *Sci. Rep.* **8**, 1–10 (2018).

Picart, P. *et al.* Multi-step biocatalytic depolymerization of lignin. *Appl. Microbiol. Biotechnol.* **101**, 6277–6287 (2017).

Ponnusamy, V. K. *et al.* A review on lignin structure, pretreatments, fermentation reactions and biorefinery potential. *Bioresour. Technol.* **271**, 462-472 (2019).

Raj, A., Reddy, M. M., Chandra, R., Purohit, H. J. and Kapley, A. Biodegradation of kraft-lignin by *Bacillus* sp. isolated from sludge of pulp and paper mill. *Biodegradation* **18**, 783-92 (2007).

Rashid, G. M. M., Taylor, C. R., Liu, Y., *et al.* Identification of manganese superoxide dismutase from *Sphingobacterium* sp. T2 as a novel bacterial enzyme for lignin oxidation. *ACS Chem. Biol.* **10**, 2286-2294 (2015).

Reiter, J., Strittmatter, H., Wiemann, L. O., Schieder, D. and Sieber, V. Enzymatic cleavage of lignin beta-O-4 aryl ether bonds via net internal hydrogen transfer. *Green Chem.* **15**, 1373–1381 (2013).

Rosini, E. *et al.* Cascade enzymatic cleavage of the β-O-4 linkage in a lignin model compound. *Catal. Sci. Technol.* **6**, 2195–2205 (2016).

Schutyser, W. *et al.* Chemicals from lignin: an interplay of lignocellulose fractionation, depolymerisation, and upgrading. *Chem. Soc. Rev.* **47**, 852-908 (2018).

Singh, R., Grigg, J. C., Qin, W., Kadla, J. F., Murphy, M. E. and Eltis, L. D. Improved manganese-oxidizing activity of DypB, a peroxidase from a lignolytic bacterium. *ACS Chem. Biol.* **8**, 700–706 (2013).

Tonin, F. *et al.* Comparison of different microbial laccases as tools for industrial uses. *New Biotechnol.* **33**, 387–398 (2016).

Tonin, F., Vignali, E., Pollegioni, L., D'Arrigo, P. and Rosini, E. A novel, simple screening method for investigating the properties of lignin oxidative activity. *Enzyme Microb. Technol.* **96**, 143–150 (2017).

Vishtal, A. and Kraslawski, A. Challenges in industrial applications of technical lignins. *BioResources* **6**, 3547–3568 (2011).

Wiermans, L., Pérez-Sánchez, M. and Domínguez de María, P. Lipase-mediated oxidative delignification in non-queous media: formation of de-aromatized lignin oil and cellulose accessible polysaccharides. *ChemSusChem* **6**: 251-255 (2013).

Zhu, D., Liang, N., Zhang, R., Ahmad, F., Zhang, W., Yang, B., Wu, J., Geng, A., Gabriel, M. and Sun, J. *ACS Sustainable Chem. Eng.* **8**: 12920-12933 (2020).

Supplementary Materials

Design and cloning of gene for MnSOD-1 enzyme

The synthetic gene encoding the MnSOD-1 enzyme from *Sphinobacterium sp.* T2 (Rashid et al., 2015) was designed by back translation of the protein sequence deposited in the GeneBank database (GI: 910751193). The gene (accession no. MT513103) was added of six codons (encoding for six histidines) to the 5′-end, of sequences corresponding to NdeI (CATATG) and XhoI (CTCGAG) restriction sites, and the codon usage was optimized for expression in *E. coli*. The MnSOD-1 cDNA was inserted in the pET24b(+) vector (Merck Millipore, Vimodrone, Italy) using the NdeI and XhoI sites, to give a 6.15-kb construct (pET24-MnSOD-1).

Expression and purification of MnSOD-1

The pET24::MnSOD-1 plasmid was transferred to the host BL21(DE3) *E. coli* strain. Cells were grown at 37 °C in Luria Bertani broth (LB, 10 g/L tryptone, 10 g/L NaCl, 5 g/L yeast extract) until an $OD_{600nm} \approx 0.7$. Protein expression was induced by adding 0.5 mM IPTG and 1 mM $MnSO_4$ (Rashid et al., 2015). Cells were collected (8600 *g*, 10 min, 4 °C) after 18 h of incubation at 15 °C, under stirring.

Cells were resuspended in lysis buffer (20 mM Tris-HCl, pH 8.0, 0.5 M NaCl, 1 mM pepstatin A, 10 µg/mL DNAse) and sonicated (5 cycles of 30 s each, with a 30 s interval on ice). The insoluble fraction of the lysate was removed by centrifugation at 39 000 *g* for 1 h at 4 °C. The total protein content in the crude extract was quantified by the biuret method (Gornall et al., 1949). The crude extract was loaded onto a HiTrap Chelating affinity column (GE Healthcare, Milan, Italy) previously loaded with 100 mM $NiCl_2$ and equilibrated with 20 mM Tris-HCl, pH 8.0, 0.5 M NaCl. The bound protein

was eluted in 20 mM Tris-HCl, pH 8.0, 0.5 M NaCl, 300 mM imidazole and subsequently dialyzed against 50 mM sodium phosphate, pH 7.8.

The recombinant protein was obtained with >90% purity, as judged by SDS-PAGE analysis (Figure S1), with a volumetric yield of ≈100 $mg_{protein}/L_{culture}$ corresponding to a five-fold increase in comparison to the previously reported figure of 19.5 $mg_{protein}/L_{culture}$ (Rashid et al., 2015). The amount of MnSOD-1 was estimated by measuring the absorbance intensity at 465 nm, using the molar extinction coefficient ε_{465nm} = 470 M^{-1} cm^{-1} (Rashid et al., 2015).

Biochemical and structural characterization

The dependence on temperature of MnSOD-1 activity was assayed in the 15-85 °C temperature range. The reaction mixture (final volume 1 mL), containing 0.5 µg of enzyme in a 50 mM Tris-HCl pH 8.2, 0.1 mM EDTA buffer, was added of 10 µL of a 25 mM pyrogallol solution (0.25 mM final concentration). The effect of dimethyl sulfoxide (DMSO) concentration (0-30% (v/v)) on MnSOD-1 activity and the enzyme stability was evaluated through the standard assay (0.5 µg enzyme, 0.25 mM pyrogallol, pH 8.2); in the latter case, the residual activity was assayed following incubation at 25 °C for 24 hours at different pH values in a multicomponent buffer (15 mM Tris, 15 mM phosphoric acid, 15 mM sodium carbonate, and 250 mM potassium chloride) in the pH 3.0–9.0 range (Harris et al., 2001). The thermal stability was assessed by the standard assay after incubation at 25 °C and 37 °C for 24 hours in 50 mM sodium phosphate buffer, pH 7.8.

All the spectral experiments were performed in 50 mM sodium phosphate buffer, pH 7.8. The fluorescence measurements were performed using a 1-mL cell in a Jasco FP-750 instrument equipped with a thermostated cell holder (Jasco, Cremella, Italy). The recordings of the tryptophan emission spectra (from 300 to 400 nm) were performed setting 280 nm as excitation wavelength, with excitation and emission bandwidths of 1 nm both. All

spectra were corrected by subtracting the emission of 50 mM sodium phosphate buffer, pH 7.8. Circular dichroism (CD) spectra were recorded on a J-810 Jasco spectropolarimeter and analyzed by means of Jasco software. The measurements in the 250- to 600-nm range were recorded using a 1 cm cell path, while for the measurements in the 190- to 250-nm region the cell path was of 0.1 cm (Caldinelli et al., 2005).

The temperature-induced modifications of secondary and tertiary structure were studied by following the CD signal at 220 nm and the tryptophan fluorescence at 332 nm. Both the spectropolarimeter and the fluorimeter were equipped with a software-driven Peltier-based temperature controller (temperature gradient of 0.5 °C/min) (Caldinelli et al., 2009).

Properties of recombinant MnSOD-1

The recombinant enzyme is active in superoxide dismutation, assessed as inhibition of 0.25 mM pyrogallol autoxidation in 50 mM Tris-HCl buffer, pH 8.2, containing 0.1 mM EDTA, at 25 °C. A specific activity of 518 ± 5.3 U/mg was apparent, a value comparable with the value of 400 U/mg reported by (Rashid et al., 2015).

Concerning the enzymatic activity at different temperatures, MnSOD-1 is marginally affected since it retained >80% activity at all temperatures tested (Figure S2). In addition, the enzyme showed more than 95% of its initial activity after 24 hours of incubation both at 25 and 37 °C. This result was confirmed by spectral analyses: the temperature sensitivity of tryptophan fluorescence (taken as a reporter of tertiary structure modifications) gave a T_m value of 74.1 ± 0.7 °C, which is close to the value obtained by monitoring the far-UV CD signal (a probe of secondary structure modification, 69 ± 0.7 °C). Furthermore, the enzymatic activity is not affected by DMSO up to 30% (v/v) concentration, maintaining a 80% of initial value (Figure S3). The investigation of the MnSOD-1 stability at different pH values highlighted a

widespread pH tolerance resulting in a >90% residual activity in the whole 3.0-9.0 pH range (Figure S4).

Spectral analyses of tertiary structure highlighted a high fluorescence intensity, although MnSOD-1 contains six Trp residues not exposed to the solvent (Figure S5A), and a low intensity of the signal in the near-UV CD spectrum (see Figure S5C). An α-helix and a β-strand content of ~42% and ~15%, respectively, were estimated from the far-UV CD spectrum by means of K2D3 software (Figure S5B): these values are in fair good agreement with data from the resolved structure (44% helical and 9% β-strands, PDB code 5A9G) (Rashid et al., 2015).

Table S1. Qualitative comparison of compounds identified after silylation of the extracts from WSL, ASWL and AIWS samples treated with Lac F/ABTS or MnSOD-1. X: compound present in the enzyme-treated sample only; XX: compound present in both the enzyme-treated sample and in the control.

	Compound	Lac F/ABTS			MnSOD-1		
		WSL	**ASWL**	**AIWL**	**WSL**	**ASWL**	**AIWL**
Aromatics	Phenyl acetic acid		X				
	4-methoxy acetophenone				X		
	4-Hydroxybenzaldehyde		X				
	Vanillin				X		
	Veratraldehyde	XX	XX	XX	X	XX	
	3,4-Dimethoxy-benzenemethanol	XX					
	Resorcinol		X				
	1-Phenoxy 2-propanol			XX	XX	XX	XX
	4-Hydroxybenzoic acid					XX	
	Veratril acetate	XX	X	XX			
	Homoveratric acid			X			
	Syringaldehyde				X	X	X
	Vanillic acid		X	X			
	3,4-Dihydroxyphenylacetic acid					X	
	Syringic acid				X		
	Aceto syringone				XX		

	p-Coumaric acid		XX			XX	XX
	Ferulic acid		XX			XX	XX
	Methyl syringate		XX			XX	X
	2,6-Dimethoxyhydroxyquinone		X	X			
Substituted biphenyls	1,3-Diphenyl-3-hydroxy-1-propanone					X	
	4-Phenylphenol	X	X				
	2,2',3,3'-Tetramethoxy-4-methyl-1,1'-biphenyl			X			
	2-Hydroxy-2',4,4'-trimethoxy-1,1'-biphenyl			X			
	Diveratryl ether	XX					X
Alkyl chains	Glycerol	X	X	XX			XX
	Propanedioic acid		X				

Table S2. Qualitative comparison of compounds identified after silylation of the extracts from SKL, ASKL and AIKS samples treated with BALL/TEMPO and from SLS treated with LAC C/TEMPO. X: compound present in the enzyme-treated sample only; XX: compound present in both the enzyme-treated sample and in the control.

	Compound	**BALL/TEMPO**			**Lac C/TEMPO**
		SKL	**ASKL**	**AIKL**	**SLS**
Aromatics	Veratryl alcohol methyl ether	X			
	3-Vanilpropanol	XX			
	3-Hydroxy-4-methoxybenzyl alcohol	XX			
	5-Methoxy-2-benzoic acid		X		
	Veratraldehyde	X			
	Vanillin	X	X	X	
	4-hydroxybenzaldehyde	X			
	Vanillic acid	XX	XX	XX	
	Veratyl alcohol	XX			XX
	1-Phenoxy-2-propanol		XX	XX	
	Apocynin	X	XX	X	
	2'-Hydroxy-5'-methoxyacetophenone		X		
	2-Methyl-2(*p*-methoxy)mandelate		X		
	3-Phenyl-2-propenoic acid	X			
	Resorcinol		X		
Alkyl chains	Glycerol		X		
	2-Propanoic acid	XX			

Figure S1

SDS-PAGE analysis of the recombinant purified MnSOD-1. The His-tagged enzyme (≈20 kDa) was recovered by a single chromatographic step on HiTrap chelating column in the presence of 0.3 M imidazole with >90% purity. MW: molecular weight (kDa), 1: crude extract (140 µg of total protein), 2: fraction eluted at 0.3 M imidazole (20 µg).

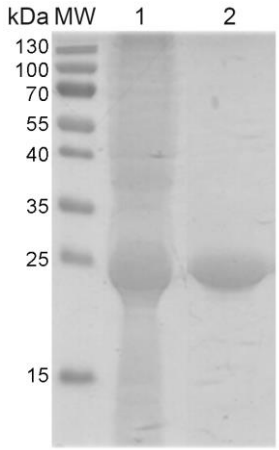

Figure S2

The superoxide dismutase activity of MnSOD-1 was evaluated using the autoxidation pyrogallol assay at different temperatures (15-85 °C). The activity at 25 °C in 50 mM Tris-HCl, pH 8.2, 0.1 mM EDTA was taken as 100%.

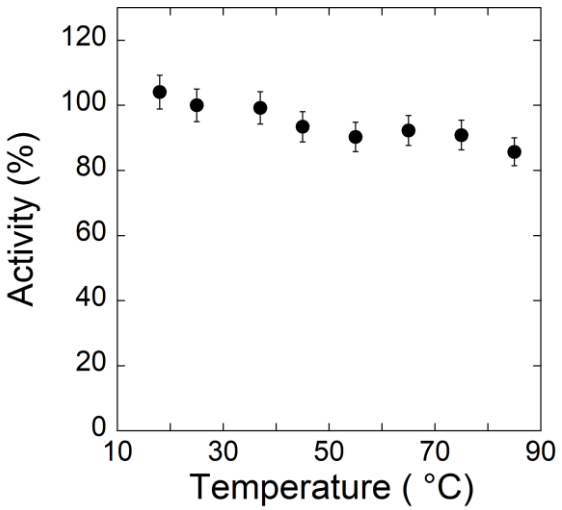

Figure S3

The superoxide dismutase activity of MnSOD-1 was evaluated using the autoxidation pyrogallol assay in the presence of different amounts of DMSO. The activity at 25 °C in 50 mM Tris-HCl, pH 8.2, 0.1 mM EDTA in absence of DMSO was taken as 100%.

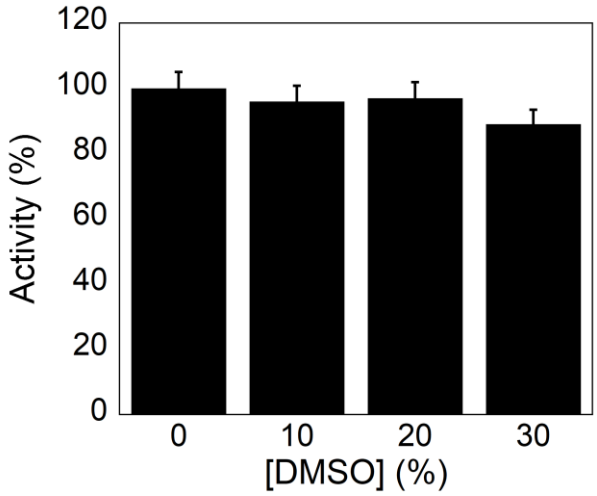

Figure S4

The MnSOD-1 stability at different pH values was evaluated incubating the enzyme for 24 h in a multicomponent buffer (pH 3.0 – 9.0). The initial activity (t_0) on 0.25 mM pyrogallol at 25 °C in 50 mM Tris-HCl, pH 8.2, 0.1 mM EDTA was taken as 100%.

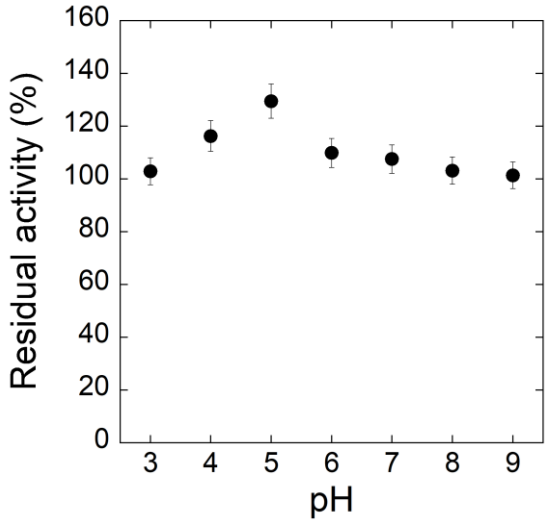

Figure S5

Spectral analysis of the recombinant MnSOD-1. A) Protein fluorescence spectrum recorded with excitation at 280 nm. B) Far-UV CD spectrum. C) Near-UV CD spectrum. All measurements were performed at 0.1 $mg_{protein}$/mL concentration, at 15 °C, in 50 mM sodium phosphate, pH 7.8.

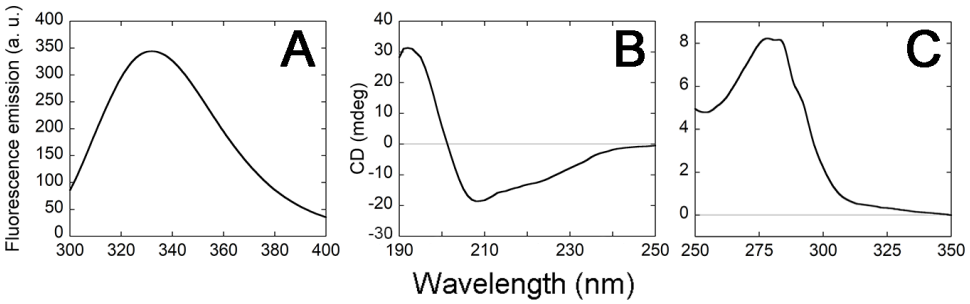

Figure S6

Identification of the optimal experimental conditions for the oxidation/degradation of the wheat straw lignin (WSL) by MnSOD-1, as detected by the colorimetric screening method.

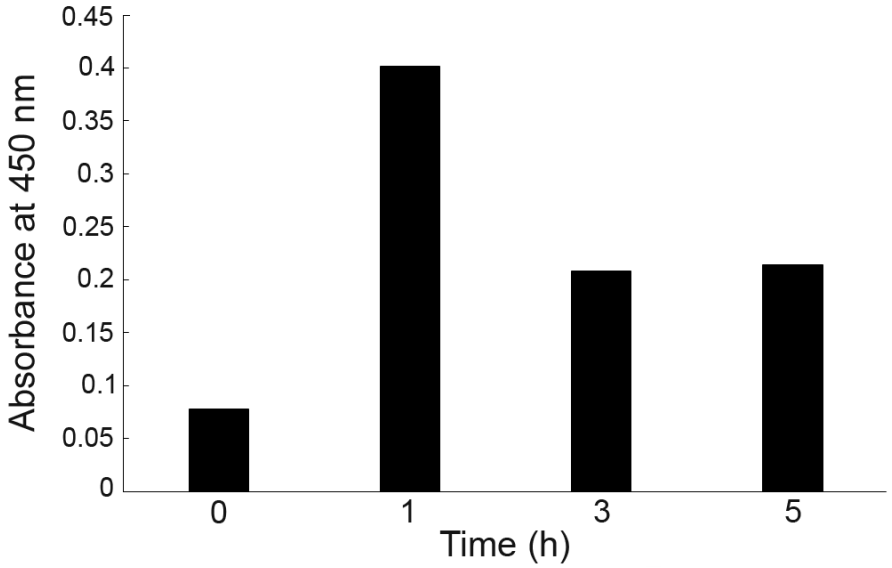

References

Caldinelli, L., Iametti, S., Barbiroli, A., *et al.* Dissecting the structural determinants of the stability of cholesterol oxidase containing covalently bound flavin. *J. Biol. Chem.* **280**, 22572-22581 (2005).

Caldinelli, L., Molla, G., Sacchi, S., Pilone, M. S. and Pollegioni, L. Relevance of weak flavin binding in human D-amino acid oxidase. *Protein Sci*. **18**, 801-810 (2009).

Harris, C. M., Pollegioni, L. and Ghisla, S. pH and kinetic isotope effects in D-amino acid oxidase catalysis: evidence for a concerted mechanism in substrate dehydrogenation via hydride transfer. *Eur. J. Biochem*. **268**, 5504-5520 (2001).

Rashid, G. M. M., Taylor, C. R., Liu, Y. *et al.* Identification of manganese superoxide dismutase from *Sphingobacterium* sp. T2 as a novel bacterial enzyme for lignin oxidation. *ACS Chem. Biol.* **10**, 2286-2294 (2015).

A multi-enzymatic one-pot reaction for the production of *cis,cis*-muconic acid

Introduction

Lignin is an aromatic three-dimensional amorphous polymer obtained by the radical polymerization of phenylpropane units (*p*-coumaryl, syringyl and guayacyl alcohols). It constitutes with cellulose and hemicellulose the so-called lignocellulosic biomass, a promising second generation renewable feedstock (Becker and Wittmann, 2019). Although lignin accounts for approximately 15-40% of lignocellulose, representing the first renewable source of aromatics on Earth, it is almost underutilized (Pollegioni et al., 2015; Vardon et al., 2015; Xu et al, 2019). In fact, as its calorific power is comparable to that of some fossil carbons (26-28 MJ/ton dry lignin), approximately 140 million tons per year of technical lignin is burned for the in loco generation of heat and power (Berlin and Balakshin, 2014; Becker and Wittmann, 2019). Nevertheless, lignin valorisation is feasible by performing its thermochemical or biological depolymerisation into value-added products (such as vanillin, cresol, catechol, gallic acid, ferulic acid) (Becker and Wittmann, 2019). These compounds represent building blocks for the sustainable synthesis of chemicals, such as adipic acid, *cis,cis*-muconic acid ((2Z,4Z)-hexa-2,4-dienedioic acid, ccMA) and terephthalic acid (Wu et al., 2017; Becker and Wittmann, 2019; Ruales-Salcedo et al., 2019). Because of the relevance of these compounds as precursors of commercial plastics, biological routes for their production have been already implemented and scaled up to the pilot scale, representing the masterpiece of lignin valorization (Vardon et al., 2015; Kohlstedt et al., 2018).

ccMA is one of the three isomers of the linear dicarboxylic muconic acid which global market is greater than $22 billion due to its relevance for the synthesis of polyamides, unsaturated polyesters, adipic acid and terephthalic acid, which are all chemicals involved in the production of a large number of plastic materials (Vardon et al., 2015; Xu et al., 2019). Currently, the industrial production of ccMA depends mainly on chemical synthesis using petroleum-based feedstocks (Xu et al., 2019). In order to limit the use of fossil-sources, the development of green alternatives for the synthesis of ccMA is a crucial objective for biotechnology (Becker and Wittmann, 2019; Ruales-Salcedo et al., 2019; Xu et al., 2019).

Recently, the feasibility of a biotechnological process for the ccMA production from an alkali pretreated lignin was demonstrated (Wu et al., 2017). The DH1 strain of *Escherichia coli* was engineered with a new anabolic pathway for the bioconversion of vanillin (obtained from the thermochemical pre-treatment of lignin) into ccMA (up to 314 mg ccMA/L culture; 0.69 g ccMA/g vanillin) (Wu et al., 2017). Nonetheless, the limits of this approach consist both in the difficulty of the microbial pathway regulation and in the set up of the optimal microbial growth conditions (Martani et al., 2017). To overcome these limitations, multi-enzymatic biocatalytic approaches could represent a suitable strategy (Schmid et al., 2001; Picart et al. 2017): system biocatalysis allows the combination of different enzymes, also from different source organisms, in a single reactor, resulting both in the generation of new routes for the product synthesis and in a high selective process (Tessaro et al., 2015; Rosini et al., 2016; Picart et al., 2017; Ruales-Salcedo et al., 2019).

In the present work, we optimized a multi-enzymatic one-pot process for the production of ccMA through the bioconversion of vanillin (the only

aromatic lignin degradation product globally commercialised) (Upton and Kasko, 2016) (Figure 1).

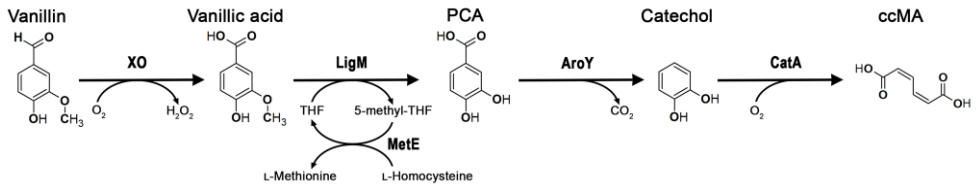

Figure 1. Scheme of the reactions involved in the multi-enzymatic bioconversion of vanillin into ccMA.

In details, the oxidation of vanillin into vanillic acid is catalyzed by the enzyme xanthine oxidase (XO). Then, the demethylation of vanillic acid into protocatechuic acid (PCA) is catalyzed by the recombinant *O*-demethylase LigM in the presence of tetrahydrofolate (THF) and of the cofactor-regeneration enzyme methyl transferase MetE (Rosini et al., 2016). PCA is converted into catechol (1,2-dihydroxybenzene) by the decarboxylase AroY. The final reaction, catalyzed by the catechol 1,2-dioxygenase (CatA), consists in the production of ccMA through the intradiolic opening of the catechol aromatic ring. The set up of this multi-enzymatic system represents a sustainable alternative for the production of a high value added product from a renewable source such as vanillin, obtained from the depolymerization of the lignocellulosic biomass.

Materials and methods

1. Reagents and enzymes

Xanthine oxidase from bovine serum milk (XO, Grade I, ammonium sulfate suspension), catalase from bovine liver (14 U/mg), tetrahydrofolate (THF), analytical grade standards of vanillin (4-hydroxy-3-methoxybenzaldehyde), vanillic acid (4-hydroxy-3-methoxybenzoic acid), protocatechuic acid (PCA or 3,4-dimethoxybenzoic acid), catechol (1,2-dihydroxybenzene), *cis,cis*-

muconic acid ((2Z,4Z)-hexa-2,4-dienedioic acid, ccMA), acetonitrile (ACS Grade, ≥99%) and formic acid (ACS Grade, ≥ 98%) were purchased by Merck (Merck KGaA, Darmstadt, Germany). Methanol of ACS Grade (≥ 99%) was purchased by Carlo Erba. The enzyme catechol 1,2-dioxygenase (CatA) from *Acinetobacter radioresistens* S13, cloned between *NdeI* site and *EcoRI* site in pET30+ (Novagen) (Caglio et al., 2009), was produced as reported by Di Nardo *et al.* (Di Nardo et al., 2009); recombinant *O*-demethylase from *Sphingobium* sp. SYK-6 (LigM) and methionine synthase from *Catharanthus roseus* (MetE) were expressed in *E. coli* and purified as previously reported by Rosini *et al.* (Rosini et al., 2016).

2. Design and cloning of the *AroY* synthetic gene

The synthetic gene encoding the protocatechuate decarboxylase AroY from *Klebsiella pneumoniae* ssp. *pneumoniae* A170-40 was previously optimized for the recombinant expression in *E. coli* (Accession no. KX774258.1) (Wu et al., 2017). The *AroY* cDNA was synthesized by TWIST Bioscience (San Francisco, USA) and cloned in the pET24(b) vector using the *BamHI* (GGATCC) and *XhoI* (CTCGAG) restriction sites. Notably, during the subcloning process, six codons (encoding for six additional histidines, His-tag) were added at the C-terminus of the *AroY* gene.

3. AroY recombinant expression in *E. coli* cells

The pET24::AroY plasmid was transferred to the BL21(DE3) *E. coli* host strain. Cells were grown at 37 °C in Terrific Broth and protein expression was induced at an OD_{600nm} ≈0.6 by adding 0.2 mM IPTG; cells were further grown at 18 °C for 18 h under shaking (Payer et al., 2017). After the harvesting of the cells by centrifugation (7000 rpm, 10 min, 4 °C) and their washing twice in 100 mM Tris-HCl, pH 8.0, cells were resuspended at the final concentration of 0.8 g cells/mL in the same buffer. Cells have been lyophilized and stored

as a dried power at 4 °C. A rehydration step (i.e. 15 minutes of incubation at room temperature on a rotatory wheel in the presence of an amount of deionized water corresponding to the one lost during lyophilisation) was performed before their use (Farnberger et al., 2017; Payer et al., 2017). Notably, the same growth and expression protocol, followed by the harvesting, washing and lyophilisation steps, were performed also for not transformed BL21(DE3) *E. coli* cells, used as control during the bioconversion reactions.

4. Protein quantification

The commercial ammonium sulfate suspension of XO was dialysed against 100 mM Tris-HCl, pH 8.0 and the amount of XO (≈150 kDa) was determined by measuring the absorbance intensity at 450 nm and using the molar extinction coefficient of 36000 M^{-1} cm^{-1} (Godber et al., 2005). The amount of purified LigM (≈55 kDa), MetE (≈85 kDa) and CatA (≈38 kDa) were estimated by measuring the absorbance intensity at 280 nm and using the following molar extinction coefficients: 107950 M^{-1} cm^{-1} (Rosini et al., 2016), 126290 M^{-1} cm^{-1} (Rosini et al., 2016), and 53560 M^{-1} cm^{-1} (Di Nardo et al., 2009), respectively.

5. Biocatalytic reaction steps for ccMA production

5.1.Oxidation of vanillin into vanillic acid

Xanthine oxidase from bovine serum milk is commercially available as an ammonium sulfate containing suspension. Its storage buffer was changed by dialysis against 100 mM Tris-HCl, pH 8.0 buffer. The oxidase activity of XO was determined on 100 μM xanthine as substrate in 100 mM Tris-HCl, pH 8.0, at 25 °C by following for 5 min the change in absorbance at 295 nm on a Jasco V-580 spectrophotometer (Cremella, Italy) and using a molar absorption coefficient of 9600 M^{-1} cm^{-1} (Godber et al., 2005). A specific activity of 1.7

± 0.2 U/mg on xanthine as substrate was determined. One enzymatic unit was defined as the amount of enzyme which converts 1 μmol of substrate in one minute, at 25 °C. The ability of XO to convert vanillin was assayed at two different pH values: the 0.5 mL reaction mixture containing 0.22 mg (0.4 U) XO and 1 mM vanillin was assayed both in Krebs-Henseleit, pH 7.4 buffer (118 mM NaCl, 4.7 mM KCl, 1.2 mM $MgSO_4$, 1.25 mM $CaCl_2$, 1.2 mM KH_2PO_4, 24 mM $NaHCO_3$, 11 mM glucose) (Panoutsopoulos et al., 2004) and in 100 mM Tris-HCl, pH 8.0. Reaction mixtures were incubated at 30 °C for 170 min on a rotatory wheel. Reaction mixtures withdrawn at different times were analysed using the HPLC method (see "HPLC analyses" paragraph).

5.2.Demethylation of vanillic acid into PCA

The LigM activity was assayed at 30 °C in the presence of 0.1 mM vanillic acid in 100 mM Tris-HCl buffer, pH 8.0, by measuring the initial rate (10 min) of a 240 min reaction (Rosini et al., 2016). Analyses were performed by HPLC as described in the "HPLC analyses" paragraph. One enzymatic unit was defined as the amount of enzyme that converts 1 μmol of substrate in one minute, at 30 °C. The vanillic acid demethylation into PCA was assayed in the presence of recombinant enzymes *O*-demethylase THF-dependent LigM (0.15 U/mg) and methionine synthase MetE, as previously described (Rosini et al., 2016). The 0.5 mL reaction mixture contained 1 mM vanillic acid, 0.1 mM THF and 2 mM L-homocysteine (the substrate of the MetE enzyme, see Figure 1), (Rosini et al., 2016) in 100 mM Tris-HCl, pH 8.0. Reaction started by adding 0.15 mg (0.02 U) LigM and 0.5 mg MetE (Rosini et al., 2016). The reaction control was assayed in the absence of enzymes. Every 2 h, 0.5 mg MetE or an equal volume of buffer were added to the mixture and in the control reactions, respectively (Rosini et al., 2016). Reaction mixture was incubated at 30 °C for 8 h on a rotatory wheel and 40 μL of sample were

withdrawn at different times and analysed by HPLC (see "HPLC analyses" paragraph).

5.3.Whole-cell decarboxylation of PCA into catechol

The AroY activity was determined in the presence of 5 mM PCA (i.e. a saturating concentration) in 100 mM Tris-HCl, pH 8.0, by measuring the initial rate of consumption of a 240 min reaction. Analyses were performed by HPLC analyses (see "HPLC analyses" paragraph). The activity for the not purified AroY (i.e. expressed in whole-cell system consisting in pET24::AroY *E. coli* transformed lyophilised cells) corresponded to 0.26 U per g of lyophilised cells. One enzymatic unit was defined as the amount of lyophilised cells (g) that converts 1 μmol of substrate in one minute, at 30 °C.

The 0.5 mL reaction mixture contained 1 mM PCA and 30 mg of lyophilised pET24::AroY transformed *E. coli* cells in 100 mM Tris-HCl, pH 8.0. The reaction control was assayed by incubating PCA with 30 mg of untransformed *E. coli* BL21(DE3) lyophilised cells, as well as omitting the substrate. Reaction mixtures were incubated at 30 °C on a rotatory wheel for 4 h. At different times, 50 μL of each sample were withdrawn and centrifuged for 10 min at 13000 rpm, 4 °C. The supernatant was subsequently treated as described in the "HPLC analyses" paragraph.

5.4.Conversion of catechol into ccMA

The CatA activity was assayed by following for 5 min the ccMA formation at 260 nm in a thermostated spectrophotometer at 30 °C. Reaction mixture (1 mL) contained 0.2 mM catechol in 50 mM HEPES, pH 8.0 (Di Nardo et al., 2009) or 0.2 mM catechol in 100 mM Tris-HCl, pH 8.0. Reaction started adding 0.9 μg CatA (0.018 mU). The product was quantified using the ccMA extinction coefficient of 17600 M^{-1} cm^{-1} at 260 nm (Di Nardo et al., 2009). One enzymatic unit was defined as the amount of enzyme that converts 1 μmol

of substrate in one minute, at 30 °C. The bioconversion of 1 mM catechol was carried out using 10 μg (0.2 U) CatA in 100 mM Tris-HCl, pH 8.0. The reaction mixture was incubated for 30 min at 30 °C on a rotatory wheel and at different times 40 μL of sample were withdrawn for HPLC analyses (see "HPLC analyses" paragraph).

6. Combination of biocatalytic steps for ccMA production

6.1.Multi-step sequential bioconversion of vanillin into ccMA

The multi-step sequential bioconversion of vanillin into ccMA was performed at 30 °C using the reaction conditions optimised for the single reactions with minimal modifications: 1 mM vanillin was incubated in 100 mM Tris-HCl, pH 8.0 with 0.22 mg (0.4 U) XO and 0.1 mg (1.4 U) catalase (the enzymes were omitted in the control mixture). After 2 h of incubation, 0.1 mM THF, 2 mM L-homocysteine, 0.15 mg (0.02 U) LigM and 0.5 mg MetE (or an equal volume of buffer) were added to the reaction mixture (or to the control). In addition, 0.5 mg of MetE were supplemented after 2, 4 and 6 h of incubation, and 0.15 mg LigM after 6 h. After 18 h, 30 mg (0.01 U) of lyophilized pET24::AroY transformed BL21(DE3) *E. coli* cells were added to the reaction mixture and incubated for 4 h. Then, 5 μg (0.1 U) CatA were added and the reaction was monitored for further 2 h. At different times, samples were analysed by HPLC in order to monitor the time course of each reaction step (see "HPLC analyses" paragraph).

6.2.One-pot bioconversion of vanillin into PCA

The bioconversion of vanillin into PCA was performed in a one-pot multi-enzymatic reaction. The 0.5 mL reaction mixture containing 1 mM vanillin, 0.1 mM THF and 2 mM L-homocysteine in 100 mM Tris-HCl, pH 8.0, was added of XO (0.22 mg, 0.4 U), LigM (0.15 mg, 0.02 U), MetE (0.5 mg) and catalase (0.1 mg, 1.4 U). The control reaction did not contain the enzymes.

The reaction mixture was incubated for 18 h at 30 °C on a rotatory wheel. The enzyme MetE (0.5 mg) was added after 2, 4, 6, and 8 h of reaction (Rosini et al., 2016); after 6 and 8 h of incubation, also 0.15 mg LigM were added. At different times, 40 μL of sample were withdrawn for HPLC analysis (see "HPLC analyses" paragraph).

6.3.One-pot bioconversion of PCA into ccMA

The mixture for one-pot bioconversion of PCA into ccMA contained 1 mM PCA, 30 mg (0.01 U) of lyophilised pET24::AroY transformed BL21(DE3) *E. coli* cells and 5 μg (0.1 U) CatA in 100 mM Tris-HCl, pH 8.0 (final volume 0.5 mL). As controls, reaction mixtures containing not transformed lyophilised BL21(DE3) *E. coli* cells or lacking the substrate PCA were used. Reaction mixtures were incubated for 3 h at 30 °C, on a rotatory wheel. Indeed, 5 μg (0.1 U) CatA or an equal volume of buffer were added after 1 h of incubation in the reaction or in the control mixtures, respectively. At different times, 40 μL of the reaction mixture were withdrawn and analysed by HPLC (see "HPLC analyses" paragraph).

6.4.One-pot bioconversion of vanillin into ccMA

The one-pot bioconversion of vanillin into ccMA was performed at 30 °C under optimised conditions by adding additional amounts of the enzymes of different times. The reaction mixture contained 0.1 mg (1.4 U) catalase, 0.15 mg (0.02 U) LigM, 0.5 mg MetE and 5 μg (0.1 U) CatA, and 10 mg (3 mU) of lyophilized pET24::AroY transformed BL21(DE3) *E. coli* cells (let to re-hydrate for 15 minutes at room temperature on a rotary wheel). The reaction was started by adding 1.1 mg (1.9 U) XO. The 0.5 mL control mixture contained 1 mM vanillin, 0.1 mM THF and 2 mM L-homocysteine in 100 mM Tris-HCl, pH 8.0 buffer. After 1, 2 and 3.5 h of incubation on a rotary wheel, 0.7 mg (1.2 U) of XO were added; after 2 and 3.5 h of incubation, 0.5 mg

MetE and 0.15 mg (0.02 U) LigM were added; after 4.5 h of incubation, 30 mg (0.01 U) of lyophilized pET24::AroY transformed BL21(DE3) *E. coli* cells were added. Lastly, 5 μg (0.1 U) CatA were further added after 6.5 h from the starting. In order to maintain the same final volume, an equal volume of 100 mM Tris-HCl buffer, pH 8.0, was added in the control mixtures.

The two-step one-pot bioconversion of vanillin into ccMA was set up in a 0.5 mL reaction mixture containing 1 mM vanillin, 0.2 mM THF, 2 mM L-homocysteine and the enzymes XO (0.7 mg, 1.2 U), LigM (0.6 mg, 0.09 U), MetE (1 mg) and catalase (0.1 mg, 1.4 U) in 100 mM Tris-HCl buffer, pH 8.0. A 0.5 mL mixture in the absence of enzymes was used as control. After 2.5 and 4.5 h of incubation at 30 °C on a rotary wheel, 0.6 mg LigM and 1 mg MetE or an equal volume of 100 mM Tris-HCl, pH 8.0 buffer were supplemented in the reaction mixture or in the control, respectively. After 5.5 h of incubation, the reaction mixture was added of 30 mg (0.01 U) of lyophilized pET24::AroY transformed BL21(DE3) *E. coli* cells and 10 μg (0.2 U) CatA: the reaction mixture was incubated for further 2.5 h at 30 °C on a rotary wheel.

6.5.Scale up of the two-step one-pot bioconversion of vanillin

The two-step one-pot production of ccMA from vanillin was assayed in a 3 mL reaction mixture containing 3 mM vanillin, 0.2 mM THF, 3 mM L-homocysteine and the enzymes XO (4.2 mg, 7 U), LigM (3.6 mg, 0.54 U), MetE (6 mg) and catalase (0.2 mg, 2.8 U) in 100 mM Tris-HCl buffer, pH 8.0. A 3 mL mixture in the absence of enzymes was used as control. After 1, 3 and 5 h of incubation at 30 °C on a rotary wheel, the reaction mixture was added of 1.8 mg LigM, 3 mg MetE and 80 μM THF. In addition, after 5 h, 60 mg (0.02 U) of lyophilized pET24::AroY transformed BL21(DE3) *E. coli* cells and 30 μg (0.6 U) CatA were added. Furthermore, MetE (3 mg) was added after 7 h while, after 9 and 12 h, 40 mg (0.01 U) and 100 mg (0.03 U),

respectively, of lyophilized pET24::AroY transformed BL21(DE3) *E. coli* cells were added. Finally, after 9 and 12 h of incubation, 30 μg (0.6 U) of CatA were added, followed by an additional aliquot of 90 μg (1.8 U) of CatA after 15 h. At different times, samples were analysed by HPLC (see "HPLC analyses" paragraph).

7. HPLC analyses

All the HPLC analyses were performed on a Jasco apparatus equipped with a Symmetry C8 column 100 Å, 5 μL, 4.6 x 250 mm (Waters, Milan, Italy) and with an UV detector set at 254 nm. The mobile phase consisted in 34.5% (v/v) methanol, 5.4% (v/v) acetonitrile and 0.1% (v/v) formic acid; the flow rate was 0.8 mL/min and the column oven was set at 30 °C (Rosini et al., 2016).
Calibration curves were obtained solubilising standards of vanillin, vanillic acid, PCA, catechol and ccMA in 100 mM Tris-HCl, pH 8.0 at the final concentration of 40 mM. Subsequently, after dilution in the 0.04 – 2 mM range, 80 μL of each sample were added with 160 μL of the mobile phase and centrifuged for 2 min at 13000 rpm, 4 °C: 20 μL of the supernatant were injected for HPLC analysis. Each value was reported as the mean of three measurements ± standard deviation. Retention times for standards of PCA, ccMA, vanillic acid, catechol and vanillin were: 5.2, 6.2, 7.2, 7.7 and 9.7 min, respectively. The calibration curves for PCA, ccMA, vanillic acid, catechol and vanillin are reported in ESI† Figure S1. In order to monitor the biocatalytic process, at different times 40 μL of reaction mixtures were withdrawn and added with 80 μL (160 μL for the two-step one-pot bioconversion) of mobile phase. After 2 min of centrifugation at 13000 rpm at 4 °C, 20 μL of supernatant were analysed by HPLC.

Results and discussion

1. Set up of single catalytic steps

The commercial enzyme XO catalyses the oxidation of a wide range of *N*-heterocycles and aldehydes (Panoutsopoulos et al., 2004). The oxidation of vanillin by XO was evaluated at two different pH values, i.e. 7.4 and 8.0. The reaction performed in Krebs-Henseleit buffer, pH 7.4, reported as the optimal condition for XO (Panoutsopoulos et al., 2004), showed the complete conversion of 1 mM vanillin into vanillic acid in 1 h at 30 °C (data not shown). On the other hand, using the optimal buffer for the multi-step one-pot bioconversion reaction (i.e. 100 mM Tris-HCl, pH 8.0), the complete conversion of 1 mM vanillin was observed after 2 h of incubation at 30 °C (Figure 2A).

The demethylation of vanillic acid into PCA was catalysed by the purified LigM/MetE bi-enzymatic system in the presence of 1 mM vanillic acid and 0.1 mM THF. Because of the known low stability (Rosini et al., 2016), 0.5 mg of MetE were added to the reaction mixture every 2 hours: after 8 h of reaction, 1 mM of PCA was produced (Figure 2B).

Concerning AroY, all the available purification protocols consist in the isolation of the inactive apoprotein followed by a time-consuming reconstitution step with the cofactor FMN (Marshall et al., 2017; Payer et al., 2017; Wang et al., 2018; Khusnutdinova et al., 2019). In order to facilitate the bioconversion, we opted for the use of transformed *E. coli* cells (grown reaching a volumetric yield of 24 g cells per litre of culture). When 1 mM PCA was mixed with 30 mg (0.01 U) of lyophilised pET24::AroY transformed *E. coli* cells (corresponding to 0.3 g wet cells) in 100 mM Tris-HCl, pH 8.0, 1 mM catechol was produced after 4 h of incubation at 30 °C (Figure 2C). No catechol formation was observed for the reaction controls assayed in the absence of substrate or in the presence of not transformed *E. coli* cells.

The enzymatic activity of CatA was evaluated spectrophotometrically at 30 °C both using its optimal buffer (i.e. 50 mM HEPES, pH 8.0) (Di Nardo et al., 2009) and 100 mM Tris-HCl, pH 8.0: the enzyme showed a similar specific activity corresponding to 21 ± 2 and 20 ± 2 U/mg, respectively. The bioconversion of 1 mM catechol catalysed by the CatA enzyme in 100 mM Tris-HCl, pH 8.0, resulted in the full conversion to 1 mM ccMA after 30 min of incubation (Figure 2D).

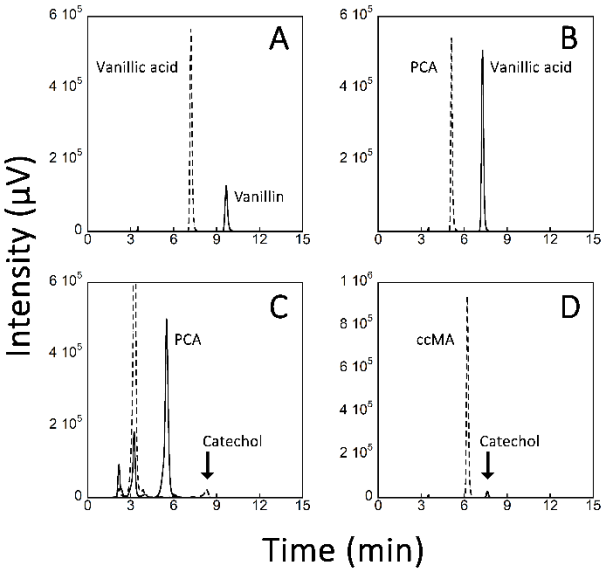

Figure 2. HPLC chromatograms of single catalytic steps in the bioconversion of (A) vanillin to vanillic acid, (B) vanillic acid to PCA, (C) PCA to catechol, and (D) catechol to ccMA. All the reactions were carried out on 1 mM substrate in 100 mM Tris-HCl (pH 8.0, 30 °C). The chromatograms show the reaction mixture at the beginning (continuous line) and at the end of the incubation (dotted line).

2. Multi-step sequential bioconversion of vanillin into ccMA

In order to demonstrate the feasibility of the process, the multi-step bioconversion of vanillin into ccMA was investigated in a sequential way (at pH 8.0, 30 °C). Firstly, 1 mM vanillin was oxidized in the presence of XO and catalase. The latter enzyme was added in order to avoid that the hydrogen peroxide formed by XO could affect the

following enzymatic steps. After 2 h of incubation 1 mM vanillin was completely converted into vanillic acid (Figure 3A); then, 0.1 mM THF, 2 mM L-homocysteine and the LigM/MetE by-enzymatic system were added. After 18 h of incubation, 1 mM vanillic acid was completely converted into 1 mM PCA (Figure 3B). Thirdly, 30 mg (0.01 U) of lyophilised pET24::AroY transformed BL21(DE3) *E. coli* cells were added to the reaction mixture: after 4 h of incubation, 1 mM PCA was fully converted into catechol (Figure 3C). Finally, the catechol conversion into ccMA was obtained in 2 hours by the adding CatA: a total of ~1 mM ccMA was formed (Figure 3D).

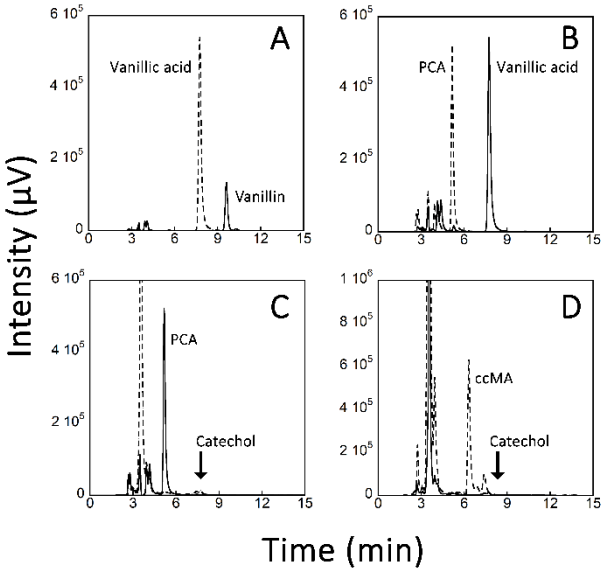

Figure 3. HPLC chromatograms of the multi-step sequential bioconversion of (A) 1 mM vanillin to vanillic acid, (B) to PCA, (C) to catechol, and (D) to ccMA, in 100 mM Tris-HCl, pH 8.0, 30 °C. The chromatograms show the elution profile of the reaction mixture at the beginning (continuous line) and at the end of each incubation (dotted line).

3. One-pot bioconversion of vanillin into ccMA

Because of the apparent difference in reaction kinetics, the optimal incubation conditions for the one-pot production of ccMA from vanillin were studied by

first combining in a one-pot mixture the components involved in the bioconversion of vanillin into PCA and subsequently those for the bioconversion of PCA into ccMA (see Figure 1).

The multi-enzymatic system composed by XO, LigM and MetE was applied in the one-pot oxidation of vanillin into vanillic acid, the THF-dependent demethylation of vanillic acid into PCA and the regeneration of the THF cofactor. A 0.5 mL solution containing 1 mM vanillin, 0.1 mM THF, 2 mM L-homocysteine, XO, LigM, MetE and catalase was incubated in 100 mM Tris-HCl, pH 8.0, at 30 °C. After 18 h of incubation, ~80% of PCA was produced: the peak corresponding to the substrate vanillin disappeared and, in addition to the peak corresponding to PCA, the intermediate reaction product vanillic acid (~0.12 mM) was still present (Figure 4A).

Then, the ccMA production from PCA was assayed in a one-pot reaction containing 1 mM PCA, lyophilised pET24::AroY transformed BL21(DE3) *E. coli* cells and CatA in 100 mM Tris-HCl, pH 8.0: after 1 h of incubation, 0.8 mM ccMA were produced. Therefore, 5 μg CatA were further added, resulting in the disappearance of the peak corresponding to PCA and the formation of 1 mM ccMA after 1 h. The bioconversion yield of 1 mM PCA to ccMA was thus ~100% in 2 h of incubation (Figure 4B).

In order to set up the one-pot bioconversion of vanillin into ccMA, 1 mM vanillin was incubated with the complete enzymatic system XO, LigM, pET24::AroY *E. coli* cells and CatA in the presence of THF, L-homocysteine and catalase in 100 mM Tris-HCl, pH 8.0 buffer, 30 °C (by adding at different times additional amounts of the enzymes, see Experimental section for details). After 7.5 h of incubation, ~0.65 mM ccMA was produced (~65% yield, Figure 4C).

An alternative strategy for the one-pot bioconversion of vanillin into ccMA consists in a one-pot two-step procedure which first leads to the production of the PCA intermediate from vanillin, followed by its direct bioconversion into

ccMA. First, the one-pot bioconversion of 1 mM vanillin into the intermediate PCA was performed using the optimized amounts of XO, LigM/MetE, THF, L-homocysteine, and catalase (see above). After ≈2 h, the peak corresponding to vanillin disappeared and after 5.5 h of incubation at 30 °C, ~0.8 mM PCA was produced (80% yield) with a residual ~0.19 mM vanillic acid. Hence, both the lyophilized pET24::AroY transformed *E. coli* cells and CatA were added to the reaction mixture and, after 2.5 h of incubation at 30 °C, the 0.8 mM PCA previously produced was fully converted into the final product ccMA, without any accumulation of the catechol intermediate. Under these conditions, the yield for the bioconversion of 1 mM vanillin into ccMA was ~80% in 8 hours.

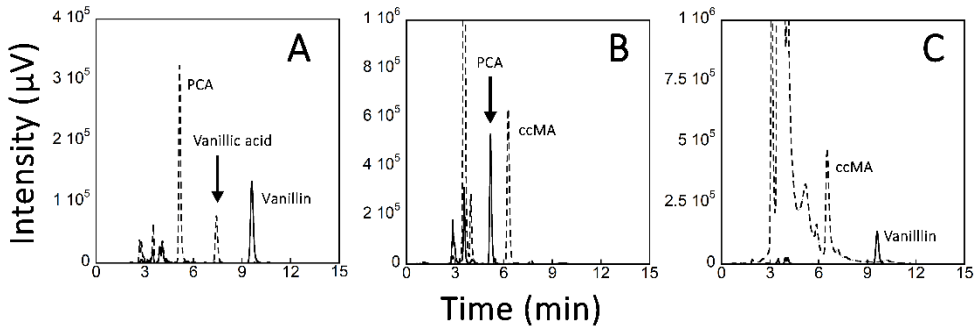

Figure 4. HPLC chromatograms of the multi-enzymatic one-pot bioconversion of (A) 1 mM vanillin into PCA, (B) 1 mM PCA into ccMA and (C) of 1 mM vanillin into ccMA, in 100 mM Tris-HCl, pH 8.0, 30 °C, at t_0 (continuous line) and at the end of incubation (dotted line).

4. Scaled up production of ccMA

Bioconversion was scaled up by increasing the vanillin concentration to 3 mM and using a 3 mL solution. The conversion was further optimized evaluating the addition of the enzymes at different times (see Experimental section) allowing full transformation of vanillin into the final product ccMA in 16 hours, with a >95% yield (Figure 5).

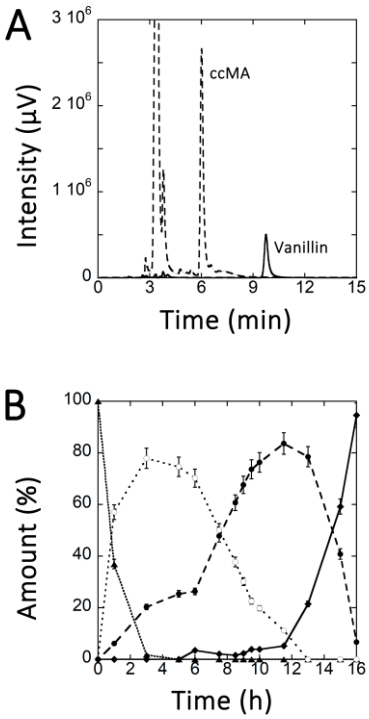

Figure 5. Bioconversion of 3 mM vanillin into ccMA, in 100 mM Tris-HCl, pH 8.0, 30 °C. (A) HPLC chromatograms of vanillin (t_0, continuous line) and of ccMA produced after 16 h (dashed line). (B) Time course of the reaction. Symbols used: (▲) vanillin, (○) vanillic acid, (●) PCA, and (♦) ccMA.

Previously, a biotechnological route for ccMA production from vanillin was reported by Wu *et al.* (Wu et al., 2017): they reported on the engineering of the *E. coli* DH1 strain with five recombinant enzymes (i.e. vanillin dehydrogenase, *O*-demethylase, protocatechuate decarboxylase, catechol dioxygenase). The transformed cells were incubated with ~3 mM vanillin and, after 48 h at 30 °C, ~2 mM ccMA were produced (0.69 g ccMA/g vanillin, 69% yield). Our work represents an improvement in terms of yields and time in comparison to the whole-cell system (Wu et al., 2017). In particular, the enzymatic process overcomes the limiting step of cell-based bioconversion, represented by the protecatechuate decarboxylase (Wu et al., 2017).

The economic aspects of this multi-enzymatic bioconversion were taken into great consideration during the design of the synthetic pathway. The cost of

ccMA is approximately 400-fold higher than that of vanillin (based on the commercial price for lab-scale amounts). Altogether, the reported lab-scale procedure allows to produce 1 g of ccMA from vanillin at approximately 70% of the commercial cost of product and with a 95% yield. The use of recombinant His-tagged enzymes (i.e. LigM, MetE and CatA), which can be easily purified with high yields in a single chromatographic step, joined with the use an efficient system for the regeneration of the LigM cofactor (which allows a reduction of the lab-scale costs from 20 to 0.07 € per mg of converted vanillic acid) (Rosini et al., 2016) represent main advantages of the proposed biocatalytic system. Remarkably, the choice to adopt *E. coli* cells expressing the enzyme protocatechuate decarboxylase AroY allowed to drastically reduce both the costs and the time required for the reconstitution of the purified inactive apoprotein AroY with its FMN cofactor (Marshall et al., 2017). Moreover, the lyophilisation step for transformed cells ensures both stability and easy storage.

Conclusions

In this work, a ready-to-use high-yield system for production of ccMA starting from vanillin was presented. In comparison with cell-based systems, the multi-enzymatic reactions allow a rapid and easy modification of the reaction parameters in order to improve both the yield and the timespan of the process. The immobilization of this multi-enzymatic system, aimed at improving the enzyme stability, could represent a further improvement pushing its use by reducing the costs. The development of this cost-effective and efficient bioconversion system is supposed to provide a green opportunity to transform lignin-deriving compounds into high value added compounds.

Acknowledgements

LP and ER thank the support of Fondo di Ateneo per la Ricerca. EV is a PhD student of the "Life Sciences and Biotechnology" course at Università degli studi dell'Insubria.

References

Becker, J. and Wittmann, C. A field of dreams: lignin valorization into chemicals, materials, fuels, and health-care products. *Biotechnol. Adv.* **37**, 107360 (2019).

Berlin, A. and Balakshin, M. Industrial lignins: analysis, properties, and applications. *Bioener. Res: Adv. Appl.,* **18**, 315-336 (2014).

Caglio, R., Valetti, F., Caposio, P., Gribaudo, G., Pessione, E. and Giunta, C. Fine-Tuning of catalytic properties of catechol 1,2-dioxygenase by active site tailoring. *Chembiochem.,* **10**, 1015-1024 (2009).

Di Nardo, G., Roggero, C., Campolongo, S., Valetti, F., Trotta, F. and Gilardi, G., Catalytic properties of catechol 1,2-dioxygenase from *Acinetobacter radioresistens* S13 immobilized on nanosponges. *Dalton T.,* **33**, 6507-6512 (2009).

Farnberger, J. E., Lorenz, E., Richter, N., Wendisch, V. F. and Kroutil, W. In vivo plug-and-play: a modular multi-enzyme single-cell catalyst for the asymmetric amination of ketoacids and ketones. *Microb. Cell Fact.,* **16**, 132 (2017).

Godber, B. L., Schwarz, G., Mendel, R. R., Lowe, D. J., Bray, R. C., Eisenthal, R. and Harrison, R., *Biochem. J.*, **388**, 501-508 (2005).

Khusnutdinova, A. N., Xiao, J., Wang, P. H., Batyrova, K. A., Flick, R., Edwards, E. A. and Yakunin A. F. Prenylated FMN: biosynthesis, purification, and Fdc1 activation. *Methods Enzymol.,* **620**, 469-488, Academic Press (2019).

Kohlstedt, M., Starck, S., Barton, N., Stolzenberger, J., Selzer, M., Mehlmann, K., Schneider, R., Pleissner, D., Rinkel, J., Dickschat, J. S., Venus, J., van Duurena, J. B. J. H. and Wittmann, C., From lignin to nylon: cascaded chemical and biochemical conversion using metabolically engineered *Pseudomonas putida*. *Metab. Eng.*, **47**, 279-293 (2018).

Marshall, S. A., Fisher, K., Cheallaigh, A. N., White, M. D., Payne, K. A., Parker, D. A., Rigby S. E. J. and Leys, D., Oxidative maturation and structural characterization of prenylated FMN binding by UbiD, a decarboxylase involved in bacterial ubiquinone biosynthesis. *J. Biol. Chem.*, **292**, 4623-4637 (2017).

Martani, F., Beltrametti, F., Porro, D., Branduardi, P. and Lotti, M., The importance of fermentative conditions for the biotechnological production of lignin modifying enzymes from white-rot fungi. *FEMS Microbiol. Lett.*, **364**, 1-18 (2017).

Panoutsopoulos, G. I., Kouretas, D. and Beedham C. Contribution of aldehyde oxidase, xanthine oxidase, and aldehyde dehydrogenase on the oxidation of aromatic aldehydes. *Chem. Res. Toxicol.*, **17**, 1368-1376 (2004).

Payer, S. E., Marshall, S. A., Bärland, N., Sheng, X., Reiter, T., Dordic, A., Steinkellner, G., Wuensch, C., Kaltwasser, S., Fisher, K., Rigby S. E. J., Macheroux, P., Vonck, J., Gruber, K., Faber, K., Himo, F., Leys, D., Pavkov-Keller, T. and Glueck, S. M. Regioselective *para*-carboxylation of catechols with a prenylated flavin dependent decarboxylase. *Angew. Chem. Int. Ed.*, **56**, 13893-13897 (2017).

Picart, P., Liu, H., Grande, P. M., Anders, N., Zhu, L., Klankermayer, J., Leitner, W., de María, P. D., Schwaneberg, U. and Schallmey, A. Multi-step biocatalytic depolymerization of lignin. *Appl. Microbiol. Biot.*, **101**, 6277-6287 (2017).

Pollegioni, L., Tonin, F. and Rosini E. Lignin-degrading enzymes. *FEBS J.*, **282**, 1190-1213 (2015).

Rosini, E., D'Arrigo, P. and Pollegioni, L. Demethylation of vanillic acid by recombinant LigM in a one-pot cofactor regeneration system. *Catal. Sci. Technol.*, **6**, 7729-7737 (2016).

Ruales-Salcedo, A. V., Higuita, J. C., Fontalvo, J. and Woodley, J. M. (Chemo-) enzymatic cascade reactions. *Z. Naturforschung C.*, **74**, 77-84 (2019).

Schmid, A., Dordick, J. S., Hauer, B., Kiener, A., Wubbolts, M. and Witholt, B. Industrial biocatalysis today and tomorrow. *Nature*, **409**, 258-268 (2001).

Tessaro, D., Pollegioni, L., Piubelli, L., D'Arrigo, P. and Servi, S. Systems biocatalysis: an artificial metabolism for interconversion of functional groups. *ACS Catal.*, **5**, 1604-1608 (2015).

Vardon, D. R., Franden, M.A., Johnson, C. W., Karp, E. M., Guarnieri, M. T., Linger, J. G., Salm, M. J., Strathmann, T. J. and Beckham, G. T. Adipic acid production from lignin. *Energy Environ. Sci.*, **8**, 617-628 (2015).

Wang, P. H., Khusnutdinova, A. N., Luo, F., Xiao, J., Nemr, K., Flick, R., Brown, G., Mahadevan, R., Edwards, E. A. and Yakunin, A. F. Biosynthesis and activity of prenylated FMN cofactors. *Cell Chem. Biol.*, **25**, 560-570 (2018).

Wu, W., Dutta, T., Varman, A. M., Eudes, A., Manalansan, B., Loqué, D. and Singh, S. Lignin valorization: two hybrid biochemical routes for the conversion of polymeric lignin into value-added chemicals. *Sci. Rep. UK*, **7**, 1-13 (2017).

Xu, Z., Lei, P., Zhai, R., Wen, Z. and Jin, M. Recent advances in lignin valorization with bacterial cultures: microorganisms, metabolic pathways, and bio-products. *Biotechnol. Biofuels*, **12**, 32 (2019).

Supplementary Materials

Figure S1. HPLC calibration curves for (A) vanillin, (B) vanillic acid, (C) PCA, (D) catechol and (E) ccMA.

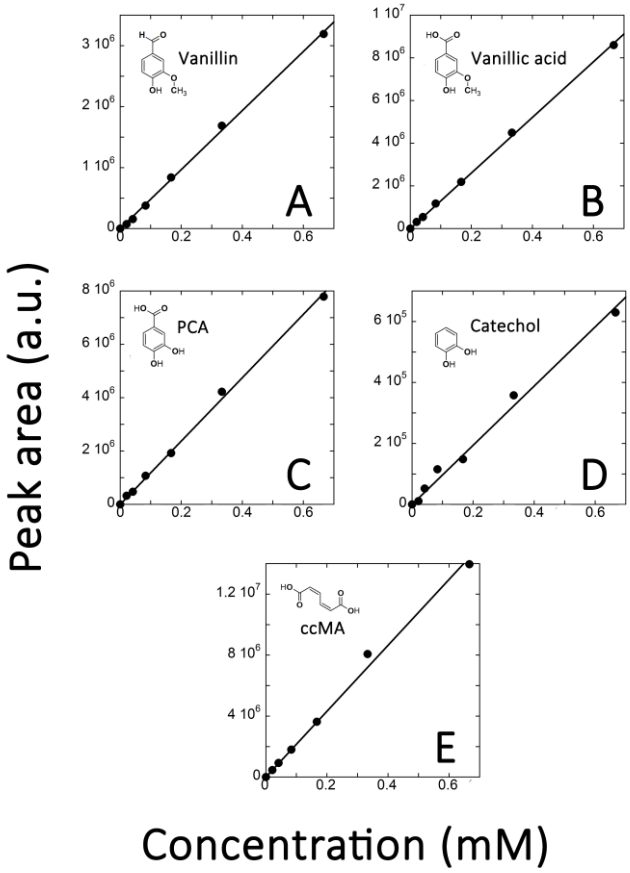

3. Discussion

"We are living on this planet as if we had another one to go to" is the lucid and disenchanted warning stated by Terri Swearingen at the Goldman Environmental Prize Ceremony, in the 1997. The constant and rapid growth of the world population, the effects of climate changes, the indiscriminate exploitation of soil and ecosystems and the strict dependence on fossil non-renewable sources are actual issues that modern society can no more ignore. In 2020, the international research organization "Global Footprint Network" calculated that the Earth Overshoot Day (which marks the date in which the demand of humanity for ecological resources and services at the present year exceeds what Earth can regenerate in that year) worryingly landed on August 22nd. Therefore, the bioeconomy paradigm, promoting a model of production which takes into account the building of a more equal society and the respect for the natural resources, emerged in the last decades as a promising solution[66–68]. Notably, the branch of the circular economy results particularly attractive in the re-thinking of the productive strategies from a "take, make, and dispose" linear chain into a more holistic approach in which value can be obtained from what is wasted (Figure 6)[48,66].

Notably, a large number of advantageous effects on economy, environment and society can be obtained from the adoption of a circular economy model as shown in Figure 1[47,66]. However, the deepen analyses of the characteristics of each territory and of its pre-existing productive network are both primary assumptions for the realisation of a targeted and integrated bioeconomy system[69].

In this view, the lignocellulosic biomass from woody feedstock's, agricultural residues, industrial wastes and municipal solid wastes, was reported as the most abundant (more than 2×10^{11} t/year worldwide[22,39]) and suitable renewable feedstock to replace chemicals and fuels from fossil sources[37]. In particular, biorefineries aim to integrate the valorisation of the carbohydrate components of the lignocellulosic biomass with that of the more recalcitrant lignin[70]. In fact, the peculiar structure of lignin, formed by phenylpropane units, makes this biopolymer the first renewable source of aromatics on Earth[2,5].

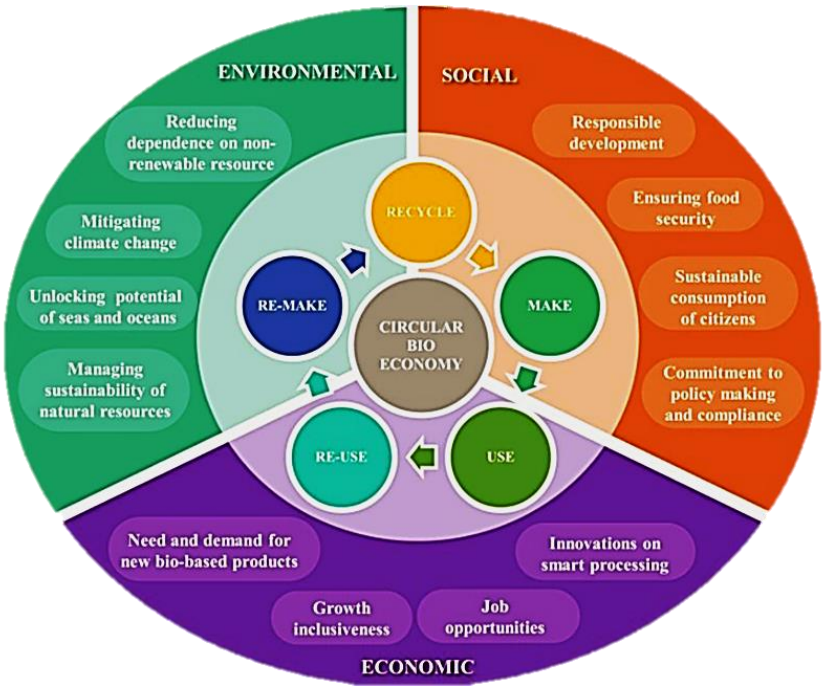

Figure 6. Scheme of the material-flow in the bio-based circular economy and of the positive impact of each step of the circular productive chain on economy, environment and society. Reprinted from reference[66].

This Ph.D. project focused on the investigation of different strategies for lignin valorisation strictly based on a biochemical approach, based on the great advantages in using enzymes, such as high-selective and efficient biocatalysts in eco-friendly and safe processes[6,60].

Firstly, the enzymatic *tool-box* available at the host laboratory and containing 26 fungal and bacterial enzymes with both ligninolytic and auxiliary-ligninolytic activities (i.e. laccases, peroxidases, β-etherases and dioxygenases) was added of two recombinant enzymes. In particular, the N246A variant of the dye-decolorizing peroxidase DypB (Rh_DypB, which was reported to have an increased manganese-peroxidase activity[62]) and the superoxide dismutase MnSOD-1, which were recently identified from the lignin-degrading bacteria *Rhodococcus jostii* RHA1[71] and *Sphinobacterium sp.* T2[61], respectively. The *Rh_DypB* and *MnSOD-1* synthetic genes were optimized for their recombinant overexpression in the BL21(DE3) strain of *Escherichia coli* and the corresponding His-tagged proteins were purified by a single

chromatographic step on nickel-chelating affinity column and biochemically characterized.

The Rh_DypB is a tetrameric heme-peroxidase belonging to the chlorite dismutase super-family (EC 1.11.1.14). Notably, the set-up of an improved expression protocol (which consists in an additional post-induction incubation under micro-aerobic conditions) allowed, for the first time, the purification with high yields (i.e. >100 mg/L) and purity (i.e. >90%) of a fully folded active holoenzyme, avoiding the need for further time-consuming and expensive reconstitution steps of the apoprotein as previously stated in[71,72] (see paragraph 3.1). Subsequently, the potential of Rh_DypB as biocatalyst was evaluated under a large number of experimental conditions and its kinetic parameters were determined for different substrates (i.e. hydrogen peroxide, manganese, ABTS and 2,6-dimethoxyphenol) as reported in paragraph 3.1. For what concerns its peroxidase activity, the reaction rates were fitted with a Michaelis-Menten equation modified to account for a substrate inhibition effect by hydrogen peroxide ($K_i \approx 2.2$ mM). Rh_DypB showed the highest substrate specificity (K_m of 0.03 mM) and enzymatic activity ($\approx 20\ s^{-1}$) for hydrogen peroxide as substrate. Moreover, the addition of manganese produced an increased up to 1.6 fold ($\approx 34\ s^{-1}$) in the peroxidase activity. Interestingly, the enzyme showed two pH optima according to the fact that a peroxidase activity (0.1 mM H_2O_2, pH 4.0) or a manganese-dependent peroxidase activity (0.1 mM H_2O_2, 2 mM Mn^{2+}, pH 6.0) was evaluated. This aspect was particularly relevant in assaying the dye-decolorizing activity in the presence of Azure B, Reactive Black 5 and Remazol Brilliant Blue R. Actually, in all the cases, the highest decolorization level was observed following manganese addition (see paragraph 3.1). The enzyme catalysed the oxidation of different phenolic and non-phenolic monomeric lignin model compounds (e.g., ABTS, 2,6-dimethoxyphenol, veratryl alcohol), besides the cleavage of the β-O-4 linkage of the lignin model dimer GGE, which is the most abundant linkage in the lignin polymer (≈ 50% of the total lignin interunit linkage)[73]. The bioconversion of GGE (12.5 µmol/min mg enzyme) produced the formation of guaiacol, with a ≈ 30% increase when ascorbic acid was added: the stabilizing effect exerted by ascorbate

probably reduced the occurrence of side radical reactions (paragraph 3.1). The characterisation of Rh_DypB highlighted its highly appreciable features as biocatalyst (including good thermal stability and tolerance to detergents and solvents), and therefore its applicability was evaluated even in the field of mycotoxins degradation, as described in paragraph 3.2.

These secondary toxic metabolites, produced by filamentous fungi mainly belonging to *Fusarium*, *Aspergillus* and *Penicillium* genera, represent an urgent problem for food and feed safety, especially in developing countries[74]. Besides physical (e.g., heat, irradiation, mechanical treatments) and chemical (e.g., peroxidation, ozonation) approaches for the detoxification of commodities, the enzymatic treatments resulted effective in reducing mycotoxin contamination both in vitro and in real matrices[74]. Nevertheless, the main bottleneck for the application of enzymes at industrial level is represented by the lack of information about the resulting degradation products, with the only exception for FUMzyme® (Biomin Holding GmbH, Getzersdorf, Austria), a commercialised feed additive which exploits the activity of a purified esterase to perform the fumonisin degradation[74].

This Ph.D. project investigated the possibility to enzymatically degrade Aflatoxin B_1 (AFB_1) which, because of its carcinogenicity, was classified in 2002 by the International Agency of Research on Cancer (IARC) as the most hazardous mycotoxin for human health[74]. In particular, the use of a previously set-up colorimetric miniaturised screening method for the detection of carbonyl groups (resulting from oxidative degradation products)[75] allowed to identify the dye-decolorizing peroxidase Rh_DypB as the most active enzyme among a selected group of potential candidates (i.e. two laccases from *Bacillus licheniformis* and *Trametes versicolor* and two manganese peroxidases from *Bjerkandera adusta* and *Phlebia* sp. Nfb19). Notably, the activity of Rh_DypB on AFB_1 was confirmed by HPLC analyses and the experimental conditions for the in vitro degradation were optimized (i.e. incubation time, amounts of hydrogen peroxide and enzyme) allowing to obtain a 96% of biotransformation yield of AFB_1 in 96 hours (see paragraph 3.2). This result demonstrates the efficiency of Rh_DypB as biocatalyst since lower concentrations

of enzyme (0.1 U/mL) and hydrogen peroxide (0.1 mM), along with high amounts of AFB_1 (1 µg/mL), were used in comparison with reported studies[76,77]. Interestingly, as demonstrated by high resolution LC-MS/MS analyses, Rh_DypB catalyses the hydroxylation of AFB_1 into the less toxic metabolite Aflatoxin Q_1 (AFQ_1), rather than the production of the more stable demethylated AFB_1 product or of the 8,9-epoxy-AFB_1 compound (which is the most toxic oxidation product arising from cytochromes and other peroxidases) (see paragraph 3.2). Consequently, Rh_DypB is also eligible in detoxification processes. In order to determine the mechanism underlying the molecular interaction between Rh_DypB and AFB_1, a site-directed mutagenesis study of putative residues involved in the AFB_1 binding identified by molecular docking has already been started.

Superoxide dismutase from the soil bacterium *Sphingobacterium sp.* T2 (MnSOD-1) belongs to the oxidoreductase family which catalyses the two-step conversion of the reactive superoxide anion into molecular oxygen and hydrogen peroxide, according to a ping-pong mechanism (SODs, EC 1.15.1.1)[78,79]. On the basis of the metal ion cofactor, four classes of SODs can be distinguished, showing a Cu/Zn binuclear centre or a mononuclear Fe, Mn or Ni centre and other structural and functional peculiarities[78,79]. The disproportionation of superoxide ($O_2^{\bullet -}$) is an essential reaction in the protection of organisms from oxidative damages, especially those provoked by the reactive oxygen species (ROS)[79,80]. Interestingly, the MnSOD-1 from *Sphingobacterium sp.* T2 showed, beside the classical superoxide dismutase activity, a lignin oxidation activity (i.e. O-demethylation activity, aryl-Cα and Cα-Cβ bond cleavage) higher than MnSODs from *E. coli* and *Thermus thermophilus*, according to a mechanism for the generation of lignin oxidants which is still unclear[61,81]. The recombinant MnSOD-1 was produced with a volumetric yield of ≈100 $mg_{protein}/L_{culture}$, corresponding to a five-fold increase in comparison to the previously reported figure of 19.5 $mg_{protein}/L_{culture}$[61], and a specific activity of 518 ± 5.3 U/mg in good agreement with the value of 400 U/mg reported by[61] (see paragraph 3.3). The MnSOD-1 enzyme showed a great stability after a 24 hours incubation at different pH values (from 3.0 to 9.0, residual activity >90%) and

retained >80% activity when assayed in the 15-85 °C temperature range (paragraph 3.3).

Based on previous studies[61,82], the ligninolytic MnSOD-1 activity was investigated on actual samples of wheat straw lignin. The identification and quantification of the obtained degradation products were part of an extensive study aimed to define the degradation yields from different unfractionated and fractionated lignin samples enzymatically treated (paragraph 3.3).

In details, a colorimetric miniaturised screening method[75] was used to identify the optimal conditions for the incubation of three different technical lignins (i.e. softwood kraft lignin, wheat straw lignin and softwood lignosulphonate) with different enzymes from the tool-box (i.e. the laccases Lac C, Lac F and BALL and the superoxide dismutase MnSOD-1). This experimental approach allowed the rapid collection and comparison of more than 240 results (i.e. > 48 different lignin/enzyme combinations), representing an efficient support in the design of scaled-up incubations (see paragraph 3.3). Notably, the data currently available from enzymatic treatments of lignin samples mainly reported qualitative results of the degradation products, with the exception for the formation of ≈ 12.5% (w/w) oily fraction of low-molecular weight compounds[63] or < 0.5 mg/g lignin for selected molecules[62,73] (paragraph 3.3). Under our optimized conditions, the highest net degradation yield (i.e. values subtracted of the amounts present in the corresponding untreated control and calculated respect to the internal standard) was obtained for the wheat straw lignin incubated with Lac F and the mediator ABTS (2 mg total monomers per gram of lignin), showing veratric acid as the main degradation product (1.2 mg/g). A figure of 0.4-0.7 mg monomers per gram of lignin was obtained by incubating the wheat straw lignin with MnSOD-1 and the softwood kraft lignin with BALL and the mediator TEMPO (paragraph 3.3). Moreover, an acetone-fractionation of the technical lignins was performed as a green and mild process to increase in homogeneity (i.e. reduction of the polydispersity) of the starting material: in all the cases, an improvement in the enzymatic degradation yield in comparison with the corresponding unfractionated samples was observed.

Interestingly, a large number of value-added compounds were identified and quantified, such as 0.4 mg of vanillin per gram of lignin either for the treatment of the fractionated wheat straw lignin with MnSOD-1 and for the treatment of the fractionated softwood kraft lignin with the BALL/TEMPO laccase/mediator system. In addition, the incubation of fractions from the wheat straw lignin with the Lac F/ABTS laccase/mediator system allowed the formation of 2 mg of veratric acid and 13.5 mg of veratraldehyde per gram of lignin (paragraph 3.3).

Although enzymatic treatments take advantage of selective catalysis to generate a reproducible process (i.e. obtainment of a homogeneous mixture enriched in a certain degradation product of interest starting from a peculiar lignin sample), the increasing in the degradation yields remains the main bottleneck for their industrial application. In this view, this quantitative study highlighted the importance to identify the optimal incubation conditions for the set-up of multi-variant enzymatic experiments (e.g., incubation time, lignin/enzyme combination, etc.). In addition, the fractionation of the lignin samples was a key point in its valorisation beside other promising strategies such as multi-enzymatic incubations and chemo-enzymatic treatments which will be further investigated.

Moreover, the lignin valorisation process focuses also on the promotion of sustainable solutions for the synthesis of value-added chemicals from its degradation products (i.e. aromatics). Accordingly, the Ph.D project also focused on the design and set-up of the one-pot multi-enzymatic bioconversion of vanillin (the only aromatic lignin degradation product globally commercialised[43]) into *cis,cis*-muconic acid (paragraph 3.4). This latter compound is one of the three isomers of the linear dicarboxylic muconic acid and its global market is greater than $22 billion, since its relevance for the synthesis of polyamides, unsaturated polyesters, adipic acid and terephthalic acid, which are all chemicals involved in the production of a large number of plastic materials[57,83]. The multi-enzymatic bioconversion involves four reactions catalysed by the enzymes xanthine oxidase, *O*-demethylase, protecatechuate decarboxylase and catechol dioxygenase. After the study of each catalytic step, the enzymes were combined in a one-pot reaction. The enzymatic

system allowed the bioconversion of 1 mM vanillin into ~0.65 mM ccMA in 7.5 hours, corresponding to a ~65% yield (paragraph 3.4). In order to further improve the bioconversion yields, the set-up of a two-step process allowed the production of ccMA with ~80% yield, in 8 hours, by starting from 1 mM vanillin (paragraph 3.4). The scaled-up bioconversion was carried out using 3 mM vanillin under optimized conditions: after ~15 hours, 1 g of ccMA was produced (>95% bioconversion) at the 70% of the commercial cost while a 69% bioconversion of 3 mM vanillin in ccMA was reported in 48 hours using a whole-cell approach (i.e. a resting *E. coli* strain transformed with the genes encoding for the enzymes involved in the synthetic pathway)[65]. Therefore, the proposed multi-enzymatic system demonstrates the efficacy of bio-catalytic pathways as innovative and more sustainable alternatives than classical synthetic processes. Notably, in order to reduce the lab-costs for the need of expensive enzymatic cofactors (i.e. the tetrahydrofolate for the *O*-demethylase and the prenylated FMN for the protecatechuate decarboxylase) on the one hand an efficient system for the tetrahydrofolate regeneration was introduced[84] and, on the other hand, the need for the laborious reconstitution of the protecatechuate decarboxylase purified in the apoprotein form was bypassed by using lyophilised cells expressing the enzyme. In order to further improve this efficient and inexpensive multi-enzymatic system, strategies for the immobilization and the re-using of the enzymes should be studied. Finally, the system could be used in combination with known ligninolytic enzymes (i.e. laccases and peroxidases) in order to design a direct flow process between the degradation of lignin and the valorisation of its degradation products through a completely bio-catalytic pathway.

In conclusion, the results collected during this Ph.D. program contribute in offering biochemically strategies for the valorisation of lignin, the most promising renewable substitute of fossil sources. The high-yield recombinant production of lignin-degrading enzymes (i.e. Rh_DypB and MnSOD-1) and their biochemically characterization were preliminary essential steps. Intriguingly, the deepening in the biochemical study of a certain enzyme may lead to the finding of new

biotechnological applications, as demonstrated by the dye-decolorizing Rh_DypB, which catalyses the degradation of both lignin and mycotoxins. Moreover, the treatment of authentic lignin samples with different enzymatic activities (i.e. laccases, superoxide dismutase) under optimized conditions (i.e. determined using conditions identified by a rapid miniaturised screening for each lignin/enzyme combination and the fractionation of lignin to generate homogenous starting samples) provided an insight on the ensuing degradation products, from a qualitative and quantitative point of view. Finally, the set-up of an efficient and inexpensive multi-enzymatic system for the one-pot bioconversion of vanillin into the value-added *cis,cis*-muconic acid demonstrated the efficacy of an innovative bio-catalysed pathway to perform lignin valorisation under eco-friendly conditions. Enzymes are extremely versatile and powerful catalysts and their contribution in the biotechnological valorisation of lignin has been well established. Therefore, the expanding of studies on their main features will allow the realisation of a consolidated biorefinery platform in which different expertise from different multi-disciplinary fields co-work to reach the shared goal of a more sustainable productive development.

4. References

1. Martone, P. T. *et al.* Discovery of lignin in seaweed reveals convergent evolution of cell-wall architecture. *Curr. Biol.* **19**, 169–175 (2009).

2. Zakzeski, J., Bruijnincx, P. C. A., Jongerius, A. L. & Weckhuysen, B. M. The catalytic valorization of lignin for the production of renewable chemicals. *Chem. Rev.* **110**, 3552–3599 (2010).

3. Petridis, L. & Smith, J. C. Molecular-level driving forces in lignocellulosic biomass deconstruction for bioenergy. *Nat. Rev. Chem.* **2**, 382–389 (2018).

4. Beckham, G. T., Johnson, C. W., Karp, E. M., Salvachúa, D. & Vardon, D. R. Opportunities and challenges in biological lignin valorization. *Curr. Opin. Biotechnol.* **42**, 40–53 (2016).

5. Kirk, T. K. & Farrell, R. L. Enzymatic 'combustion': the microbial degradation of lignin. *Ann. Rev. Microbiol* **41**, (1987).

6. Pollegioni, L., Tonin, F. & Rosini, E. Lignin-degrading enzymes. *FEBS J.* **282**, 1190–1213 (2015).

7. Hatakeyama, H., & Hatakeyama, T. Lignin structure, properties, and applications. *Biopolymers* (pp. 1-63). Springer, Berlin, Heidelberg, (2009).

8. Berlin, A. & Balakshin, M. Industrial lignins: analysis, properties, and applications. In *Bioenergy Research: Advances and Applications* (pp. 315-336). Elsevier (2014).

9. Vanholme, R., Demedts, B., Morreel, K., Ralph, J. & Boerjan, W. Lignin biosynthesis and structure. *Plant Physiol.* **153**, 895–905 (2010).

10. Pandey, M. P. & Kim, C. S. Lignin depolymerization and conversion: a review of thermochemical methods. *Chem. Eng. Technol.* **34**, 29–41 (2011).

11. Derkacheva, O. & Sukhov, D. Investigation of lignins by FTIR spectroscopy. *Macromol. Symp.* **265**, 61–68 (2008).

12. Whetten, R. & Sederoff, R. Lignin biosynthesis. *Plant Cell* **7**, 1001–1013 (1995).

13. Baucher, M., Monties, B., Montagu, M. Van & Boerjan, W. Critical reviews in plant sciences biosynthesis and genetic engineering of lignin. *CRC. Crit. Rev. Plant Sci.* **17**, 125–197 (1998).

14. Ralph, J. *et al.* Lignins: Natural polymers from oxidative coupling of 4-hydroxyphenyl-propanoids. *Phytochem. Rev.* **3**, 29–60 (2004).

15. Capanema, E. A., Balakshin, M. Y. & Kadla, J. F. A comprehensive approach for quantitative lignin characterization by NMR spectroscopy. *J. Agric. Food Chem.* **52**, 1850–1860 (2004).

16. Wen, J. L., Sun, S. L., Xue, B. L. & Sun, R. C. Recent advances in characterization of lignin polymer by solution-state nuclear magnetic resonance (NMR) methodology. *Materials (Basel).* **6**, 359–391 (2013).

17. Martínez, Á. T. *et al.* Biodegradation of lignocellulosics: Microbial, chemical, and enzymatic aspects of the fungal attack of lignin. *Int. Microbiol.* **8**, 195–204 (2005).

18. Li, X. & Zheng, Y. Biotransformation of lignin: mechanisms, applications and future work. *Biotechnol. Progr.* (2019). doi:10.1002/btpr.2922

19. Kamimura, N., Sakamoto, S., Mitsuda, N., Masai, E. & Kajita, S. Advances in microbial lignin degradation and its applications. *Curr. Opin. in Biotechnol.* **56**, 179–186 (2019).

20. Becker, J. & Wittmann, C. A field of dreams: lignin valorization into chemicals, materials, fuels, and health-care products. *Biotechnol. Advances* **37**, (2019).

21. Lee, S., Kang, M., Bae, J. H., Sohn, J. H. & Sung, B. H. Bacterial valorization of lignin: strains, enzymes, conversion pathways, biosensors, and perspectives. *Front. Bioeng. Biotechnol.* **7**, (2019).

22. Li, C. *et al.* Recent advancement in lignin biorefinery: with special focus on enzymatic degradation and valorization. *Bioresour. Technol. Rep.* **291**, (2019).

23. Bugg, T. D. H., Ahmad, M., Hardiman, E. M. & Singh, R. The emerging role for bacteria in lignin degradation and bio-product formation. *Curr. Opin. Biotechnol.* **22**, 394–400 (2011).

24. Picart, P., De María, P. D. & Schallmey, A. From gene to biorefinery: microbial β-etherases as promising biocatalysts for lignin valorization. *Front. Microbiol.* **6**, 1–8 (2015).

25. Rosini, E. *et al.* Cascade enzymatic cleavage of the β-O-4 linkage in a lignin model compound. *Catal. Sci. Technol.* **6**, 2195–2205 (2016).

26. Wang, W. *et al.* Efficient, environmentally-friendly and specific valorization of lignin: promising role of non-radical lignolytic enzymes. *World J. Microbiol. Biotechnol.* **33**, 1–14 (2017).

27. Regalado, C., García-Almendárez, B. E. & Duarte-Vázquez, M. A. Biotechnological applications of peroxidases. *Phytochem. Rev.* **3**, 243–256 (2004).

28. Singh, R. S., Singh, T. & Pandey, A. Microbial enzymes: an overview. *Adv. Enzyme Technol.* (pp. 1-40). Elsevier (2019).

29. Tien, M. & Kirk, T. K. Lignin-degrading enzyme from the *Hymenomycete Phanerochaete chrysosporium* burds. *Science,* **221**, 661–663 (1983).

30. Ten Have, R. & Teunissen, P. J. M. Oxidative mechanisms involved in lignin degradation by white-rot fungi. *Chem. Rev.* **101**, 3397–3413 (2001).

31. Ruiz-Dueiias, F. J., Camarero, S., Pérez-Boada, M., Martínez, M. J. & Martínez, Á. T. A new versatile peroxidase from *Pleurotus*. *Biochem. Soc. Trans.* (2001).

32. de Gonzalo, G., Colpa, D. I., Habib, M. H. M. & Fraaije, M. W. Bacterial enzymes involved in lignin degradation. *J. Biotechnol.* **236**, 110–119 (2016).

33. Yoshida, T., Tsuge, H., Konno, H., Hisabori, T. & Sugano, Y. The catalytic mechanism of dye-decolorizing peroxidase DyP may require the swinging movement of an aspartic acid residue. *FEBS J.* **278**, 2387–2394 (2011).

34. Rodríguez Couto, S. & Toca Herrera, J. L. Industrial and biotechnological applications of laccases: a review. *Biotechnol. Adv.* **24**, 500–513 (2006).

35. Fatma, S. *et al.* Lignocellulosic biomass: a sustainable bioenergy source for future. *Protein Pept. Lett.* **25**, (2018).

36. Marriott, P. E., Gómez, L. D. & Mcqueen-Mason, S. J. Unlocking the potential of lignocellulosic biomass through plant science. *New Phytol.* **209**, 1366–1381 (2016).

37. Liguori, R. & Faraco, V. Biological processes for advancing lignocellulosic waste biorefinery by advocating circular economy. *Bioresour. Technol.* **215**, 13–20 (2016).

38. Bajwa, D. S., Pourhashem, G., Ullah, A. H. & Bajwa, S. G. A concise review of current lignin production, applications, products and their environment impact. *Ind. Crops Prod.* **139**, 111526 (2019).

39. Tuck, C. O., Pérez, E., Horváth, I. T., Sheldon, R. A. & Poliakoff, M. Valorization of biomass: deriving more value from waste. *Science (80-.).* **337**, 695–699 (2012).

40. Constant, S. *et al.* New insights into the structure and composition of technical lignins: a comparative characterisation study. *Green Chem.* **18**, 2651–2665 (2016).

41. Chio, C., Sain, M. & Qin, W. Lignin utilization: a review of lignin depolymerization from various aspects. *Renew. Sustain. Energy Rev.* **107**, 232–249 (2019).

42. Abejón, R., Pérez-Acebo, H. & Clavijo, L. Alternatives for chemical and biochemical lignin valorization: hot topics from a bibliometric analysis of the research published during the 2000-2016 period. *Processes* **6**, (2018).

43. Upton, B. M. & Kasko, A. M. Strategies for the conversion of lignin to high-value polymeric materials: review and perspective. *Chem. Rev.* **116**, 2275–2306 (2016).

44. Holladay, J. E., White, J. F., Bozell, J. J. & Johnson, D. Top value-added chemicals from biomass volume II - Results of screening for potential candidates from biorefinery lignin. Prepared for the U.S. Department of Energy under Contract DE-AC05-76RL01830. **II**, (2007).

45. Ragauskas, A. J. *et al.* Lignin valorization: improving lignin processing in the biorefinery. *Science (80-.).* **344**, (2014).

46. Abdelaziz, O. Y. *et al.* Biological valorization of low molecular weight lignin. *Biotechnol. Adv.* **34**, 1318–1346 (2016).

47. Aguilar, A., Wohlgemuth, R. & Twardowski, T. Perspectives on bioeconomy. *New Biotechnol.* **40**, 181–184 (2018).

48. Anastasiades, K., Blom, J., Buyle, M. & Audenaert, A. Translating the circular economy to bridge construction: lessons learnt from a critical literature review. *Renew. Sustain. Energy Rev.* **117**, 109522 (2020).

49. Indipendent Group of Scientists appointed by the Secretary-General. *Global Sustainable Development Report 2019*. (2019).

50. Schroeder, P., Anggraeni, K. & Weber, U. The relevance of circular economy practices to the sustainable development goals. *J. Ind. Ecol.* **23**, 77–95 (2019).

51. International Renewable Energy Agency (IRENA). Global energy transformation: a roadmap to 2050. (2018). ISBN : 978-92-9260-121-8

52. Chakar, F. S. & Ragauskas, A. J. Review of current and future softwood kraft lignin process chemistry. *Ind. Crops Prod.* **20**, 131–141 (2004).

53. Vishtal, A. & Kraslawski, A. Challenges in industrial applications of technical lignins. *Bioresour. Technol.* **6**, 3547–3568 (2011).

54. Hossain, M. M. & Aldous, L. Ionic liquids for lignin processing: dissolution, isolation, and conversion. *Aust. J. Chem.* **65**, 1465–1477 (2012).

55. Liu, Z. H. *et al.* Identifying and creating pathways to improve biological lignin valorization. *Renew. Sustain. Energy Rev.* **105**, 349–362 (2019).

56. Chen, Y. *et al.* Kraft lignin biodegradation by *Novosphingobium sp.* B-7 and analysis of the degradation process. *Bioresour. Technol.* **123**, 682–685 (2012).

57. Xu, Z., Lei, P., Zhai, R., Wen, Z. & Jin, M. Recent advances in lignin valorization with bacterial cultures: microorganisms, metabolic pathways, and bio-products. *Biotechnol. Biofuels* **12**, (2019).

58. Lin, B. & Tao, Y. Whole-cell biocatalysts by design. *Microb. Cell Fact.* **16**, 1–12 (2017).

59. De Carvalho, C. C. C. R. Enzymatic and whole cell catalysis: finding new strategies for old processes. *Biotechnol. Adv.* **29**, 75–83 (2011).

60. Ruales-Salcedo, A. V., Higuita, J. C., Fontalvo, J. & Woodley, J. M. Design of enzymatic cascade processes for the production of low-priced chemicals. *Zeitschrift fur Naturforsch. - Sect. C J. Biosci.* **74**, 77–84 (2019).

61. Rashid, G. M. M. *et al.* Identification of manganese superoxide dismutase from *Sphingobacterium* sp. T2 as a novel bacterial enzyme for lignin oxidation. *ACS Chem. Biol.* **10**, 2286–2294 (2015).

62. Singh, R. *et al.* Improved manganese-oxidizing activity of DypB, a peroxidase from a lignolytic bacterium. *ACS Chem Biol* **8**, 700–706 (2013).

63. Picart, P. *et al.* Multi-step biocatalytic depolymerization of lignin. *Appl. Microbiol. Biotechnol.* **101**, 6277–6287 (2017).

64. Gasser, C. A. *et al.* Sequential lignin depolymerization by combination of biocatalytic and formic acid/formate treatment steps. *Appl. Microbiol. Biotechnol.* **101**, 2575–2588 (2017).

65. Wu, W. *et al.* Lignin valorization: two hybrid biochemical routes for the conversion of polymeric lignin into value-added chemicals. *Sci. Rep.* **7**, (2017).

66. Ubando, A. T., Felix, C. B. & Chen, W. H. Biorefineries in circular bioeconomy: a comprehensive review. *Bioresour. Technol. Rep.* **299**, (2020).

67. Aguilar, A., Wohlgemuth, R. & Twardowski, T. Perspectives on bioeconomy. *New Biotechnol.* **40**, 181–184 (2018).

68. Aguilar, A., Twardowski, T. & Wohlgemuth, R. Bioeconomy for sustainable development. *Biotechnol. J.* **14**, (2019).

69. Korhonen, J., Honkasalo, A. & Seppälä, J. Circular economy: the concept and its limitations. *Ecol. Econ.* **143**, 37–46 (2018).

70. Korányi, T. I., Fridrich, B., Pineda, A. & Barta, K. Development of 'Lignin-First' approaches for the valorization of lignocellulosic biomass. *Molecules* **25**, 2815 (2016).

71. Ahmad, M. *et al.* Identification of DypB from *Rhodococcus jostii* RHA1 as a lignin peroxidase. *Biochemistry* **50**, 5096–5107 (2011).

72. Singh, R., Grigg, J. C., Armstrong, Z., Murphy, M. E. P. & Eltis, L. D. Distal heme pocket residues of B-type dye-decolorizing peroxidase: arginine but not aspartate is essential for peroxidase activity. *J. Biol. Chem.* **287**, 10623–10630 (2012).

73. Reiter, J., Strittmatter, H., Wiemann, L. O., Schieder, D. & Sieber, V. Enzymatic cleavage of lignin β-O-4 aryl ether bonds via net internal hydrogen transfer. *Green Chem.* **15**, 1373–1381 (2013).

74. Loi, M., Fanelli, F., Liuzzi, V. C., Logrieco, A. F. & Mulè, G. Mycotoxin biotransformation by native and commercial enzymes: present and future perspectives. *Toxins (Basel).* **9**, (2017).

75. Tonin, F., Vignali, E., Pollegioni, L., D'Arrigo, P. & Rosini, E. A novel, simple screening method for investigating the properties of lignin oxidative activity. *Enzyme Microb. Technol.* **96**, 143–150 (2017).

76. Yehia, R. S. Aflatoxin detoxification by manganese peroxidase purified from *Pleurotus ostreatus*. *Brazilian J. Microbiol.* **45**, 127–133 (2014).

77. Wang, J., Ogata, M., Hirai, H. & Kawagishi, H. Detoxification of aflatoxin B_1 by manganese peroxidase from the white-rot fungus *Phanerochaete sordida* YK-624. *FEMS Microbiol. Lett.* **314**, 164–169 (2011).

78. Robinett, N. G., Peterson, R. L. & Culotta, V. C. Eukaryotic copper-only superoxide dismutases (SODs): a new class of SOD enzymes and SOD-like protein domains. **293**, 4636–4643 (2018).

79. Cannio, R., Fiorentino, G., Morana, A., Rossi, M. & Bartolucci, S. Oxygen: friend or foe? Archaeal superoxide dismutases in the protection of intra- and extracellular oxidative stress. *Front. Biosci.* **5**, d768-779 (2000).

80. Miller, A. Superoxide dismutases: active sites that save, but a protein that kills. *Curr. Opin. Chem. Biol.* **8**, 162–168 (2004).

81. Rashid, G. M. M. *et al. Sphingobacterium sp.* T2 manganese superoxide dismutase catalyzes the oxidative demethylation of polymeric lignin via generation of hydroxyl radical. *ACS Chem. Biol.* **13**, 2920–2929 (2018).

82. Lancefield, C. S. *et al.* Investigation of the chemocatalytic and biocatalytic valorization of a range of different lignin preparations: the importance of β-O-4 content. *ACS Sustain. Chem. Eng.* **4**, 6921–6930 (2016).

83. Vardon, D. R. *et al.* Adipic acid production from lignin. *Energy Environ. Sci.* **8**, 617–628 (2015).

84. Rosini, E., D'Arrigo, P. & Pollegioni, L. Demethylation of vanillic acid by recombinant LigM in a one-pot cofactor regeneration system. *Catal. Sci. Technol.* **6**, 7729–7737 (2016).

Acknowledgments

The Ph.D. program represented for me more than an extraordinary opportunity of high-level formation and professional training: it was also an important period of personal formation and growth.

Therefore I sincerely want to thank my supervisor Prof. Loredano Pollegioni for the trust he placed in me, allowing me to work in the stimulating laboratory he directs.

I want to kindly thank my tutor Ph.D. Elena Rosini for her immense disponibility and her constant support, even in the most challenging moments. She represents for me a model of professionality and of true passion for research.

Special thanks to all my collegues of The Protein Factory laboratory: they made me feel part of a great team.

Thinking about the past three years, I can only be extremely greatful to my parents and my sister Sara for always encouraging me to give my best, with patience and perseverance.

Last but not least, a big thank you to Luca for his precious suggestions and motivational support and to my friends, especially Linda, Ludovica, Federica, Simona, Andrea and “I Soci” for staying next me, unconditionally.